AMP Deaminase 3 in Skeletal Muscle Atrophy: Regulation of Protein Degradation and Contractile Performance

by

Patrick R. Davis

October, 2015

Director of Dissertation: Jeffrey J. Brault

Major Department: Kinesiology

Skeletal muscle atrophy is characterized by depressed cellular energetics, increased rates of protein degradation, contractile deficits and loss of muscle mass. A potential regulator of these impairments is the metabolic enzyme AMP Deaminase 3, which is highly upregulated during most if not all types of atrophy. The goals of the present dissertation were: 1) to investigate the role of AMPD3 on energetics and contractile characteristics of skeletal muscle during atrophy and 2) to determine the effects of AMPD3 in muscle cells on adenine nucleotide content and protein degradation.

AMPD3 was knocked down by electroporation of shRNA plasmids into mouse soleus muscle during denervation-induced atrophy. One week later, muscles were removed, electrically stimulated, and contractile function measured. Muscle homogenates were analyzed by UPLC and western blot. Denervation increased AMPD3 protein expression by 67%, while knockdown reduced AMPD3 by 60%. Knockdown of AMPD3 increased half relaxation times in both innervated and denervated muscles

during tetanic and high intensity fatiguing contractions. Neither low intensity contractions nor overexpression of AMPD3 in non-atrophying muscles altered half relaxation time.

To determine the effects of AMPD3 on protein degradation, AMPD3 was overexpressed by adenovirus in C2C12 myotubes. Adenine nucleotides, protein degradation rate, and indices of the major protein degradative pathways were measured. Overexpression of AMPD3 resulted in a 40% loss of ATP and an increase in IMP. Protein degradation rate was 38% greater while protein synthesis was unchanged, which resulted in a net loss of protein and myotube atrophy. Surprisingly, the autophagy activator ULK1 and apparent autophagic flux were unchanged. Further, proteasome subunit contents and in-vitro proteasome activity were similarly unchanged. However, consistent with greater protein degradation, total ubiquitinated conjugates decreased.

The increase in half relaxation time with AMPD3 knockdown is consistent with the role of AMPD in preserving the free energy of ATP hydrolysis and SERCA function. Overexpression of AMPD3 also resulted in a loss of adenine nucleotides and acceleration of protein degradation, suggesting that a fall in ATP activates proteasomal degradation in-vivo. These exciting findings identify AMPD3 as a novel regulator of skeletal muscle performance and protein degradation during atrophy.

AMP Deaminase 3 in Skeletal Muscle Atrophy: Regulation of Protein Degradation and Contractile Performance

A Dissertation

Presented to

The Faculty of the Department of Kinesiology

East Carolina University

In partial fulfillment of the requirements for the degree

Doctor of Philosophy in Bioenergetics and Exercise Science

by

Patrick R. Davis

October, 2015

AMP Deaminase 3 in Skeletal Muscle Atrophy: Regulation of Protein Degradation and Contractile Performance

by
Patrick R. Davis

APPROVED BY:

DIRECTOR OF DISSERTATION _____
Jeffrey J. Brault, Ph.D.

COMMITTEE MEMBER _____
Carol A. Witczak, Ph.D.

COMMITTEE MEMBER _____
David A. Brown, Ph.D.

COMMITTEE MEMBER _____
P. Darrell Neufer, Ph.D.

CHAIR OF THE DEPARTMENT OF KINESIOLOGY _____
Stacey Altman, J.D.

DEAN OF THE GRADUATE SCHOOL _____
Paul Gemperline, Ph.D.

Acknowledgements

The completion of this dissertation was made possible through numerous contributions of knowledge, time, support, and funding. I would first like to thank my advisor Dr. Brault who has been a critical part to my development through the doctoral program and has funded the vast majority of my research. I would also like to thank Dr. Witczak for her advice on experimental protocols and career options as well as allowing me to use much of her research equipment. Dr. Brown and Dr. Neufer have both been a great help through their comments on my dissertation development, and through the classroom instruction that I received from them. Several fellow students and research assistants have provided their help to me along the way, including Steven Roseno, Lance Bollinger, Kimberly Benton, and Denise Schmidt. I am thankful to the American College of Sports Medicine who funded my grant proposal. And finally, I would be remised if I did not express my deepest gratitude to my family Lindsay, Jack and Peter. You all bring joy into my life and have been unconditionally supportive of me through this program, for which I am sincerely grateful.

Table of Contents

List of Tables

List of Figures

Abbreviations

AEC,	Adenylate Energy Charge
AK,	Adenylate Kinase
AMPD,	AMP Deaminase
AMPK,	AMP Activated Protein Kinase
CK,	Creatine Kinase
COPD,	Chronic Obstructive Pulmonary Disorder
CP,	Creatine Phosphate
EDL,	Extensor Digitorum Longus
FTI,	Force-Time Integral
ΔG_{ATP},	Free Energy of ATP Hydrolysis
GFP,	Green Fluorescent Protein
KO,	Knockout
P_i,	Inorganic Phosphate
PCA,	Perchloric Acid
SERCA,	Sarcoendoplasmic Reticulum Calcium ATPase
shAMPD3,	AMPD3 Knockdown
shNEG,	Negative Control Knockdown
shRNA,	Short Hairpin RNA
SR,	Sarcoendoplasmic Reticulum
UPLC,	Ultra Performance Liquid Chromatography
WT,	Wild-Type

Chapter One

Introduction

Skeletal muscle atrophy, loss of muscle mass, is a debilitating condition because those who suffer from it are limited in activities of daily living (26), have decreased quality of life (149), and increased risk of all-cause mortality (4, 94, 118, 144). Because muscle has critical roles in locomotion, respiration, and whole body metabolism, maintaining muscle mass can contribute to many aspects of improved quality of life. Most notably, the loss of muscle mass results in a loss of contractile filaments (27, 28, 153), reduced strength (75, 146), and lower power (148). Clinically, atrophy is often referred to as cachexia, the involuntary loss of muscle mass, and is often associated with wasting states such as cancer and cardiac heart failure. Additionally, atrophy can be referred to as sarcopenia, the age related loss of muscle mass.

The loss of muscle mass is indeed a major concern of atrophy; however, loss of mass alone does not explain all the negative effects of atrophy. For example, increased fatigue (160), loss of mitochondrial content (108, 156), disrupted energetics (29, 33), reduced specific force (123, 131), and impaired contractile kinetics (53, 116, 123) are all observed during atrophy but are not solely a result of the loss of mass. Therefore, any treatment designed to address any of these issues or the loss of mass may alleviate some of the burden of atrophy. There is a lack of pharmacological treatments for atrophy and only exercise has been shown to be an effective treatment for atrophy (51). For example strength/resistance training increases muscle mass (131), force (131, 148), and power (148) in conditions of atrophy. Additionally, endurance training can

improve mitochondrial content (63, 68), prevent loss of mass during atrophy (63, 64), and normalize the adenylate energy charge and ATP levels (33) in atrophying muscle.

Skeletal muscle atrophy is often comorbid with other disease and injury states such as cancer, chronic obstructive pulmonary disease (COPD), diabetes, renal failure, and sepsis as well as with disuse, starvation, and paralysis. The presence of these comorbidities makes exercise, the only known effective treatment of atrophy, difficult or impractical for the large number of people who suffer from atrophy. There are an estimated 5 million people in the US alone that suffer from severe muscle wasting or cachexia (101), 7-14 million people who suffer sarcopenia-related disability in the US and EU (51). The estimated cost of managing sarcopenia-related disability is $18.5 billion in the US alone (74). In Japan it is estimated that 8.2% of men and 6.8% of women suffer from sarcopenia (162). Therefore, the discovery of new targets to treat atrophy is of great importance in order to improve quality of life, relieve suffering, and improve outcomes of disease. Treatment of atrophy may allow for more effective or more aggressive treatment of the underlying disease.

Reduced Muscle Function/Performance

The reduced performance of the muscle during atrophy is a major impediment to the quality of life for those who suffer from atrophy. For example, the loss of muscle mass contributes to an increased fear of falling, decreased mobility, and decreased muscle performance (149). The mechanisms behind the decreased of muscle performance can begin to be unfolded by an examination of muscle contractile characteristics. There are several contractile characteristics of the muscle elicited by

both twitch (a single depolarization of the muscle) and tetanic (multiple depolarizations which summate and fuse the muscle) contractions, which become impaired when the muscle atrophies. Maximal force measurements such as absolute force (mN or g) or specific force (N/g or mN/cm^2) are reduced. The fatigability or endurance capacity of muscle is also affected by atrophy. This is often demonstrated over a series of repeated contractions where the atrophied muscle is not able to maintain the same percentage of initial force output as a control muscle. Also time dependent variables such as time to peak force, rate of force development, and rate of relaxation show impairments during atrophy. All of these factors individually diminish muscle performance but when compounded together can severely reduce quality of life.

Maximal Force. The loss of maximal force or strength has been well documented in humans under several atrophic conditions such as bed rest (8, 148), immobilization (71), cancer cachexia (157), COPD (9, 31), and diabetes (10). Additionally, loss of force has been seen in many rodent models of atrophy. For example, after two weeks of denervation (severing of the sciatic nerve) in mice, the extensor digitorum longus (EDL) lost about 20% of its tetanic force production while the soleus lost about 40% (85). Twitch tension is reduced to 55% of control after 14 days and down to 21% of control after 42 days of denervation atrophy in rats (160). In mice with cancer cachexia, tetanic force is reduced by 25% and 30% in the soleus and EDL respectively (123). The reduction in maximal absolute force during atrophy can be largely attributed to the loss of muscle mass or fiber cross sectional area. However, some loss of force cannot be explained purely by the loss of muscle mass, as evidenced by reduced specific force during atrophy.

Specific force, the force normalized to weight or cross sectional area of the muscle, can indicate whether other factors besides muscle mass are contributing to force production. A reduced specific force has been observed in mouse models of atrophy including denervation (2, 48, 76), hind limb unloading (131), and in cancer cachexia (123). While the specific mechanisms that account for this reduction in specific force are not known, it appears that the reduction in the number of available actin and myosin cross bridges is not a the only cause (48). A reduction in the specific force during atrophy indicates that the observed reduction in maximal tetanic force was due to more than just the loss of mass and may be explained by other factors such as energetics. For example, accumulation of metabolic products of ATP hydrolysis can influence force and power output of the muscle independently of changes in muscle mass. Accumulations of ADP have been shown to slow the rate of cross bridge cycling (30) and increased [P_i] can reduce peak force (37, 105).

Fatigue. The loss of endurance capacity is a common but less appreciated component of skeletal muscle atrophy. In humans, following 20 days of unilateral lower limb suspension (ULLS) there are marked decrements in endurance performance in the muscle. These participants experienced an average 11% decrease in VO_{2peak} during an exhaustive one-legged cycling test (136) when compared to the ambulatory limb. Additionally, the suspended limb reached exhaustion 10% quicker than the ambulatory limb (3). Patients with atrophy from diabetic neuropathy also exhibited increased fatigability. During a single maximal voluntary isometric contraction, force production dropped 21% more rapidly in atrophying muscles than in healthy matched controls (3). In a mouse model of cancer cachexia, the soleus muscle lost force production more

rapidly and dropped to a lower percentage of initial force than a healthy control during a 10 minute fatigue protocol (123). Additionally, in disuse models of atrophy such as denervation and hind limb unloading fatigue is also accelerated in mouse soleus (92) and in rats (53, 131, 160). The increase in fatigability during atrophy is a common component and can be dissociated from the loss of muscle mass and maximal force.

A likely factor in the increase in fatigability during atrophy is a reduction in mitochondrial content (14, 108) and function (29, 156). During atrophy mitochondria are lost at a greater rate than muscle mass, resulting in a lower mitochondrial content for a given volume of muscle (14). Furthermore, the function of the remaining mitochondria is impaired as demonstrated by decreased maximal ADP-stimulated state 3 respiration. This has been demonstrated following 3 and 7 days of hind limb unloading (18), 14 days of immobilization (98), and 7 days of denervation (106). The reduction in mitochondrial content and maximal respiration during atrophy contributes to the reduced maximal rate of ATP synthesis (29, 140). Additionally, at submaximal workloads, a smaller mitochondrial content requires a larger increase in [ADP] to elicit a given increase in mitochondrial ATP synthesis (41). As a consequence, the muscle becomes more dependent on anaerobic ATP synthesis pathways which results in more rapid fatigue.

Contraction Kinetics. The kinetics of contraction are slower during atrophy. For example, the half relaxation time (time required after stimulation for force to drop to half of maximal) is longer during denervation atrophy and cancer cachexia (2, 53, 123, 158, 160). The relaxation of the muscle is highly dependent on the ability of the sarcoendoplasmic reticulum calcium ATPase (SERCA) pump to re-sequester Ca^{2+} into the sarcoendoplasmic reticulum (SR). A slower relaxation time can be due to a change

in the composition of the SERCA isoforms or to a decrease in the activity of SERCA. Ca^{2+}clearance from the sarcoplasm was severely impaired in the flexor digitorum brevis (FDB) muscles of hind limb unloaded rats (159) as well as Ca^{2+}uptake by the SR following immobilization (146) suggesting that SERCA activity might be reduced during disuse atrophy. Changes in the composition of the SERCA pump isoforms during atrophy depends on the muscle type and model of atrophy. For example, a reduction in the content of SERCA1 (fast type) was seen in denervation in soleus muscle of rats although no change in SERCA2a (slow type) was observed (143). This isoform shift would be expected to result in a slower rate of Ca^{2+} re-sequestration and hence an increase in relaxation time. However, in contrast, there was an increase in both SERCA1 and SERCA2a in the EDL in a cancer cachexia model of atrophy (46), which may increase the rate of Ca^{2+} uptake and shorter relaxation time. While the exact mechanisms of slowed relaxation during atrophy are not known, the impairment itself may increase the energy burden for each contraction. During the relaxation phase, force production begins to drop as available myosin binding sites on the actin filaments are covered by tropomyosin. However, this process is not instantaneous, and ATP is still being consumed by the myosin ATPases through the relaxation phase, albeit at a reducing rate. The more rapidly Ca^{2+} can be re-sequestered into the SR, the more rapidly the myosin binding sites are covered and ATP usage by the myosin ATPase will decrease. Therefore, a slower relaxation time leads to more ATP consumption per contraction.

The time taken to reach peak force is also increased during both disuse and systemic atrophy (53, 123, 158). An increase in the time to peak force increases the

denominator of the power calculation (force x distance/time), and results in a reduced power output. Loss of power severely reduces performance of the muscle and increases risks for injury, especially for the elderly. For example, lower muscle power (measured by chair stand) is an independent predictor of falls and potential fractures in the elderly (103). The increase in time to peak force during atrophy may be explained by a change in the fiber type distribution of the muscle. Type II fibers have a shorter time to peak force and, thereby, are more powerful than type I fibers. A reduction of type II fibers and/or an increase in type I fibers would reduce the power output of the whole muscle. However, shifts in fiber type during atrophy are not the same between systemic and disuse types of atrophy.

There are clear shifts in fiber type during atrophy (38); however, these shifts are not the same between species, strains, muscles, or models of atrophy (25). In general during systemic atrophy conditions there is a shift in muscle fiber type from fast to slow fibers. For example, with glucocorticoid administration there is a shift from type IIb to type IIa in the masseter muscle (154). Conversely, there is an opposite shift from slow to fast fibers in disuse atrophy. In denervation-induced atrophy there is a loss of type I fibers in the rat soleus and an increase in type IIa fibers as early as 7 days post denervation but not earlier (70). However, despite direction of the fiber type shift, the contractile kinetics are impaired. It then follows that shifts in the fiber type distribution of muscle during atrophy do not adequately explain the increase in time-to-peak force.

Energetic Disruption During Atrophy

One possible explanation of impaired contractile characteristics may be a depressed energetic profile. For example, reduced [ATP] content has been reported in denervation (92) cancer cachexia (33, 46) and spinal cord contusion (140). Additionally, increased [ADP] (110), a reduced free energy of ATP hydrolysis (ΔG_{ATP}) (29, 42, 54, 77, 110, 140), and a loss of phosphocreatine (110, 140) and creatine (140) have been observed during atrophy. These energetic deficits are found in healthy, albeit atrophying, muscles which have reached a new steady-state phenotype with depressed energetics. Furthermore, a number of the contractile characteristics have been shown to be sensitive to perturbations in energetics. For example, muscle relaxation is slower in the presence of increased [ADP] (56). Additionally, high levels of [ADP] can slow cross bridge cycling, by preventing the dissociation of the myosin head from the actin filament, and thereby reduces the rate of force development (30). Elevated levels of [P_i] have been shown to reduce the peak force and power in skinned fibers (37, 105), likely because elevated P_i increases the time the cross bridge cycle spends in the low/no force phase of AM • ADP • P_i (62, 114). Taken together, it is reasonable to suspect that energetics may play a factor in some of the contractile impairments observed during atrophy.

In healthy muscle, the adenine nucleotide pool size is tightly regulated. The equilibrium reaction of the creatine kinase enzyme[1] buffers reductions in [ATP] by consuming creatine phosphate (CP) to phosphorylate ADP and form ATP. Additionally,

(1) ADP + CP → ATP + Creatine

the adenylate kinase enzyme[2] (AK), another equilibrium reaction, limits accumulation of ADP by consuming two ADP molecules to form one ATP and one AMP. Furthermore,

$$(2)\ ADP + ADP \rightarrow ATP + AMP$$

AMP deaminase[3] (AMPD) will limit AMP accumulation by degrading AMP to IMP,

$$(3)\ AMP + H_2O \rightarrow IMP + NH_3$$

displacing the equilibrium of the adenylate kinase reaction toward ATP production. All three of these reactions help to maintain the ΔG_{ATP}[4], where ΔG°_{ATP} equals -30.5 kJ/mol

$$(4)\ \Delta G_{ATP} = \Delta G^{\circ}_{ATP} + RT\ln([ADP] \bullet [P_i]/[ATP])$$

(34) during perturbations in energy demand. At rest the ΔG_{ATP} is maintained at approximately -65 kJ/mol and during intense exercise the ΔG_{ATP} can decline to -54 kJ/mol (155) in submaximal and -51 kJ/mol (56) in near maximal exercise.

A collapse of the ΔG_{ATP} is catastrophic to any living organism and is therefore tightly regulated. Even small reductions in the ΔG_{ATP}, on the order of 5 kJ/mol, have been shown to inhibit activities of key ATPases. For example, the Na/K ATPase activity is reduced and directionality can even be reversed at a reduced ΔG_{ATP} (52, 107). Likewise, under resting conditions the SERCA pump requires a large portion of the maximal yield of the ΔG_{ATP} in order to maintain the 1:10,000 Ca^{2+} gradient across the sarcoendoplasmic reticulum membrane (21, 59). Chen et al. observed in cardiac muscle the free energy requirement of the SERCA was -49.5 kJ/mol (21). Accumulation of ADP during exercise can reduce the ΔG_{ATP} and compromise the function of the SERCA pump. Reduced activity of the SERCA pump would decrease the rate of Ca^{2+} clearance from the sarcoplasm and would prolong tension development, or in other words, slow muscle relaxation. Indeed Dawson et al. observed increased relaxation times when the

ΔG_{ATP} was depressed by 15-20 kJ/mol in contracting muscle (35). If the ΔG_{ATP} were to drop far enough (to approx. -41 kJ/mol), reversal of the SERCA pump could expel Ca^{2+} into the sarcoplasm, resulting in rigor mortis and eventual death of the myofiber. Therefore, preservation of the ΔG_{ATP} during high energy demands is of utmost importance to the survival of muscle and organism.

It is clear that the function of the muscle is dramatically compromised during atrophy (reduced force, specific force, increased fatigability, slower contractile kinetics, and disrupted energetics). Although the loss of muscle mass can account for some of the contractile impairments, such as loss of maximal force, it cannot account for many others (fatigue resistance, specific force, time to peak force, half relaxation time). Energetics seemingly plays a role in some of these characteristics. Exercise, the only effective treatment of atrophy, improves the energetic profile (adenylate energy charge, [ATP], etc.) in atrophying muscle (33), however it is unknown if improvement of the energetic profile itself can improve muscle health and function during atrophy.

Loss of Muscle Mass

While there are many functional changes to the muscle during atrophy, as described above, the loss of protein and muscle mass is also of great concern. Preventing or limiting atrophy and/or increasing muscle mass may be beneficial for many who suffer from chronic disease. In a study of patients with chronic heart failure, those who also exhibited cachexia had a mortality rate of 50% within 18 months of follow-up compared to just 7% of those who did not exhibit cachexia (4). Skeletal muscle mass is also a valid independent predictor of all-cause mortality (118, 144).

Because atrophy is often comorbid with other chronic disease, treatment or prevention of muscle mass loss can allow for more effective or direct treatment of the underlying disease and help improve outcomes.

Skeletal muscle mass in adults is largely controlled by the rates of protein synthesis and protein degradation. When the balance between protein synthesis and protein degradation is shifted toward degradation, there is a net loss of protein and muscle will atrophy. There are two main pathways by which proteins are degraded, the ubiquitin-proteasome and the autophagy-lysosome system. It is widely recognized that both the ubiquitin-proteasome and autophagy-lysosome are upregulated during skeletal muscle atrophy (17, 81, 90, 106, 163), and make significant contributions to the loss of muscle mass. However, there are some who argue that it is a reduction in protein synthesis and not an acceleration of protein degradation that leads to atrophy (36, 121). This balance between protein degradation and synthesis is model specific and may differ between humans and rodents. For example, in denervation atrophy protein synthesis has been shown to increase (115). Regardless, the balance between protein synthesis and degradation is critical to maintaining healthy muscle content and treatments that target either may improve outcomes of disease.

The initial loss of muscle mass can occur rapidly as the rate of protein degradation is accelerated. For example, after just 24 hours of fasting in mice, the rate of protein degradation is increased 49% (161) and by 48 hours 14% of muscle weight can be lost (72). Additionally, 18-69 hours of mechanical ventilation was associated with a striking 50% reduction in fiber cross sectional area in the diaphragm (83). After an initial increase in protein degradation in response to the atrophy stimulus, the rate slows

until a new steady state is reached and further loss of muscle mass is minimal (130, 160). Early treatment of atrophy is therefore critical to thwart excessive loss of muscle mass.

AMPD3, a Potential Target for the Treatment of Atrophy

The signaling events that initiate muscle atrophy have received much attention in the past decade (81, 130, 134, 163). However, much still remains unknown, particularly with regards to how energetics may contribute to the activation of atrophy. It has been previously demonstrated that the disruption of the mitochondrial network can initiate atrophy (125), which suggests that impaired energetics may contribute to muscle atrophy. Furthermore, impaired energetics, whether it be lower [ATP] (46, 92, 140), increased [ADP] (110), decreased [CP] (110, 140) , or reduced ΔG_{ATP} (29, 42, 54, 77, 110, 140) has been observed in many atrophy conditions. The adenine nucleotides, and energetics in general, are known to be involved in several signaling mechanisms. For example, the AMP activated protein kinase (AMPK) is activated by AMP and is involved in several signaling cascades that regulate muscle mass (133). It is currently unknown if disrupted energetics can be an initiating event of atrophy or if it is a response to atrophy.

While there are several potential regulators of energetics only some are differentially expressed during most atrophy conditions. The atrophy process is regulated, at least in part, by a coordinated transcriptional program of atrophy related genes (atrogenes). The atrogenes consist of approximately 130 genes that are up or down regulated during several types of atrophy such as cancer cachexia, fasting,

chronic renal failure, diabetes, and denervation (81, 130), and potentially all types of atrophy. One of the most highly induced atrogenes (up to 100 fold) is AMP Deaminase isoform 3 (AMPD3) (81, 97). Additionally, others have reported increases in protein content of AMPD3 (47) as well as activity (7, 47) in denervation induced atrophy. However, reason for the upregulation of AMPD3 and its role during atrophy are completely unknown.

AMP Deaminase (AMPD) is an important energetic regulator as it helps to maintain high ratios of ATP/ADP/AMP and thus preserve the ΔG_{ATP} (55, 56). During high energy demands such as exercise, the content of AMP increases in the cell. AMPD removes AMP from the adenine nucleotide pool which in turn favors the forward direction of the adenylate kinase reaction (see equation 2). The combined actions of AMPD and adenylate kinase help to limit ADP accumulation and maintain the ΔG_{ATP}[4]. The induction of AMPD3 may be a response to the increased energetic challenge of muscle atrophy. On the contrary, increased AMPD3 may cause an energetic challenge itself by creating excessive adenine nucleotide degradation.

AMP Deaminase Isoforms

There are three different isoforms of AMP Deaminase, AMPD1, AMPD2, and AMPD3. However, in skeletal muscle only two isoforms are expressed. AMPD1 is the predominant form in muscle. AMPD3 is expressed to a lesser extent than AMPD1 but is highly upregulated during atrophy. AMPD2 protein is not found in skeletal muscle but is the predominant isoform in non-muscle tissue. The total activity of AMPD is highest in skeletal muscle, approximately 50-100 fold greater than non-muscle tissue.

The AMP Deaminases degrade AMP to IMP (see equation 3), which is central to maintaining the adenylate energy charge[5] (AEC) (19, 91) by limiting the accumulation of

(5) Adenylate Energy Charge = ([ATP] + ½ [ADP]) / ([ATP) + [ADP] + [AMP])

AMP in the muscle. In resting muscle the AEC is normally maintained around 0.8-0.9. This also serves to maintain the free energy of ATP hydrolysis, ΔG_{ATP}. In fact, removal of AMPD1 by knockout results in drop of the AEC of approximately 25% in resting soleus muscles (112).

Both AMPD1 and AMPD3 are located in the sarcoplasm and form a tetramer composed of varying amounts of each isoform (45, 47, 100). The two AMPD isoforms, 1 and 3, appear to be differentially regulated. Both have a primary binding domain within the C-terminal for actomyosin (86). AMPD1 localizes near the myosin ATPase and will bind to myosin (66). During contraction and reduced pH, AMPD1 binds to myosin and its activity is increased (40, 126, 127). The binding of AMPD1 to myosin occurs when energy demand is not balanced, such as during intense contractions, and precedes any significant accumulation of IMP (127).

Conversely, AMPD3 is more active basally and is known to bind to membranes rather than myosin. The membrane binding of AMPD3 has been attributed to the N-terminal sequence (87), which has also been shown to suppress contractile filament binding (86). When AMPD3 binds to the membrane there is a subsequent reduction in its activity (87, 111). Membrane binding of AMPD3 can be induced when pH is reduced (87, 141). In human erythrocytes, AMPD3 binds to the cytoplasmic side of the membrane with a drastic drop in activity and increase in protein stability (111).

The post-translational modifications of AMPD are not well understood. Although, protein kinase C has been shown to phosphorylate AMPD resulting in a 3-fold decrease in the K_m without affecting V_{max} (147). An additional study by Tullson et al. has confirmed phosphorylation-induced alterations in AMPD kinetics. In this study treatment of muscle homogenates with acid phosphatase resulted in removal of negative cooperativity and an increased K_m (151). Furthermore Ca^{2+} has been shown to activate AMPD3 in erythrocytes through binding of calmodulin (88).

Interestingly, an AMPD1 nonsense mutation (C34T), which results in a truncated inactive peptide, is among the most common mutations in humans. Roughly 20% of the general Caucasian population are heterozygous of the CT, and 2% are homozygous TT for the AMPD1 C34T mutation (99, 104). AMP Deaminase deficiencies or mutations have been associated with muscle weakness (44), reduced sprint performance (43) and muscle cramps (39, 44), and increased perceived exertion (122). Sprint and power type athletes are more likely to not have the C34T mutation, implying AMPD is important for intense efforts (50). However, there is some inconsistency in the symptoms with AMPD1 mutations as some patients are asymptomatic. Hanische et al. found no relationship between AMPD deficiency and exertion-induced complaints in over 400 subjects (57). Additionally, the C34T mutation did not appear to have any effect on exercise capacity in the elderly (109).

A whole body AMPD1 knockout (KO) mouse was recently generated and characterized, displaying no obvious difference in phenotype (1). Following 5 minutes of electrical stimulation of the EDL, AMPD1 knockout mice exhibit large increases in [ADP] and [AMP] and a significant drop in the adenylate energy charge compared to wild type

(WT) controls (112). The maximal tetanic force was similar between WT and AMPD1 KO in the EDL and soleus, however, the baseline force during a fatigue protocol was higher in AMPD1 KO soleus muscle compared to WT (112). An AMPD3 KO mouse also exhibits no overtly adverse phenotype but did have elevated levels of ATP in erythrocytes (22). Unfortunately, measurements of muscle contractile function and protein degradation have not been measured in the AMPD3 knockout mice.

The Role of AMPD3 in Atrophy

During denervation atrophy, content of AMPD1 remains steady or decreases slightly while AMPD3 content increases and total AMPD activity increases 34% (47). Traditionally AMPD is thought to help maintain energetics during high energy demand (55, 56, 91), hence its activation during contraction. However, the upregulation of AMPD3 during atrophy occurs when energy demand presumably is not as high as typically necessary of AMPD activity. The differential regulation of AMPD1 and AMPD3 also suggest during atrophy there may be a greater need for basal AMPD activity as evidence by the increased proportion of AMPD3 to the total AMPD activity. This increase in AMPD3 content and AMPD activity is of interest because the energetic disruption, rather than maintenance, that may result from nucleotide cycling or loss of adenine nucleotides may be a signal to induce atrophy. Currently it is unknown if AMPD3 is able to exert any influence on overall protein degradation or synthesis. Additionally, the upregulation of AMPD3 may be in response to the energetic challenge of atrophy, such as the drop in the ΔG_{ATP} (29, 42, 54, 110, 140). It's also unknown if the

upregulation of AMPD3 attenuates some of the loss of contractile function, such as increased half relaxation time, or if it contributes to contractile impairments.

Statement of the Problem

Skeletal muscle is essential for quality of life because of its critical roles in locomotion, respiration, and whole body metabolism. During atrophy, the loss of muscle mass and muscle function severely impairs the quality of life and survival rates of those who are affected. Currently, there is a lack of sufficient treatments for the loss of muscle mass or loss of muscle function during atrophy. The only known effective treatment, exercise, may be impossible or impractical for many who suffer from atrophy. One exciting potential regulator of atrophy is AMPD3, which is highly upregulated during several types of atrophy. In a healthy muscle AMPD is activated by high energy demands in order to help maintain favorable energetics. It may be the case that the upregulation of AMPD3 during atrophy may help to maintain muscle energetics and performance in a state of declining function. However, the upregulation of AMPD3 during atrophy can present a unique energy challenge to the muscle by creating a drain on the total adenine nucleotide pool, which may contribute to activation of protein degradation. This dissertation will address some of the effects of AMPD3 upregulation on skeletal muscle as the role of AMPD3 during atrophy is currently unknown.

Chapter Two

AMP Deaminase 3 upregulation during skeletal muscle atrophy improves muscle relaxation in mouse soleus

Abstract

Skeletal muscle atrophy severely impairs contractile function of muscle making tasks of daily living more difficult and results in a loss of quality of life. The purpose of this study was to determine whether the upregulation of AMPD3 during atrophy improved relaxation time of muscle, which is sensitive to reductions in the free energy of ATP hydrolysis, during intense contractions. AMPD3 was knocked down by RNAi during denervation-induced atrophy or overexpressed in the mouse soleus. Following one week of denervation or overexpression, soleus muscles were removed and electrically stimulated and contractile function measured. One week of denervation resulted in a 20% loss of mass and an increase in AMPD3 protein expression of 67%. Knockdown of AMPD3 during denervation reduced AMPD3 by 60%. Denervation reduced AMPD1 protein expression by 36%. Half relaxation time in denervated muscles is shorter during high intensity fatiguing contractions. Knock down of AMPD3 in denervated muscles resulted in a 33% increase in half relaxation time during high intensity contractions. Denervation increased tetanic half relaxation time from 0.041 to 0.049 ms and knockdown of AMPD3 further increased half relaxation time to 0.054 ms. SERCA1 and SERCA2 protein content were not different with denervation or knockdown. Low intensity contractions did not alter half relaxation time of the soleus muscles nor did overexpression of AMPD3 in non-atrophying muscles. Our results suggest that the

upregulation of AMPD3 during skeletal muscle atrophy improves muscle relaxation during high intensity fatiguing contractions. AMPD3 may attenuate some of the loss of muscle power and performance common to atrophy.

Introduction

Skeletal muscle atrophy is common to many different disease states such as cancer, renal failure, and diabetes as well as during starvation, disuse, and denervation. During skeletal muscle atrophy, muscle function and power are dramatically impaired, making tasks of daily living more difficult (73), increases risk of falls in the elderly (103), and results in a loss of quality of life (137). Most notably, maximal force is reduced, which can be largely attributed to the overall loss of muscle mass/cross sectional area (2, 5, 123). However, other impairments are evident. For example, in cancer cachexia and denervation induced atrophy, specific force (2, 65, 102), half relaxation time (2, 53, 65, 116), and time to peak force (53, 123) are also impaired, all of which contribute to reduced muscle power output. The mechanisms that account for these impairments during atrophy are currently unknown.

A possible explanation of impaired contractile characteristics may be the depressed energetic profile of atrophy. For example, during several types of atrophy there is a net loss of [ATP] (33, 46, 92, 140), increased [ADP] (110), reduced free energy of ATP hydrolysis (ΔG_{ATP}) (29, 42, 54, 77, 110), and a loss of phosphocreatine (CP) (110, 140) and creatine (140). These energetic deficits are found in healthy, albeit atrophying, muscles that have reached a new steady-state phenotype. Furthermore, a number of the contractile characteristics have been shown to be sensitive to perturbations in energetics. For example, half relaxation time is greater in the presence of increased [ADP] and reduced ΔG_{ATP} (56). Additionally, high levels of [ADP] can slow cross bridge cycling and the time to peak force (30). Elevated levels of P_i have been shown to reduce the peak force and power in skinned fibers (37, 105). It is therefore

reasonable to suspect that energetics may play a factor in some of the contractile impairments observed during atrophy.

Skeletal muscle maintains favorable energetics during high energy demands, when ATP consumption outpaces ATP production, by the concerted actions of adenylate kinase (AK: ADP + ADP → ATP + AMP) and AMP Deaminase (40, 91). Removal of AMP by AMP Deaminase (AMPD: AMP + H_2O → IMP + NH_3) favors ADP clearance and ATP production by AK. Taken together, these enzymes preserve the ΔG_{ATP} because they limit ADP accumulation and promote ATP production. However, the cost of sustained AMPD activity is an overall loss of adenine nucleotides, which can be resynthesized only during recovery (16, 150). During skeletal muscle atrophy, AMPD, specifically isoform 3 (AMPD3), is highly upregulated (47, 81, 97), while AMPD1 content remains stable, and results in an increase in total AMPD activity (47). Currently the effects of AMPD3 upregulation during atrophy on muscle function are unknown.

In the present study, we sought to investigate the role of increased expression of AMPD3 on energetics and contractile characteristics of skeletal muscle during atrophy. We used short hairpin RNA (shRNA) to knockdown AMPD3 protein in mouse soleus muscle during denervation-induced atrophy. Because of the increased AMPD activity during atrophy and the importance of AMPD activity in maintaining the ΔG_{ATP}, we hypothesized that knockdown of AMPD3 during atrophy would result in impairments of muscle half relaxation time which is sensitive to the ΔG_{ATP}.

Methods

Expression Plasmid and shRNA Generation

Plasmid encoding mouse AMPD3 was purchased from Open Biosystems and subcloned into the CMV driven pIRES-hrGFP II vector (Agilent Technologies). The empty pIRES-hrGFP II vector was used as a control. To knockdown AMPD3 protein, we designed three different shRNA oligos against mouse AMPD3 (Table 1) using Invitrogen's web based RNAi designer (https://rnaidesigner.lifetechnologies.com/rnaiexpress/) and inserted them into pcDNA 6.2-GW/EmGFP-miR vector using Invitrogen's BLOCK-iT RNAi Expression Vector Kit with EmGFP. A negative control plasmid (shNEG) containing a hairpin forming sequence that is designed to not target any vertebrate genes (5'-GAAATGTACTGCGCGTGGAGACGTTTTGGCCACTGACTGACGTCTCCACGCAGTACATT-3') was provided with the kit and was used as a negative control. To test the efficacy of the knockdown, each plasmid was transfected into C2C12 myoblasts using FuGene 6 (Promega). mRNA was extracted with Trizol Reagent (Thermo Fischer) and real time PCR done for AMPD3 normalized to RPLPO using SybrGreen (Thermo Fischer). The shRNA plasmid with the greatest knockdown effect was used in all subsequent experiments (shAMPD3).

Animal Procedures

Adult male CD-1 mice were purchased from Charles River (Raleigh, NC) and housed in Association for Assessment and Accreditation of Laboratory Animal Care approved housing. Mice were approximately 30 grams at the time of muscle collection. They were housed 4 mice per cage, and given free access to food and water and a 12

hr light/dark cycle. All animal procedures were approved by the East Carolina University Animal Care and Use Committee.

Expression or shRNA plasmids were transferred into skeletal muscle by electroporation, as done previously (14). In brief, mice were anesthetized with isoflurane (2-3%) in oxygen and an incision was made in the anterior lower hind limb allowing access to the soleus muscle. Plasmid DNA (0.5 μg/μl knockdown plasmids, 1.0 μg/μl overexpression plasmids) was injected lengthwise into the soleus (10 μl), using a Hamilton microliter syringe. Electrical pulses were applied using BTX ECM 830 electroporator (Holliston, MA) as the muscle was sandwiched between two opposing stainless steel paddles (10 volts, 5x20 ms pulses at 250 ms intervals). Incisions were closed with Vicryl (polyglactin 910) sutures.

Atrophy was induced by sciatic nerve sectioning as done previously at the same time as electroporation (14). An incision was made in the lateral mid-thigh of the hind limb. The sciatic nerve was exposed by blunt dissection and a 2-3 mm section was removed. Sham operation on the contralateral limb was done to expose the sciatic nerve without sectioning the nerve. The incisions were closed with surgical glue, and buprenex (0.03 mg/kg body weight) was administered sub-cutaneously as a post-operative analgesic.

Muscle Contraction

Mice were anesthetized with isoflurane and euthanized by cervical dislocation. The proximal and distal tendons of soleus muscles were ligated with 2.0 silk sutures and placed in oxygenated (95% O_2, 5% CO_2) Krebs-Henseleit bicarbonate buffer (25 mM $NaHCO_3$, 118 mM NaCl, 4.7 mM KCl, 1.2 mM $MgSO_4 \cdot 7H_2O$, 1.2 mM KH_2PO_4, 1.2

mM $CaCl_2$•$2H_2O$, 5 mM glucose, 0.15 mM sodium pyruvate) at their approximate in vivo resting length. Muscles were maintained in the Krebs-Henseleit buffer at 37°C for approximately 40 minutes prior to contractile measurements.

Muscles were secured to a dual mode force transducer (Aurora Scientific) and field-stimulated via platinum electrodes (Aurora Scientific). Optimal length was determined using 0.3 ms pulses and the length tension relationship. Following another 5-10 minute rest period, muscles were either subjected to a high intensity (150 Hz pulse frequency, 500 ms train duration, 1 train per second, for 60 seconds) or low intensity (50 Hz pulse frequency, 250 ms train duration, 1 train every 2 seconds, for 600 sec) contraction protocol using 610A DMC v5.4 (Aurora Scientific) or kept at their resting length for approximately 5 additional minutes. Muscles were then rapidly cut from sutures, blotted dry, and snap frozen between liquid nitrogen cooled tongs. Contraction characteristics were analyzed using 611A DMA software v5.2 (Aurora Scientific). Each contraction was analyzed individually using the high throughput feature. For measurements of half relaxation time, the window for analysis was set to start with the last electrical pulse of each stimulation train and end just prior to the next stimulation. Force-time integral is the area under the force-time curve for each contraction.

Protein Analysis

Muscles were homogenized using Bio-Gen PRO200 Homogenizer (Pro Scientific, Oxford, CT) and proteins extracted in a RIPA Buffer (1% NP-40, 0.5% Sodium Deoxycholate, 0.1% SDS, 50 mM Tris-HCl, 50 mM NaF, 5 mM Sodium Pyrophosphate, 2 mM Sodium Orthovanate) containing a protease inhibitor cocktail (Roche Complete). Total protein content was determined by BCA assay (Pierce) using

bovine serum albumin as a standard. Equal amount of protein were separated by SDS-polyacrylamide gel electrophoresis then transferred to polyvinylidene difluoride (PVDF) membranes. Equal loading and even transfer were confirmed by Ponceau S staining of membranes. Antibodies were purchased from abcam (AMPD3: ab118230, SERCA2: ab3625), Thermo Scientific (AMPD1: PA5-23172) and the Developmental Studies Hybridoma Bank (SERCA1: CaF2-5D2). Secondary antibodies conjugated to HRP (Cell signaling-7074S, Thermo Scientific-31441) were used and identified using Western Chemiluminesce HRP Substrate from EMD Millipore. Band intensities were captured using a Bio-Rad Chemi Doc XRS imager and analyzed using Image Lab software (Bio-Rad) with weights calculated from Pageruler Plus protein ladder (ThermoFisher).

Nucleotide Measurements

Nucleotides were extracted from muscles by homogenization (glass-on-glass) in ice-cold 0.5 N perchloric acid. Extracts were neutralized by addition of ice-cold KOH and centrifugation at 4°C. Samples were stored at -80°C until analysis. The concentration of adenine nucleotides (ATP, ADP, AMP) and degradation products (IMP, adenine, and inosine) were determined by ultra-performance liquid chromatography (UPLC) using a Waters Acquity UPLC H-Class system as done previously (15).

Statistical Analysis

All data are expressed as mean ± standard error of the mean. Significant differences were assessed using repeated measures two-way ANOVA (for comparisons including muscle fatigue protocols and protein content), two-way ANOVA (for comparisons of tetanic contraction characteristics and nucleotides), one-way ANOVA (for comparisons of rates of fatigue), and t-test (for comparing AMPD3 overexpression,

max force and half RT). If significance was detected by ANOVA, Sidak or Tukey's post hoc analysis was used for multiple comparisons. All analyses were performed using GraphPad Prism for Windows, version 6.05 with the alpha level set at $p<0.05$ to detect significance.

Results

Knockdown of AMPD3 during denervation atrophy.

Three different plasmids were initially tested for knockdown of AMPD3 (Table 2.1). Protein degradation was induced in cultured C2C12 myoblasts by serum starvation, as done previously (13), which increased AMPD3 mRNA expression by 3.3 fold (Figure 2.1). shRNA plasmid A had no effect on AMPD3 mRNA. However, plasmid B prevented the serum starvation induced increase in AMPD3 mRNA ($p<0.01$) but did not knock AMPD3 down basally. Plasmid C had the best knockdown effect with a significant main effect of AMPD3 knock down and was used in all subsequent experiments (hereafter referred to as shAMPD3).

To determine the extent by which our knockdown plasmid (shAMPD3) can decrease AMPD3 in adult muscles, soleus muscles were electroporated with shNEG or shAMPD3 at the same time as sciatic nerve sectioning. One week after denervation/electroporation, the AMPD3 protein content was significantly less in muscles treated with shAMPD3 compared to those treated with shNEG ($p<0.01$ main effect) (Figure 2.2A). Tukey corrected multiple comparisons showed significant differences between shAMP3 and shNEG in denervated legs. Knockdown of AMPD3 did not affect AMPD1 protein levels but AMPD1 protein content was reduced during atrophy ($p<0.05$) (Figure 2.2B), which supports other findings that there appears to be a shift in the ratio of AMPD isoforms from AMPD1 to AMPD3 during atrophy (47).

Denervation results in a complete loss of motor control of the lower limb muscles and represents a severe type of inactivity. One week of denervation resulted in a significant loss of muscle mass in the soleus ($p<0.0001$) compared to the innervated

muscle (Figure 2.2D). There was a 22% loss of muscle mass in shNEG solei and a 19% loss of muscle mass in shAMPD3 solei but there was no significant difference between shNEG and shAMPD3.

Adenine Nucleotides.

AMPD degrades AMP (AMP + $H_2O \rightarrow$ IMP + NH_3) and thereby functions as a regulator of the total adenine nucleotide pool (ATP + ADP + AMP) (132, 152). To determine if a reduced amount of AMPD3 may alter the adenine nucleotide pool in resting muscle, we measured the concentration of adenine nucleotides (ATP, ADP, and AMP) and degradation products (IMP and adenine) in homogenates of muscles that were collected in the resting/pre-contracted state. There were no significant differences detected in metabolites between innervated and denervated muscles nor was there any effect of AMPD3 knockdown (Table 2.2). However, there was a trend of reduced [ATP] in shAMPD3:Innervated.

Characteristics of Single Tetanic Contractions.

To determine whether AMPD3 affects contractile characteristics, soleus muscles electroporated with shAMPD3 were isolated and electrically stimulated in vitro. In response to a single tetanic contraction, muscles with knockdown of AMPD3 produced significantly greater max force ($p<0.05$) (Figure 2.3A). However, the differences in force output were eliminated when normalized to muscle mass i.e., the specific force did not differ between groups (Figure 2.3B). The half relaxation time (Figure 2.3C) was significantly longer in denervated muscles ($p<0.0001$ main effect) as well as in muscles that had AMPD3 knocked down ($p<0.05$ main effect). Between the two denervated groups, knockdown of AMPD3 significantly increased half relaxation time ($p<0.05$).

Additionally, there was a main effect of AMPD3 knockdown to increase the force-time integral ($p<0.05$) (Figure 2.3D), which is consistent with the increased force and longer half relaxation time.

High Intensity Contractions.

AMP deamination is expected to be most active during periods of high energy demand (126, 127). Therefore, a high intensity fatigue protocol (150 Hz pulse frequency, 500 ms train duration, 1 train per second, for 60 seconds) was used to create an energy demand that would result in AMP production and thus high levels of AMPD activity. Solei of all groups fatigued to approximately 25-30% of their initial force by 60 seconds (Figure 2.4A). A linear regression for each group was calculated from 5-15 seconds to determine the rate of fatigue. These time points were chosen because force was decreasing in all groups after 5 seconds and there was a visual inflection point around 15 seconds in both denervated groups. The rate of fatigue (Figure 2.4B) was greater in the denervated muscles compared to the innervated ($p<0.001$ main effect). Between the two knockdown groups, the denervated muscle had a significantly greater rate of fatigue compared to innervated ($p<0.05$).

The relaxation rate of muscle is largely dependent on the ability of the sarcoendoplasmic reticulum calcium ATPase (SERCA) to re-sequester Ca^{2+} into the endoplasmic reticulum. SERCA can become less active when the ΔG_{ATP} is reduced (21, 35), such as during high energy demands. Because the relationship between relaxation rate and the ΔG_{ATP} as well as the role of AMPD in maintaining the ΔG_{ATP}, we examined the half relaxation time of each contraction during the fatigue protocol. Knockdown of AMPD3 significantly increased half relaxation time in both the denervated and

innervated muscles for roughly the last 10 and 20 contractions respectively, compared to the innervated group (Figure 2.4C). When comparing the two denervated groups, knock down of AMPD3 resulted in an approximately 33% longer half relaxation time for each of the last 30 contractions (0.071 ms vs. 0.053 ms by 30 seconds and 0.087 ms vs. 0.066 ms by 60 seconds). However, there was no significant difference between the two knockdown groups.

Increases in the half relaxation time might be explained by a reduced total SERCA protein content or by shifts between isoforms of SERCA. To test for this we blotted for SERCA 1 and SERCA 2 in muscle homogenates. Neither denervation nor knockdown of AMPD3 altered SERCA 1 or SERCA 2 protein content (Figure 2.5). Because SERCA activity can be altered by the energetic state of the muscle, we measured nucleotides in muscles immediately post-contraction. Following the high intensity protocol, [ATP] was significantly reduced and [IMP] was significantly increased (Table 2.3). The increase in [AMP] was did not reach statistical significant ($p=0.059$). However, there were no significant differences in the metabolites between innervated and denervated muscles nor was there any effect of AMPD3 knockdown. The contraction protocol was sufficiently intense to cause a loss of total adenine nucleotides.

Low Intensity Contractions.

During high energy demands, which fatigue muscles to 20-25% of initial force by 60 seconds, knockdown of AMPD3 resulted in longer half relaxation times of the muscle, so we next tested if the same would be true during a lower energy demand. A low intensity fatigue protocol (50 Hz pulse frequency, 250 ms train duration, 1 train every 2 seconds, for 600 sec) fatigued muscles to approximately 50% of initial force by

600 seconds (Figure 2.6A). The rate of fatigue calculated between 10 and 200 seconds in the two denervated groups was significantly higher compared to both the innervated and shAMPD3 groups ($p<0.0001$) (Figure 2.6B). Rate of fatigue did not differ between the two innervated groups. The half relaxation time during the low intensity protocol did not differ significantly between groups (Figure 2.6C). Following low intensity contractions there was a significant increase in [IMP] (Table 2.4) in denervated muscles compared to innervated muscles($p<0.05$), however, there was no effect of knockdown on IMP levels.

Overexpression of AMPD3.

It is unclear if the effects of AMPD3 knockdown we observed during atrophy are dependent on other factors associated with atrophy such as other atrogenes, or if AMPD3 acts independently. Therefore, we over expressed AMPD3 in non-atrophying soleus muscles and subjected them to the same high intensity contraction protocol as the atrophying muscles. Electroporation of plasmid encoding AMPD3 in solei resulted in a 16 fold increase in AMPD3 protein compared to electroporation of a GFP encoding plasmid (Figure 2.7A). Despite this increase in AMPD3 protein, there was no difference in tetanic maximum force or half relaxation time in GFP vs AMPD3 (Figure 2.7B,C). Additionally, during high intensity fatiguing contractions there was no differences in fatigue or half relaxation (Figure 2.7D, E). There was a significant loss of [ATP] and increase in [ADP], [AMP], and [IMP] following contraction (Table 2.5). However, there was no effect of AMPD3 overexpression on any nucleotides.

Discussion

In this study we tested the hypothesis that knockdown of AMPD3 during atrophy would result in impairments of muscle half relaxation time. Indeed, knockdown of AMPD3 in denervated soleus muscles increased half relaxation time of a single tetanic contraction and during high intensity fatiguing contractions while there was no change in SERCA. We did not detect any significant differences of AMPD3 knockdown on nucleotides in resting or contracted muscle, although this does not rule out transient changes during intense contractions. Therefore we conclude that upregulation of AMPD3 during atrophy improves the half relaxation time of the soleus muscle in mice.

Atrophying muscles have an upregulation of AMPD3 and have been shown to have an increased half relaxation time (2, 53, 123, 158). Our study agrees with these previous findings (Figure 2.3C) and extends previous findings to demonstrate that half relaxation time actually is reduced in denervated muscle by 5 seconds of high intensity fatiguing contractions (Figure 2.4C). When the upregulation of AMPD3 during atrophy is prevented by shRNA, the half relaxation time is roughly 33% longer by the time the muscle fatigues to 35% of initial force. These finding indicate that the upregulation of AMPD3 during atrophy improves relaxation kinetics of the muscle during high intensity contractions.

Muscle relaxation is dependent on Ca^{2+} dissociation from troponin c which will then cover the myosin binding site on actin and prevent cross bridge formation. Slowed relaxation of the muscle likely suggests that Ca^{2+} handling has been decelerated. For example, reduced activity of SERCA would prolong Ca^{2+} re-sequestration and lengthen the duration of the contraction (35). This could easily be explained by a reduction in

SERCA protein content, or even a shift from the fast (type 1) toward the slow (type 2) isoforms. Our findings with one week of denervation atrophy do not demonstrate any reduction in SERCA protein content or a shift between the two different isoforms, which agrees with the one week findings of Schulte et al. (139). Therefore, the slowing of relaxation cannot be explained by SERCA protein content in this study.

A likely explanation for the slowed relaxation of muscles while AMPD3 is knocked down could be reduced SERCA activity due to a reduced ΔG_{ATP}, which would increase the Ca^{2+} transit time and prolong muscle relaxation. SERCA requires a large yield of the ΔG_{ATP} to maintain the ~1:10,000 Ca^{2+} gradient across the endoplasmic reticulum (21, 59). Previous observations put the free energy requirement of the SERCA (ΔG_{SERCA}) around 50 kJ/mol (21, 59, 80), while ΔG_{ATP} in resting muscle typically yields -60-65kJ/mol (21, 56). This small difference in the energy requirements of SERCA and available energy from ATP hydrolysis highlights how important maintenance of the ΔG_{ATP} is to preserve normal function of the muscle. Even with small reductions in the ΔG_{ATP} (<5 kJ/mol), Dawson et al. saw slowed relaxation in frog skeletal muscle (35). Additionally, slowed relaxation has been observed in mice lacking the adenylate kinase enzyme during a high intensity contraction protocol with a calculated ΔG_{ATP} of -45.6 kJ/mol (56), which is below the requirement for the SERCA pump. Knockdown of AMPD3 would be anticipated to reduce total AMPD activity, which during high energy demands would increase [AMP] content as well as [ADP] content via product inhibition of the AK reaction, the result would be a drop in the ΔG_{ATP}. Taken together, our results indicate that knockdown of AMPD3 in both innervated and denervated muscle slows

muscle relaxation during high intensity contractions, likely as a result of a reduced ΔG_{ATP} and reduced SERCA activity.

The nucleotide measurements taken following the high intensity contraction protocol (Table 2.3) show a significant loss of [ATP] and increase in [IMP] indicating that AMPD was active during the protocol. The high intensity protocol that we utilized had a 50% duty cycle whereas the protocol in a study by Hancock et al., that elicited a drop in the ΔG_{ATP} to -52 kJ/mol, had a less intense 20% duty cycle (56). While we were not able to calculate the ΔG_{ATP} in our muscles because the phosphocreatine peak was not clearly resolved, it's likely that the ΔG_{ATP} in these muscles was substantially reduced below resting levels based on the measurement by Hancock et al. from a less intense fatigue protocol.

The increase in half relaxation of a single tetanic contraction (Figure 2.3C) during atrophy is consistent with the previous literature (2, 53, 123, 158). This seems to be due to factors of Ca^{2+} handling unrelated to the energetic state of the cell, as we did not detect any differences in the nucleotides of the resting muscles (Table 2.2). A possible explanation of the increased relaxation time could be partially depolarized mitochondria during atrophy which have been shown to contribute to dysfunctional Ca^{2+} clearance from the sarcoplasm (159). Decreases in parvalbumin can impair Ca^{2+} clearance but this is an unlikely factor in the soleus muscle since there is little parvalbumin in type I fibers (60).

The increase in AMPD3 protein we observed during denervation atrophy is consistent with previous findings (7, 23, 47, 81). The AMPD enzyme in muscle is made up of a tetramer of AMPD proteins which can vary in composition of AMPD1 and

AMPD3 (47, 58). The reduction in AMPD1 and increase in AMPD3 protein content we observed suggests a shift to a greater reliance on AMPD3 for total AMPD activity during atrophy and is consistent with the findings of Fortuin et al (47). Increased AMPD activity during atrophy could lead to excessive adenine nucleotide degradation which may result in a loss of adenine nucleotides. Because of this we anticipated that in the AMPD3 overexpressing and resting denervated muscles we would observe a reduction of total adenine nucleotides while knockdown of AMPD3 in denervated muscles would attenuate this loss. Although we were not able to detect a significant loss of adenine nucleotides it is likely that during rest there may not be enough energy demand to create [AMP] in sufficient quantities for increased AMPD activity; therefore net degradation of the adenine nucleotide pool would not occur. This finding (Table 2.2) is supported by Hancock et al. who observed no change in total adenine nucleotides in AK knockout mice under resting conditions (56) which further suggests that AMPD may be most important during high energy demands.

When energy demand was increased by electrical stimulation and muscles were fatigued, we did observe a loss of total adenine nucleotides and an increase in [IMP] (Tables 2.3, 2.4) in both the high and low intensity protocols as compared to the resting values, which is in agreement of the observations of others (61, 95). Following the low intensity fatigue protocol the loss of adenine nucleotides was greater than during the high intensity protocol. Additionally, [AMP] was significantly elevated following the low intensity protocol, whereas the increase was not significant ($p=0.059$) in the high intensity protocol. This is likely an effect of the duration of the protocol where there was more time for [AMP] degradation than in the short (60 second) high intensity protocol.

We did not see any differences in nucleotides in denervated or AMPD3 knocked down muscles. This was surprising as we anticipated an increased [IMP] formation and greater loss of adenine nucleotides in the denervated muscle (which has higher AMPD3 content), with attenuation of these measures in the AMPD3 knockdown muscle. One possible explanation of why we did not see any changes in nucleotides between groups following fatiguing contractions is because at the time point of measurement, ATP supply and demand had been matched and the need for AMP deamination was reduced. By 60 seconds in our high intensity protocol and 10 min in our low intensity protocol the muscles were no longer fatiguing as indicated by maintenance of force production. At this point ATP consumption would have had to drop to a level that was met by ATP supply and the need for AMP deamination was likely minimal. In support of this, Hancock et al. observed in AK null mice, a transient increase in 5% relaxation time that returned to control levels during a high intensity fatigue protocol (56). Future studies will need to address the kinetics of the adenine nucleotide pool degradation during repeated fatiguing contractions, perhaps by ^{31}P-NMR.

Overexpression of AMPD3 in non-atrophying muscle had no measurable effects on any of the contractile characteristics (Figure 2.7) or on adenine nucleotide degradation (Table 2.5). It is likely that there are other factors associated with atrophy that are necessary to enable the AMPD3 induced improvement of muscle relaxation. One possible factor could be the protein IMP dehydrogenase 2 (IMPDH2) which is also an atrogene, and upregulated during atrophy (81, 130). IMPD2 degrades IMP, the product of the AMPD reaction, and would favor an increase in AMPD activity by reducing product inhibition. Future studies could overexpress IMPD2 along with AMPD3

in muscle to determine if upregulation of the two enzymes are necessary to improve muscle relaxation.

In summary our results indicate that the upregulation of AMPD3 during atrophy leads to a shortening of muscle relaxation kinetics during high intensity contractions. The improvement in muscle relaxation is likely due to improved ΔG_{ATP} which is better able to support higher levels of SERCA activity during the high energy demand. These findings have implications for most if not all types of atrophy since AMPD3 is upregulated in many types of atrophy (81).

Tables and Figures

Table 2.1. Primers used to generate AMPD3 knockdown plasmids 5’ to 3’.

A Forward	TGCTGTTTACCAGGAGGCTAGCTGTAGTTTTGGCCACTGACTGACTACAGCTACTCCTGGTAAA
A Reverse	CCTGTTTACCAGGAGTAGCTGTAGTCAGTCAGTGGCCAAAACTACAGCTAGCCTCCTGGTAAAC
B Forward	TGCTGTACTCAGGCATAGCATAGGGTGTTTTGGCCACTGACTGACACCCTATGATGCCTGAGTA
B Reverse	CCTGTACTCAGGCATCATAGGGTGTCAGTCAGTGGCCAAAACACCCCTATGCTATGCCTGAGTAC
C Forward	TGCTGTTGAGATTTCTTCAGAGGCGTGTTTTGGCCACTGACTGACACGCCTCTAGAAATCTCAA
C Reverse	CCTGTTGAGATTTCTAGAGGCGTGTCAGTCAGTGGCCAAAACACGCCTCTGAAGAAATCTCAAC

Table 2.2. Nucleotides in resting soleus muscles

	n	ATP	ADP	AMP	IMP	Adenine	TAN + IMP
Innervated	8	3.90 ± 0.53	1.10 ± 0.15	0.040 ± 0.004	0.012 ± 0.002	0.022 ± 0.004	5.053 ± 0.683
Denervated	7	3.45 ± 0.76	1.02 ± 0.21	0.041 ± 0.004	0.014 ± 0.003	0.020 ± 0.004	4.522 ± 0.970
shAMPD3:Innervated	10	2.79 ± 0.28	0.87 ± 0.09	0.051 ± 0.016	0.030 ± 0.010	0.014 ± 0.002	3.739 ± 0.350
shAMPD3:Denervated	10	4.00 ± 0.60	1.17 ± 0.17	0.049 ± 0.010	0.017 ± 0.003	0.021 ± 0.004	5.237 ± 0.779

Values are expressed as µmol/g. Means ± SEM. TAN=Total Adenine Nucleotides

Table 2.3. Nucleotides in high intensity contracted soleus muscles

Treatment	n	ATP*	ADP	AMP	IMP**	Adenine	TAN + IMP
Innervated	10	2.75 ± 0.33 (-1.15)	1.04 ± 0.15 (-0.06)	0.067 ± 0.020 (0.027)	0.292 ± 0.099 (0.280)	0.017 ± 0.003 (0.005)	4.170 ± 0.563 (-0.883)
Denervated	11	2.27 ± 0.46 (-1.16)	0.82 ± 0.11 (-0.19)	0.055 ± 0.009 (0.015)	0.279 ± 0.092 (0.265)	0.013 ± 0.001 (0.007)	3.477 ± 0.553 (-1.045)
shAMPD3:Innervated	10	2.36 ± 0.25 (-0.43)	0.95 ± 0.08 (-0.08)	0.065 ± 0.015 (0.014)	0.205 ± 0.037 (0.175)	0.016 ± 0.003 (-0.002)	3.578 ± 0.357 (-0.161)
shAMPD3:Denervated	10	2.60 ± 0.21 (-1.40)	1.14 ± 0.17 (-0.03)	0.067 ± 0.012 (0.018)	0.372 ± 0.130 (0.355)	0.017 ± 0.002 (0.004)	4.197 ± 0.474 (-1.040)

Values are expressed as µmol/g. Means ± SEM. TAN = Total Adenine Nucleotides. Values in ( ) indicate difference from resting levels (Table 2). *p<0.01, **p<0.0001 main effect from resting values.

Table 2.4. Nucleotides in low intensity contracted soleus muscles

	n	ATP‡	ADP†	AMP‡	IMP*‡	Adenine	TAN + IMP‡
Innervated	9	1.77 ± 0.34 -(2.13)	0.77 ± 0.19 -(0.33)	0.074 ± 0.022 (0.034)	0.227 ± 0.093 (0.215)	0.010 ± 0.002 -(0.012)	2.847 ± 0.680 -(2.206)
Denervated	9	1.41 ± 0.08 -(2.04)	0.62 ± 0.05 -(0.4)	0.069 ± 0.011 (0.028)	0.476 ± 0.093 (0.462)	0.009 ± 0.001 -(0.011)	2.582 ± 0.212 -(1.940)
shAMPD3:Innervated	7	1.93 ± 0.50 -(0.86)	0.84 ± 0.23 -(0.03)	0.097 ± 0.021 (0.046)	0.302 ± 0.103 (0.272)	0.011 ± 0.003 -(0.003)	3.178 ± 0.833 -(0.561)
shAMPD3:Denervated	7	1.76 ± 0.16 -(2.24)	0.76 ± 0.06 -(0.38)	0.097 ± 0.017 (0.048)	0.542 ± 0.077 (0.525)	0.015 ± 0.001 -(0.006)	3.155 ± 0.255 -(2.082)

Values are expressed as µmol/g. Means ± SEM. TAN=Total Adenine Nucleotides. Values in ( ) indicate difference from resting levels (Table 2). * $p<0.05$ main effect of denervation. †$p<0.05$ ‡$p<0.001$ main effect from resting values

Table 2.5. Nucleotides in high intensity contracted AMPD3 overexpressing soleus muscles

	n	ATP*	ADP*	AMP**	IMP**	Adenine	TAN + IMP
GFP Resting	7	2.55 ± 0.19	0.64 ± 0.05	0.024 ± 0.002	0.018 ± 0.004	0.017 ± 0.001	3.22 ± 0.230
GFP Contracted	9	2.23 ± 0.13	0.82 ± 0.04	0.039 ± 0.003	0.220 ± 0.031	0.015 ± 0.001	3.308 ± 0.178
AMPD3 Resting	5	2.57 ± 0.24	0.66 ± 0.07	0.025 ± 0.003	0.017 ± 0.002	0.017 ± 0.001	3.269 ± 0.303
AMPD3 Contracted	10	1.99 ± 0.20	0.72 ± 0.07	0.035 ± 0.002	0.184 ± 0.026	0.016 ± 0.001	2.930 ± 0.291

Values are expressed as µmol/g. Means ± SEM. TAN=Total Adenine Nucleotides. Main effect of contraction * $p<0.05$ ** $p<0.0001$

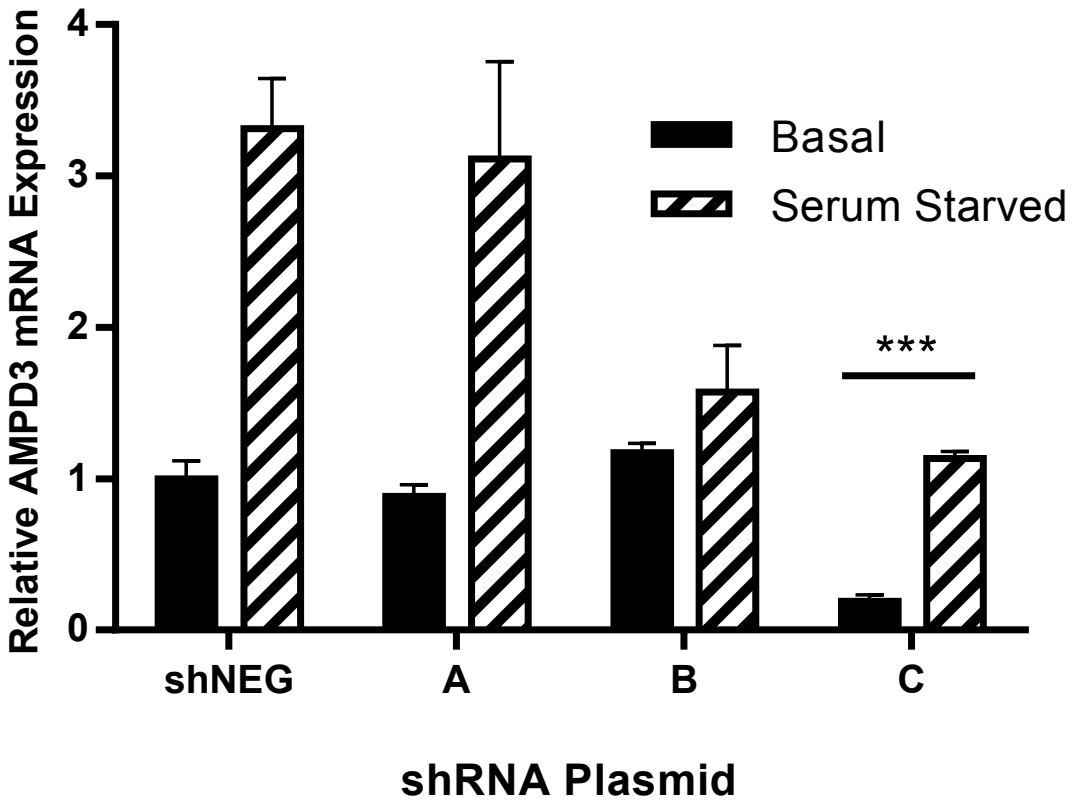

Figure 2.1. AMPD3 expression with shRNA transfection. C2C12 myoblasts were transfected with 3 shRNA plasmids targeted to AMPD3 or a negative control. Culture media was replaced with serum free media for 18 hours to simulate atrophy and induce AMPD3 expression. Means ± SEM. n=3. ***p<0.001 vs shNEG

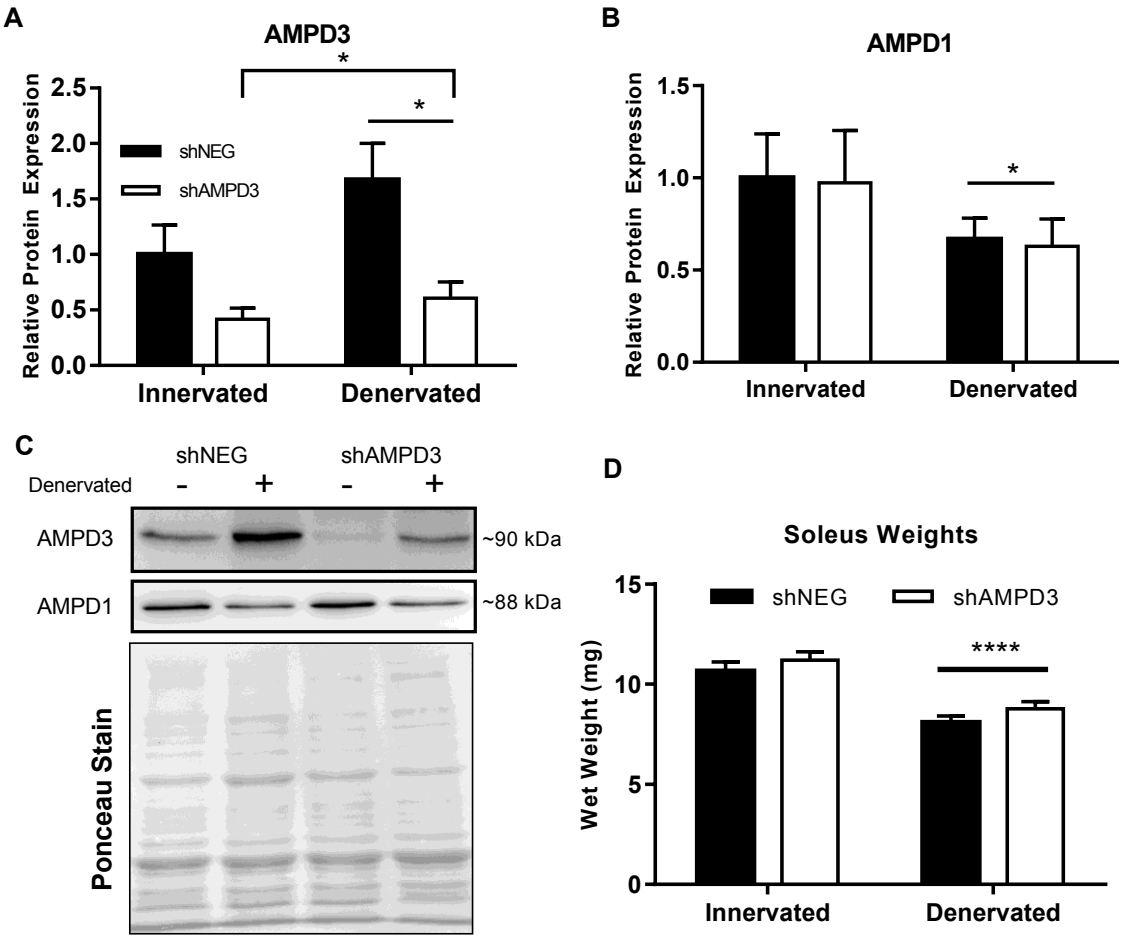

Figure 2.2. Knockdown of AMPD3 reduces AMPD3 protein content. Mouse soleus muscles were electroporated with shAMPD3 or shNEG concurrent with unilateral lower limb denervation. (A) Soleus wet weights after 1-week of denervation (B) AMPD3 protein content relative to shNEG:Innervated. n=7 shNEG, 8 shAMPD3 (C) AMPD1 protein content relative to shNEG:Innervated. n=7 shNEG, 8 shAMPD3 (D) representative western blot of images of AMPD3 and AMPD1 protein expression and Ponceau S staining. Means ± SEM. Brackets are main effect of knockdown, bars are main effect of denervation *p<0.05, ****p<0.0001

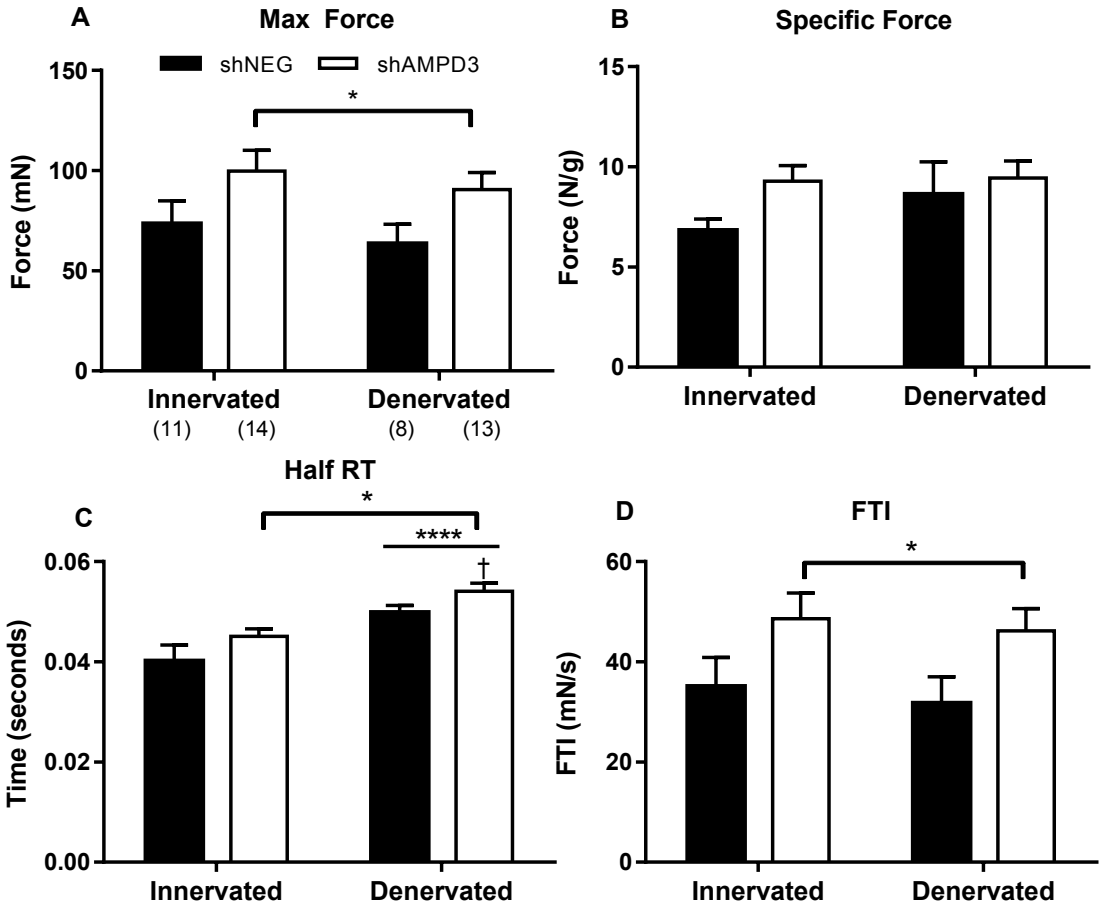

Figure 2.3. Knockdown of AMPD3 increases max force, half relaxation time, and force-time integral. Contractile characteristics of the soleus in response to a single 150 Hz 500 ms electrical stimulation. (A) Absolute maximal tetanic force (B) specific tetanic force (C) half relaxation time (D) force-time integral (area under the force-time curve). Means ± SEM, Values in ( ) are n for each group. *p<0.05 main effect of knockdown, ****p<0.0001 main effect of denervation, †p<0.05 vs shNEG:Denervated.

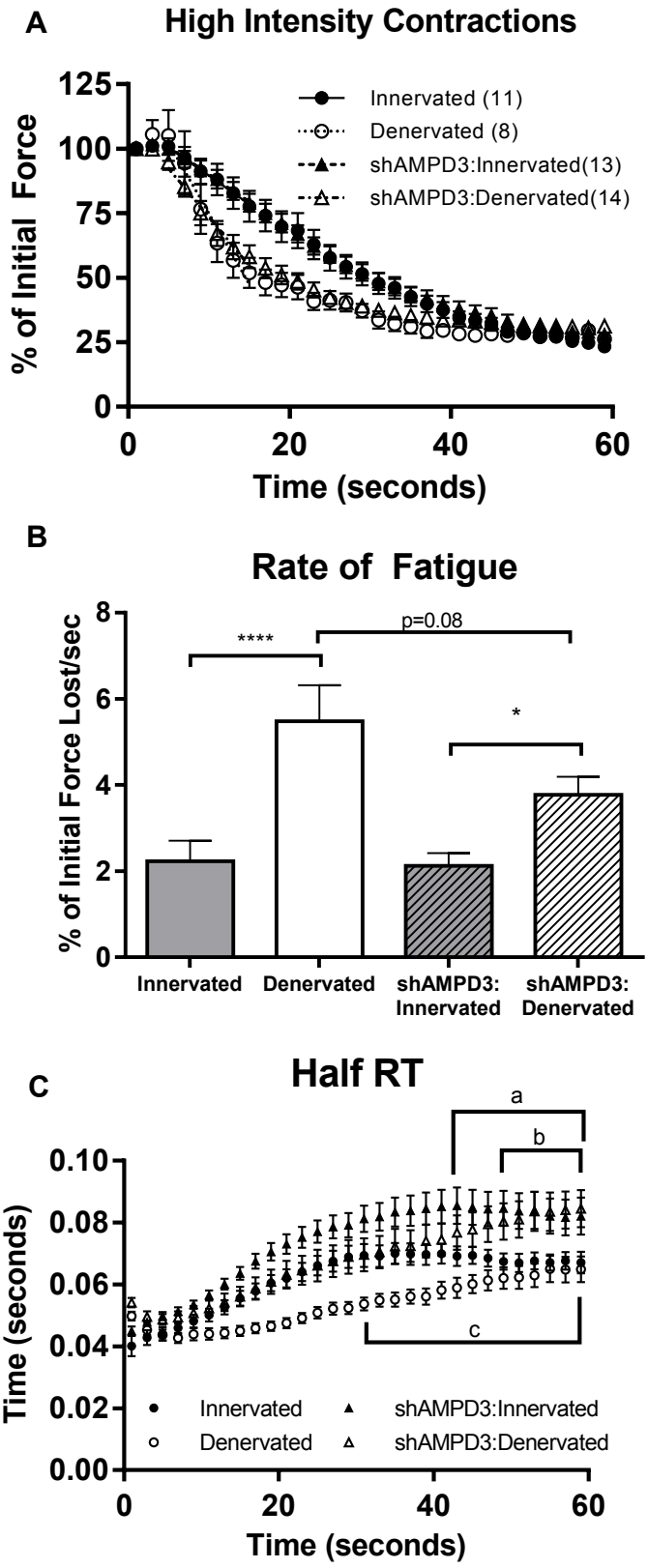

Figure 2.4. During high intensity fatiguing contractions AMPD3 knockdown increases relaxation time, denervation increases rate of fatigue. Mouse soleus muscle was electrically stimulated for 60 seconds with a high intensity fatigue protocol (50% duty cycle, 1 tetani per second). (A) Percent of initial force during high intensity fatigue protocol, n's are given in figure legend (B) rate of initial fatigue as determined by linear regression of the fatigue protocol between 5-15 seconds (C) half relaxation time during high intensity fatigue protocol. Every other contraction plotted for clarity (A&C). Means ±SEM. **** $p<0.0001$ vs Innervated, †$p<0.05$ vs shAMPD3:Innervated. Significance of Tukey post-hoc multiple comparisons, a,b $p<0.05$ vs Innervated, c $p<0.05$ vs shAMPD3:Denervated

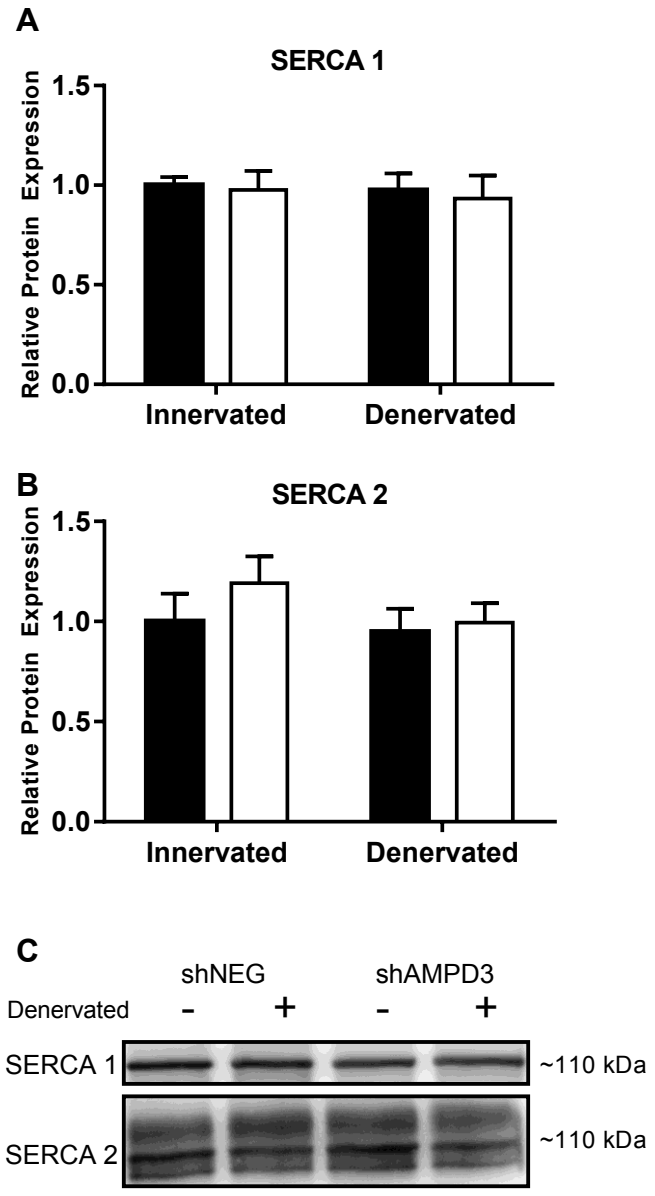

Figure 2.5. SERCA protein content does not change with AMPD3 knockdown or denervation atrophy. Western blot analysis of soleus muscle homogenates following 1-week of denervation and AMPD3 knockdown or negative control (A) SERCA1 protein content relative to shNEG:Innervated (B) SERCA2a protein content relative to shNEG:Innervated (C) representative western blot images. Mean ±SEM n=7 shNEG, 8 shAMPD3

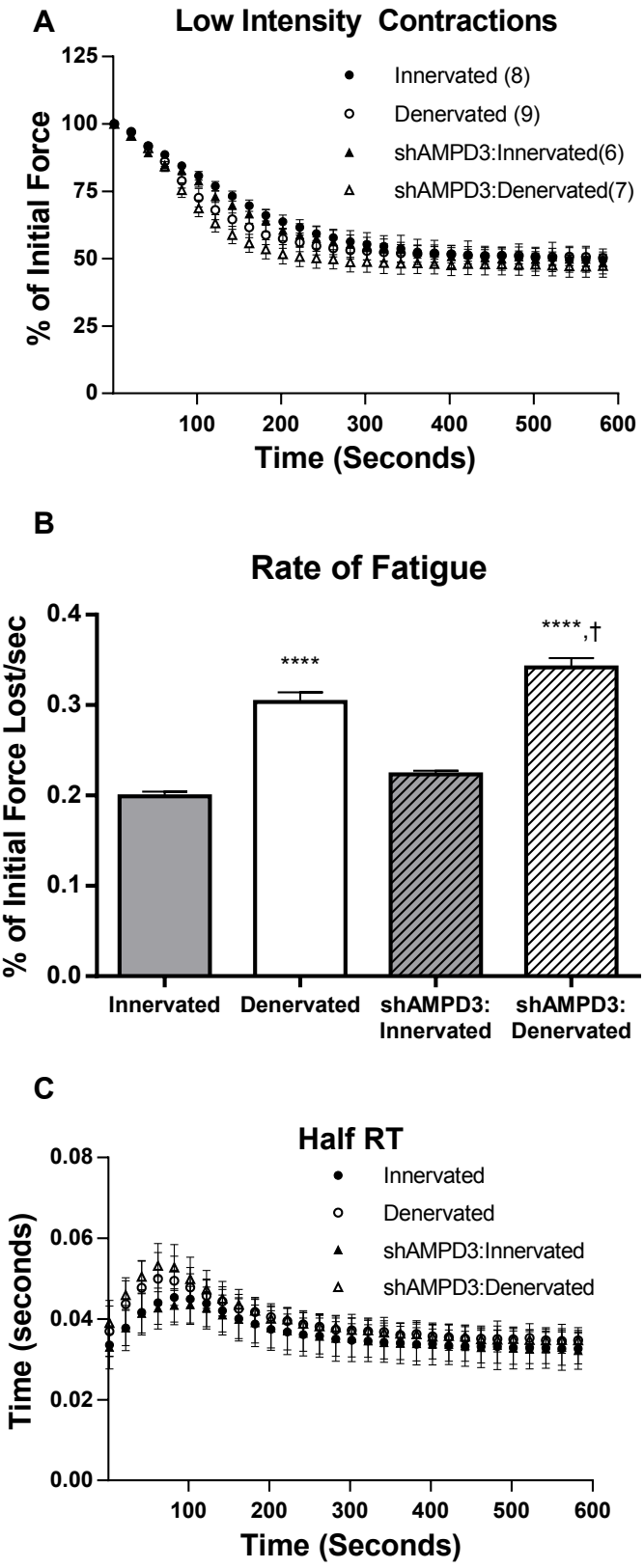

Figure 2.6. AMPD3 knockdown does not increase relaxation time during low intensity contractions. Mouse soleus muscle was electrically stimulated for 600 seconds with a low intensity fatigue protocol (12.5% duty cycle, 1 contraction every 2 seconds). (A) Percent of initial force during low intensity fatigue protocol, n's are given in figure legend (B) rate of initial fatigue as determined by linear regression of the fatigue protocol between 5-100 seconds (C) half relaxation time during low intensity fatigue protocol. Every 10^{th} contraction plotted for clarity (A&C). Means ±SEM. ****p<0.0001 vs. Innervated and shAMPD3:Innervated, † p<0.01 vs Denervated

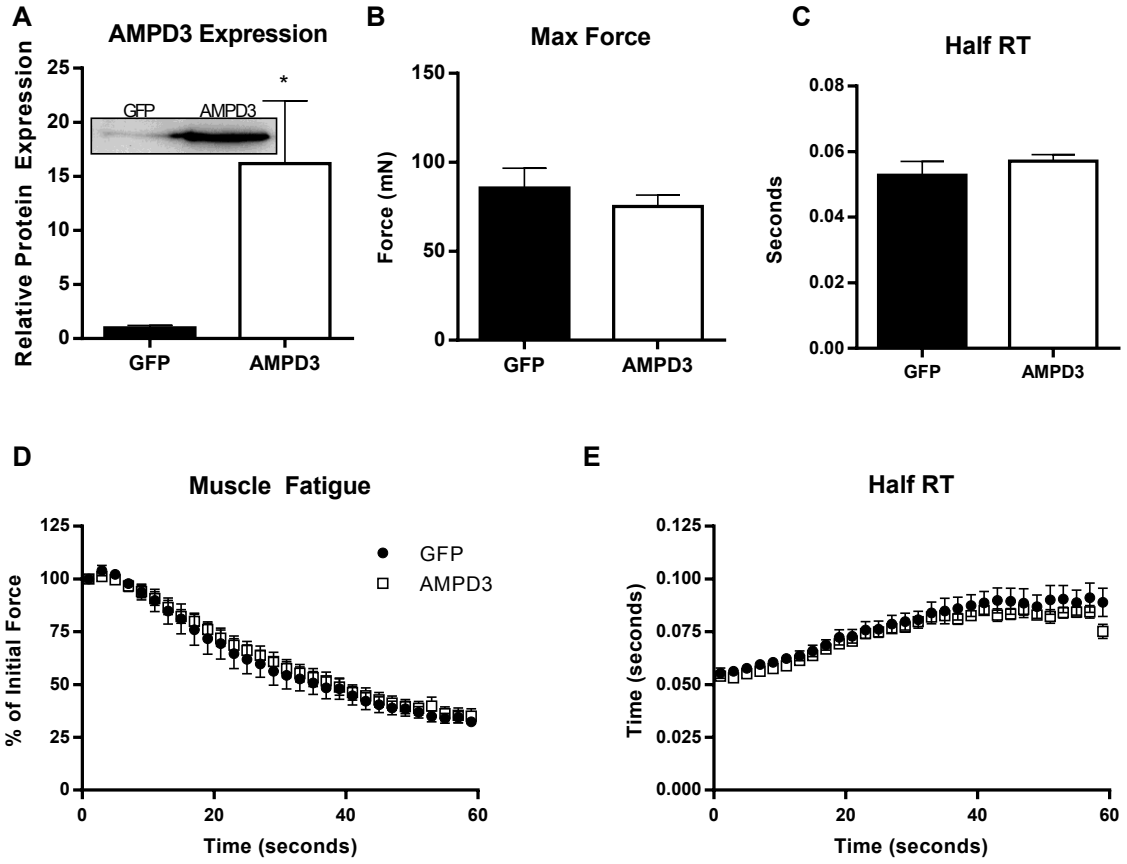

Figure 2.7. AMPD3 overexpression alone does not alter muscle performance. Mouse soleus muscle was electroporated with an AMPD3 or GFP expressing plasmid for 1 week then subjected to a high intensity contraction protocol. (A) Relative AMPD3 protein expression in electroporated soleus muscles (B) Absolute maximal tetanic force (C) half relaxation time of a tetanic contraction (D) percent initial force during high intensity fatigue protocol, (E) half relaxation time during high intensity contractions. D&E every other contraction is plotted for clarity. Means ±SEM. n=16 for protein expression; n=6 for tetanic; for fatigue protocol n=7 GFP, n=9 AMPD3. *p<0.05 vs. GFP

Chapter Three

AMP Deaminase 3 overexpression accelerates protein degradation in C2C12 myotubes

Abstract

Protein degradation dramatically increases during skeletal muscle atrophy leading to a net loss of protein and muscle mass. Because AMPD3 is highly induced in several types of muscle atrophy, we tested the hypothesis that AMPD3 overexpression would reduce the total adenine nucleotide pool and activate protein degradation. In C2C12 myotubes AMPD3 overexpression by adenovirus resulted in an increase in total AMPD activity of 2-fold and 9-fold after 24 and 48 hours of infection. By 72 hours of AMPD3 overexpression, [ATP], [ADP], and total adenine nucleotides were reduced by 40, 35, and 40%, [IMP] was increased, and the adenylate energy charge remained the same. Total and phospho AMPK were not altered over the 72 hours. The protein degradation rate was 38% greater than GFP controls but protein synthesis rates were not significantly different, resulting in a net loss of protein and loss of myotube size with AMPD3 overexpression. Neither the flux nor makers of the autophagy-lysosome system were increased. There was no increase in several subunits of the proteasome and in-vitro proteasome activity was not increased however, total ubiquitination decreased. Our results suggest that AMPD3 overexpression accelerates protein degradation, likely by in-vivo activation of the 26s proteasome in response to reduced ATP content.

Introduction

Protein degradation dramatically increases during skeletal muscle atrophy leading to a net loss of protein and muscle mass (14, 27, 138). The atrophy process is regulated, at least in part, by a coordinated transcriptional program of atrophy related genes (atrogenes). The atrogenes consist of approximately 130 genes that are either up or down regulated during several types of atrophy such as fasting, cancer cachexia, renal failure, diabetes, and denervation (81, 130). Many of the atrogenes, such as FoxO (135, 163), PGC-1a (134), Atrogin-1/MAFbx (11), JunB (117), and Bnip3 (90), have been identified to independently regulate protein degradation. Some of these atrogenes have direct effects on the protein degradation pathways, but not all atrogenes directly influence the degradation machinery. One of the most highly induced atrogenes (up to 100 fold) is AMP Deaminase isoform 3 (AMPD3) ($AMP + H_2O \rightarrow IMP + NH_3$). The degradation of AMP by AMPD helps to maintain high ratios of ATP/ADP by shifting the equilibrium of the adenylate kinase (AK) reaction ($ADP + ADP \rightarrow ATP + AMP$) toward ATP synthesis. The combined actions of AMPD and AK support the perseveration of the free energy of ATP hydrolysis (ΔG_{ATP}) during high rates of ATP consumption (55, 56). Additionally, sustained AMPD activity can lead to a reduction of [ATP] and the total adenine nucleotide pool content, and thereby acts as a regulator of the adenine nucleotide pool (95, 96). However, it is unknown if the upregulation of AMPD3 typical of muscle atrophy is able to exert any influence on protein degradation.

AMPD exists as a tetramer composed of two different isoforms in skeletal muscle (45, 100). AMPD1 is the predominant form, while roughly 5% of basal AMPD activity can be attributed to AMPD tetramers that contain at least one AMPD3 subunit (47). The

influence of AMPD3 is dramatically increased during atrophy when 35% of AMPD activity is attributed to tetramers containing AMPD3. Importantly these isoforms appear to be differentially regulated. AMPD1 will bind to myosin with a resultant increase in activity during muscle contractions and lower pH (40, 66, 126, 127). Conversely, AMPD3 is more active basally, but when pH is reduced, it binds to membranes (111) with a subsequent reduction in activity (87). The increase in AMPD3 during atrophy suggests a shift in the control of AMPD to a more basally active AMPD tetramer.

Traditionally AMPD is thought to help maintain energetics (a high ATP/ADP and ΔG_{ATP}) during high energy demand (55, 56, 91), but it also functions as a regulator of the total adenine nucleotide pool. The increase in AMPD3 protein and total AMPD activity during atrophy is of interest because the energetic disruption, rather than maintenance, that may result from excessive adenine nucleotide degradation may be a signal that induces atrophy. The proteasome, which is the major site of protein degradation (124), is more active when [ATP] is reduced (89). This phenomena has been reported in both cardiac (49) and skeletal muscle (32), and in-vivo cell culture (69) as well as in isolated preparations (24, 69, 84). Importantly, the activation of the proteasome by the loss of [ATP] occurs within a physiological range of [ATP] (69). Changes in energetics such as, loss of [ATP] (33, 42, 46, 92, 140), loss of phosphocreatine [CP] (42, 140), reduced ATP synthesis rate (29, 140), and increased [ADP] (110), and increased [P_i] (42) have been reported in atrophy. Currently it is unknown if the upregulation of AMPD3 during atrophy helps to maintain energetics or if it contributes to overall protein degradation.

The purpose of the present study was to investigate the effects AMPD3 overexpression in muscle on energetics and protein degradation. To investigate this we used adenovirus to overexpress AMPD3 or GFP in C2C12 myotubes. We tested the hypothesis that AMPD3 overexpression will lead to a loss of adenine nucleotides and an increase in the rate of protein degradation.

Methods

Animal Procedures

Adult, male C57BL/6 mice were purchased from Charles River (Raleigh,NC). All animal procedures were approved by the East Carolina University Animal Care and Use Committee. Mice were housed 4 per cage in housing approved by Association for Assessment and Accreditation of Laboratory Animal Care and provided ad libitum access to standard chow and water. Atrophy of the lower hind limb muscles was induced between 7-9 weeks of age (approx. 30g) by unilateral sciatic nerve sectioning (denervation), as done previously (14). 5-14 days later mice were anesthetized by an intraperitoneal injection of ketamine:xylazine (100:10 mg/kg) and euthanized by cervical dislocation. The plantaris muscle was removed, frozen in liquid nitrogen, and stored at -80°C until analysis. Muscles were homogenized and RNA was extracted in Trizol Reagent (Life Technologies) using a Bio-Gen PRO200 Homogenizer (Pro Scientific, Oxford, CT). Real time-PCR was done for AMPD3 and normalized to RPLPO using SybrGreen (Thermo Fischer).

Cell Culture

C2C12 myoblasts were grown in Dulbecco's modified Eagle's medium (DMEM) with 10% fetal bovine serum, penicillin (100 U/mL), and streptomycin (100 µg/mL) until 75-90% confluent. Media was switched to DMEM with 2% horse serum and penicillin/streptomycin to induce differentiation into multinucleated myotubes. Adenovirus was used to overexpress GFP or AMPD3. Custom made adenovirus, serotype 5 (DE1/E3), for the co-expression of AMPD3 and GFP was purchased from

Vector Biolabs (Malvern, PA). The use of adenovirus allows near 100% transfection efficiency into myotubes, which was confirmed visually by GFP fluorescence.

Protein Analysis

Proteins were extracted from cells with perchloric acid (PCA) or RIPA buffer and were then quantified by BCA Assay (Pierce). Equal amounts of protein were separated by SDS-PAGE (5-15% polyacrylamide, depending on target) then transferred to polyvinylidene difluoride (PVDF) membranes. Equal loading and transfer were confirmed by Ponceau S staining. Primary antibodies were purchased from ABCAM (AMPD3; ab118230), ThermoFisher (AMPD1; PA-23172), Enzo (19s Rpt6 PW9265; 19s Rpt5 PW8770; 20s β5 PW8895; Ubiquitin PW8810), Cell Signaling (AMPKα #5831; P-AMPK #2531; LC3B #3868; ULK1 #8054; P-ULK1 #5869), and Developmental Studies Hybridoma Bank (MHC A4.1025). Secondary antibodies conjugated to HRP (Cell Signaling #7074, ThermoFisher #31444) were used and visualized with Western Chemiluminesence HRP Substrate (EMD Millipore). Band intensities were captured using a Bio-Rad Chemi Doc XRS imager and analyzed using Image Lab Software (Bio-Rad) with weights calculated from Pageruler Plus protein ladder (ThermoFisher)..

Degradation of Long-lived Proteins

Degradation rate of long-lived proteins was determined from the release of the essential amino acid tyrosine as previously described (12, 14). On day 4 of differentiation, proteins were radiolabeled with L-[3,5-^{3}H]-tyrosine (5 μCi/mL) for 24 hours. After radio-labeling, cells were incubated with 2mM non-radioactive tyrosine for one hour, then repeated for another hour, in order to wash out and prevent re-incorporation of L-[3,5-^{3}H]-tyrosine into the cell proteome as well as to allow for the

breakdown of short-lived proteins. Cells were then infected with either GFP or AMPD3 adenovirus in media containing 2mM non-radioactive tyrosine (time 0). Samples of the media were taken at 18, 20, 22, 24, and 30 hours. The experiment was repeated two other times with media samples being taken between 24 and 72 hours. Trichloroacetic acid (TCA) was added to media samples to 10% final concentration in order to precipitate proteins. Following final time point, media was completely removed and C2C12 myotubes were solubilized in 0.2 N NaOH. Radioactivity was measured in the TCA soluble supernatants and in myotubes. The rate of protein degradation was calculated as the mean slope of the regression lines calculated between 24-30 hours.

Protein Synthesis

C2C12 myotubes were infected with either GFP or AMPD3 adenovirus for 24, 48, or 72. On day 7 of differentiation, myotubes were pulsed with L-[3,5-^{3}H]-tyrosine for two hours then washed twice with phosphate buffered saline (PBS). Proteins were precipitated with 10% TCA and pelleted by centrifugation. Protein pellets were re-suspended in 0.1 N NaOH for total protein measurement by BCA (Pierce). Radioactivity was measured in a scintillation counter and the protein synthesis rate was calculated and normalized to total protein content.

Nucleotide Measurements

Nucleotides were extracted from C2C12 myotubes in ice cold 0.5 N PCA. Cells were lysed by sonication, and protein was pelleted by centrifugation. Protein pellets were re-suspended in 0.2 N NaOH for protein estimation by BCA Assay (Pierce). Supernatants were neutralized by the addition of ice cold 1 N KOH and centrifugation at 4°C. Samples were stored at -80°C until analysis. Adenine nucleotide concentrations

(ATP, ADP, AMP) and degradation products (IMP, adenine, and inosine) were determined by ultra-performance liquid chromatography (UPLC) using a Waters Acquity UPLC H-Class system and a Acquity UPLC HSS T3 1.8 µm, 2.1 mm X 150 mm column (Waters) as done previously (15). The adenylate energy charge (AEC) was calculated as the mole fraction of ATP plus 0.5 the mole fraction of ADP as described by Atkinson (6).

$$[(ATP) + 0.5(ADP)] / [(ATP) + (ADP) + (AMP)]$$

AMPD Activity

Total AMPD activity was determined by the formation of IMP in cell homogenates as done previously (128). Myotubes were collected using cell lifters in a homogenization buffer (100 mM KCl, 50 mM Imidazole, 1 mM DTT, pH 7.0) and lysed in a Dounce Homogenizer. Homogenates were added to reaction buffer (150 mM KCl, 50 mM Imidazole, 10 mM AMP, pH 7.0, 30°C) to start the reaction. Fractions of the reaction mixture were removed after 2, 5, and 10 minutes and enzymatic activity was inhibited by addition of 0.5 N PCA followed by neutralization with 1.0 N KOH. IMP was measured in supernatants by UPLC. AMPD activity was calculated by the rate of IMP formation and normalized to total protein content.

Myotube Area

Myotube area was quantified by analyzing the amount of myosin heavy chain coverage as done previously (12). In brief, after 72 hours of AMPD3 or GFP overexpression, myotubes were washed in a cytoskeletal stabilizing buffer (CSB) (80 mM PIPES, 5 mM EGTA, 1mM $MgCl_2$, 40 g/L PEG 35,000, pH 7.4), fixed with 4% PFA in CSB, permeabilized with 0.2% triton X-100 in CSB, and blocked with goat serum.

Primary antibody, which detects all isoforms of myosin heavy chain, (#A4.1025; DHSB, U Iowa) incubation was done overnight at 4°C followed by secondary antibody (AlexaFluor 647) incubation at room temperature for 1 hour. Nuclei were stained with DAPI and cells were imaged using a 10x objective. Ten images, from evenly distributed regions, in each well of a 6-well plate were captured. A total of 6 wells (60 images) were imaged for each condition. Images were split to individual components and converted to threshold images using ImageJ64 (NIH). The area representing myosin heavy chain and number of nuclei were measured from the threshold images.

Autophagy Flux

The flux through autophagy was estimated by the accumulation of LC3 II in myotubes (79). C2C12 myotubes were infected with Ad.GFP or Ad.AMPD3 on day 5 of differentiation. On day 7 myotubes were treated with 0.1 μM Concanamycin A, a specific inhibitor of the lysosomal proton pump, or DMSO/vehicle for 6 hours. This results in an accumulation of the lipidated form of LC3 (LC3 II) which is proportional to the rate of autophagy (145). Following concanamycin A treatment, proteins were collected in RIPA buffer and LC3 I and LC3 II were identified by western blot as described above.

Proteasome Activity

Activity of the chymotrypsin-like site of the proteasome was measured as described by Kisselev and Goldberg (12, 78) using the flurogenic peptide substrate Suc-LLVY-AMC (Bachem; Bubendorf, Switzerland). In brief, myotubes were lifted from plates with trypsin-EDTA and centrifuged in 1.7 mL Eppendorf tubes. Cell pellets were re-suspended and permeabilized in a cytosolic extraction buffer (50 mM Tris-HCl, 250

mM Sucrose, 5 mM $MgCl_2$, 0.5 mM EDTA, 1 mM DTT, 2 mM ATP, 0.025% Digitonin) then centrifuged again. The supernatant containing the cytosolic extract was added to 10 volumes of proteasome activity buffer (50 mM Tris-HCl, 40 mM KCl, 5 mM MgCl2, 1 mM DTT, 0.5 mM ATP, 0.05 mg/mL BSA) along with Suc-LLVY-AMC (100 μM final) in a black 96-well plate. Samples were excited at 380 nm and absorbance was measured at 460 nm over 15 min. Results were normalized to total protein content (DC protein assay, Bio-Rad).

Statistics

All data are expressed as mean ± standard error of the mean. Significant differences were assessed using two-way ANOVA (for comparisons of AMPD Activity, % degraded, protein synthesis, LC3 I and II, and proteasome subunits) with Sidak post hoc analysis for multiple comparisons if significance was detected. One-way ANOVA was used for comparisons of nucleotides, mRNA, ULK1, and AMPK with a Bonferroni post hoc analysis for multiple comparisons if significance was detected. Unpaired student t-tests were used for comparisons of degradation rate, total protein, myotube size, ubiquitin, and proteasome activity. All analyses were performed using GraphPad Prism for Windows, version 6.05 with the alpha level set at $p<0.05$ to detect significance

Results

Upregulation of AMPD3 precedes loss of mass.

Previous studies have shown that the atrophy-induced upregulation of AMPD activity by AMPD3 occurs rapidly, within 36 hours of denervation (47). To examine the relationship between AMPD3 upregulation and muscle mass we measured both in 5 and 14 day denervated mouse muscles. After 5 days of denervation there was no change in muscle mass (Figure 3.1A) while AMPD3 was upregulated 10-fold (Figure 3.1B). AMPD3 mRNA remained elevated (8-fold) after 14 days of denervation and plantaris muscle had atrophied 23%. Inosine monophosphate dehydrogenase 2 (IMPDH2), which degrades a product of the AMPD reaction (IMP), was upregulated 1.5-fold after 14 days of denervation (Figure 3.1C). The upregulation of AMPD3 mRNA occurs prior to any loss of muscle mass.

AMPD3 overexpression increases protein and activity.

Overexpression of AMPD3 by adenoviral delivery resulted in a time dependent increase in AMPD3 protein (Figure 3.2A). AMPD1 content was below detection limits until 48 hours. Neither AMPD3 nor AMPD1 were detectable at time 0 (Figure 3.2A). AMPD3 overexpression resulted in increased total AMPD activity of nearly 2-fold over GFP control by 24 hours and 8.6-fold by 48 hours (Figure 3.2B).

AMPD3 degrades the total adenine nucleotide pool but does not activate AMPK.

To determine how AMPD3 overexpression affected nucleotide levels over time, adenine nucleotides and IMP were measured at several time points post AMPD3 infection. [ATP] and [ADP] progressively declined 40% and 35% respectively, over 72 hours (Figure 3.3A-B). [AMP] was reduced 25% by 72 hours but was not statistically

significant (Figure 3.3C). [IMP] was increased at 36 and 72 hours post-infection (Figure 3.3D). The total adenine nucleotide pool (TAN; ATP+ADP+AMP) was 40% smaller by 72 hours of AMPD3 overexpression (Figure 3.3E), which highlights the role of AMPD in regulating the size of the TAN pool. The adenylate energy charge, ATP/ADP ratio, and ATP/AMP ratio, all of which are indicative of the ΔG_{ATP}, did not change over the time course of infection (Figure 3.3F-H). Consistent with a constant ATP/AMP ratio and adenylate energy charge, neither total AMPK nor Thr172 phosphorylation were not altered (Figure 3.4).

Protein degradation is accelerated.

AMPD3 overexpression resulted in greater amounts of degraded protein by 18 hours (Figure 3.5A). By 30 hours 42.4% of protein was degraded in Ad.GFP while 46.0% of protein was degraded in Ad.AMPD3. In repeated experiments the percent degraded remained significantly greater in AMPD3 infected cells out until 72 hours, the last time point tested (Data not shown). The protein degradation rate was calculated as the average slope of the regression lines for each sample between 24 and 30 hours because the lines were most divergent within this time frame. Protein degradation rate was 38% greater in AMPD3 infected myotubes compared to GFP infected control (Figure 3.5B).

Protein synthesis was determined by giving a 2 hour pulse of [^{3}H]-tyrosine and measuring the incorporation of radioactivity into protein extracts from myotubes. There were no significant differences in protein synthesis rates between AMPD3 or GFP infected myotubes at any time point tested (Figure 3.5C). To determine if the increase in protein degradation with unchanging protein synthesis led to a net loss of total protein,

we quantified the total protein content from each well. The total protein content is significantly reduced by 16% following 72 hours of AMPD3 overexpression compared to GFP control (Figure 3.5D) indicating a net loss of total protein has occurred.

Increased protein degradation reduces myotube size.

Skeletal muscle loses protein and becomes smaller during atrophy. To further investigate the observed net loss of protein on the size of myotubes, we measured myotube size of AMPD3 and GFP infected myotubes. Myotubes were identified by the presence of myosin heavy chain (Figure 3.6A). In agreement with the loss of total protein, AMPD3 infected myotubes were smaller than the GFP infected controls (Figure 3.6A&B) reflecting a similar state of atrophy observed in intact skeletal muscle. There was no measurable difference in the total number of nuclei between AMPD3 or GFP infected myotubes (Figure 3.6C) indicating that there was no measurable loss of cells or apoptosis with AMPD3 treatment.

Autophagy flux is not altered with AMPD3 overexpression.

Protein degradation occurs through two main pathways, the autophagy/lysosome and ubiquitin/proteasome pathways. To account for the increased overall protein degradation, we measured the flux of autophagy by the accumulation of LC3 I and LC3 II in myotubes treated with concanamycin A, which inhibits acidification of lysosome. LC3 I is cytosolic while LC3 II is lipidated and is present in the membranes of autophagosomes. LC3 I was increased with concanamycin A treatment but there was no difference between GFP and AMPD3 infected myotubes (Figure 3.7A). Likewise, there was significant accumulation of LC3 II with concanamycin A but no difference between AMPD3 and GFP infected cells. The ratio of LC3 II to LC3 I was not different

between GFP and AMPD3 in concanamycin A treated myotubes (Figure 3.7A). Therefore, the estimated flux through autophagy was not increased with AMPD3 overexpression.

ULK1, which phosphorylates Beclin-1 and is necessary for autophagy (129), did not change with AMPD3 overexpression (Figure 3.7B). The AMPK phosphorylation site on ULK1, Ser555, was less phosphorylated following AMPD3 overexpression which tended to reduce the P-ULK1/ULK1 ratio (Figure 3.7B). These data demonstrate that autophagy was not increased, but may have been slightly down regulated.

Ubiquitin-Proteasome Pathway is not upregulated.

Because the rate of autophagic flux was not increased by AMPD3 overexpression, we next measured several markers of the other predominant protein degradation pathway, the ubiquitin-proteasome pathway. Components of the proteasome, namely the 19S RTP5 and RTP6 and 20S β5 subunits were not increased during the AMPD3 infection time course (Figure 3.8A). The 20S β5 subunit was reduced at 24 hours but not at any other time. The activity of the chymotrypsin-like site of the proteasome, determined in-vitro with a fixed [ATP] of 0.72 mM, was not different between GFP or AMPD3 groups (Figure 3.8B). This in-vitro assay is conducted in cytosolic extracts and is not dependent on ubiquitination and reflects the maximal flux capacity of the chymotrypsin-like site of the proteasome. The amount of total poly- and mono-ubiquitinated protein was reduced after 48 hours of AMPD3 overexpression (Figure 3.8C).

Discussion

In this study we tested the hypothesis that overexpression of AMPD3 in skeletal muscle would lead to a loss of adenine nucleotides and an increased rate of protein degradation. Indeed, when AMPD3 was overexpressed by adenovirus in C2C12 myotubes, we observed a loss of adenine nucleotides and an increase in the protein degradation rate. Furthermore, the increase in protein degradation rate was sufficient to explain most of the observed loss of total protein. This exciting finding implicates AMPD3 and perhaps energetics as overall contributors to protein degradation in muscle atrophy.

A likely cause of some of the energetic perturbations observed during atrophy is AMPD3, which is highly upregulated during most, if not all, types of atrophy (81, 97). AMPD has two major functions within skeletal muscle. The first is to maintain a favorable ATP/ADP ratio by shifting the equilibrium of the AK reaction toward ATP synthesis (55, 91) and the second is to regulate the size total adenine nucleotide pool (20, 132). In our study we observed a reduction in [ATP], [ADP], and total adenine nucleotides while [IMP] increased (Figure 3.3) clearly demonstrating that increased AMPD activity can degrade the total adenine nucleotide pool. Importantly, neither the adenylate energy charge, ATP/ADP, nor ATP/AMP ratios changed (Figure 3.3F-H), which suggests the free energy of ATP hydrolysis ΔG_{ATP} is preserved with AMPD3 overexpression.

During denervation atrophy, AMPD3 mRNA was significantly elevated by 5 days post denervation and remained elevated out to 14 days (Figure 3.1B). It is interesting to note that the upregulation of AMPD3 mRNA occurred prior to any significant loss of

muscle mass (Figure 3.1A). Additionally, IMPDH3 mRNA was upregulated by 14 days post denervation (Figure 3.1C) which agrees with past findings (130). In our cell culture model, overexpression of AMPD3 by adenovirus resulted in a time dependent increase in both AMPD3 protein content and AMPD activity (Figure 3.2).

The major finding of this study is that AMPD3 overexpression accelerates overall protein degradation in skeletal muscle. The rate of protein degradation was 17% greater in AMPD3 infected myotubes compared to GFP infected controls (Figure 3.5B) while protein synthesis rates were not different between GFP and AMPD3 infected myotubes (Figure 3.5C). Using the following equation, the increased degradation rate in AMPD3 infected cells fully accounts for the total protein loss by 72 hours where $[A_o]$ is the protein content of GFP infected cells, $[A_t]$ is the protein content of AMPD3 infected cells, k is the difference in degradation rate, and t is time.

$$log\ ([A_0] / [A_t]) = kt / 2.303$$

It is commonly known that during skeletal muscle atrophy there is a net loss of proteins and muscle fibers become smaller. This finding has also been reported during simulated atrophy in myotubes (12). In our study AMPD3 overexpression also resulted in smaller myotubes than GFP (Figure 3.6). The same number of nuclei between GFP and AMPD3 infected myotubes suggests that AMPD3 overexpression did not result in detectable cell death (Figure 3.6C).

The two major components of overall protein degradation are the ubiquitin-proteasome system and the lysosome-autophagy system (97, 163). Because we detected an increase in total protein degradation, it would be expected that either or both the ubiquitin-proteasome or lysosome-autophagy pathways would be upregulated.

We therefore measured components of each of these systems to address how AMPD3 was accelerating overall protein degradation. We treated AMPD3 and GFP infected myotubes with concanamycin A which inhibits the lysosomal proton pump and stops lysosomal dependent proteolysis. This results in an accumulation of LC3 II, the extent of which is dependent on the rate of autophagy (79, 82). In these samples there was no difference in the accumulation of LC3-I or LC3-II protein or in the ratio of LC3-II/LC3-I between AMPD3 and GFP infected cells, which indicates that the flux of autophagy was not increased with AMPD3 overexpression. Whereas increases in LC3 II or the LC3-II/LC3-I ratio have been reported in others cases of atrophy (90, 97, 106). Additionally, we measured the content and phosphorylation of ULK1. There was no change in ULK1 content following AMPD3 infection (Figure 3.7B) and phosphorylation of ULK1 at Ser555 decreased following infection, which further suggest that autophagy was not upregulated with AMPD3 overexpression. Our findings demonstrate that AMPD3 does not directly influence autophagy, which is commonly upregulated during atrophy (90, 97, 106). It follows then that AMPD3 acts independently of the autophagy/lysosome pathway to increase protein degradation.

We next examined the ubiquitin-proteasome system for any differences with AMPD3 overexpression. The protein contents of several components of the proteasome did not increase with AMPD3 overexpression (Figure 3.8A), suggesting that proteasome content was not different. Using a flurogenic peptide substrate, Suc-LLVY-AMC, that is specific for the chymotrypsin-like site of the proteasome (78), we measured the maximal flux capacity of the proteasome in cytosolic extracts. There was no difference in the maximal activity of the proteasome between AMDP3 and GFP infected myotubes

(Figure 3.8B). However, this measurement takes place in-vitro with an exogenous supply of ATP which masks intracellular ATP concentration across samples and therefore does not reflect the intracellular ATP conditions. Additionally, the Suc-LLVY-AMC peptide does not need to be ubiquitinated in order to enter the proteasome. These are important distinctions to make, since reduced intracellular ATP levels have been shown to activate the proteasome (24, 32, 49, 69, 84) and there is a significant loss of [ATP] in AMPD3 infected cells (Figure 3.3A). We can calculate the mM concentration of [ATP] at time 0 and 72 hours to be 3.16 mM and 1.84 mM respectively with the assumption that water content of C2C12 myotubes to be similar to that of skeletal muscle (0.78 ml per g) (67) and the protein content to be 24% of total weight (16). This allows for comparison with the findings of Huang et al. who observed an increase in the activity of the 26S proteasome as [ATP] was reduced from 4 mM to 0.125 mM (69). It is reasonable to suspect a similar activation of the 26S proteasome in our experiments with a drop in [ATP] from 3.16 to 1.84 mM.

The possible mechanism behind the increased proteasome activity with reduced [ATP] was proposed by Smith et al. (142) who argue that when 4 ATP molecules bind the 19s cap there is suboptimal joining with the 20S core. However, when only 2 ATP molecules bind the 19S cap it allows for a better association with the 20S core to form the 26S proteasome and results in maximal catalytic activity. The likelihood of ATP binding to the 19S cap is dependent on the concentration of ATP within the cell. We suspect that the reduction in [ATP] with AMPD3 overexpression decreases ATP binding to the 19S cap which results in a greater formation of the 26S proteasome and increased proteasome activity in-vivo.

Furthering the idea that the reduction of [ATP] activates the proteasome is our observation of a reduction in total ubiquitinated proteins when AMPD3 is overexpressed. Making the assumption that the rate of ubiquitination by the E3 ubiquitin ligases remains the same, while the activity of the 26s proteasome increases, we anticipated there would be a reduction in the amount of total ubiquitinated proteins in AMPD3 infected myotubes, as accelerated protein degradation would reduce the pool of ubiquitinated proteins. Indeed, we did see a reduction in the amount of total ubiquitination in our AMPD3 infected myotubes after 48 hours of AMPD3 overexpression (Figure 3.8C). This is in contrast to what happens during atrophy when total protein ubiquitination increases markedly (27, 93, 97). However, the activation of the atrogene profile during atrophy (81, 130) directly upregulates the major muscle ubiquitin ligases, Atrogin-1 (135) and MuRF (27). When we overexpress a single atrogene, AMPD3, the entire set of atrogenes is not expected to be activated, and any increases in Atrogin-1 or MuRF are not anticipated. Taken together, our results indicate that AMPD3 overexpression activates the proteasome but does not increase ubiquitination.

In summary our results indicate that overexpression of AMPD3 in skeletal muscle accelerates protein degradation. Increased AMPD3 expression results in a degradation of the adenine nucleotide pool and ATP content while the adenylate energy charge is preserved. The increase is protein degradation is likely due to activation of the proteasome by the reduced ATP content with AMPD3 overexpression. These findings are exciting in that they identify AMPD3 as a new and novel regulator of skeletal muscle atrophy.

Tables and Figures

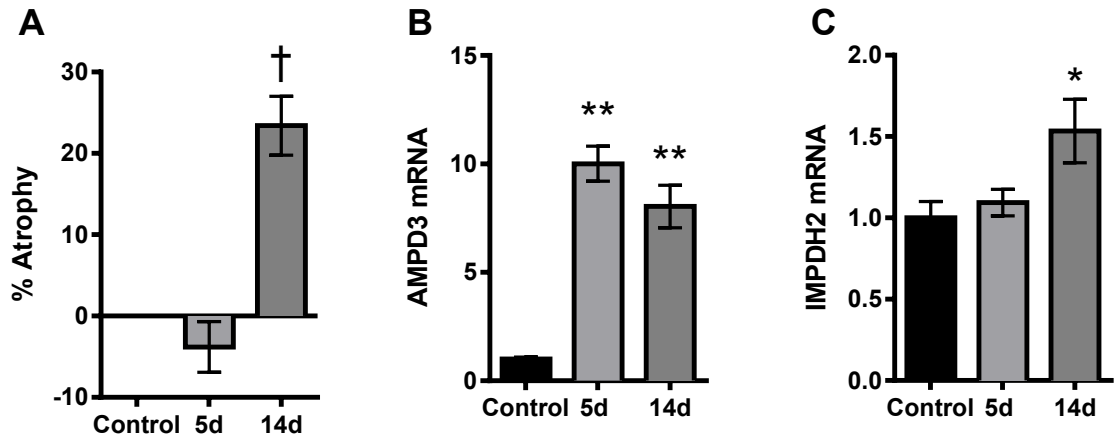

Figure 3.1. Denervation atrophy rapidly induces AMPD3. C57BL/6 mice were denervated to induce atrophy of the lower hind limb muscles. Plantaris muscles were removed, weighed, and mRNA was extracted. (A) Plantaris % atrophy after 5- and 14-days of denervation. (B) AMPD3 mRNA expression. (C) IMPDH2 mRNA expression. Means ± SEM. n=10. † $p<0.0001$ vs 5-day. *$p<0.05$ vs control. **$p<0.0001$ vs control.

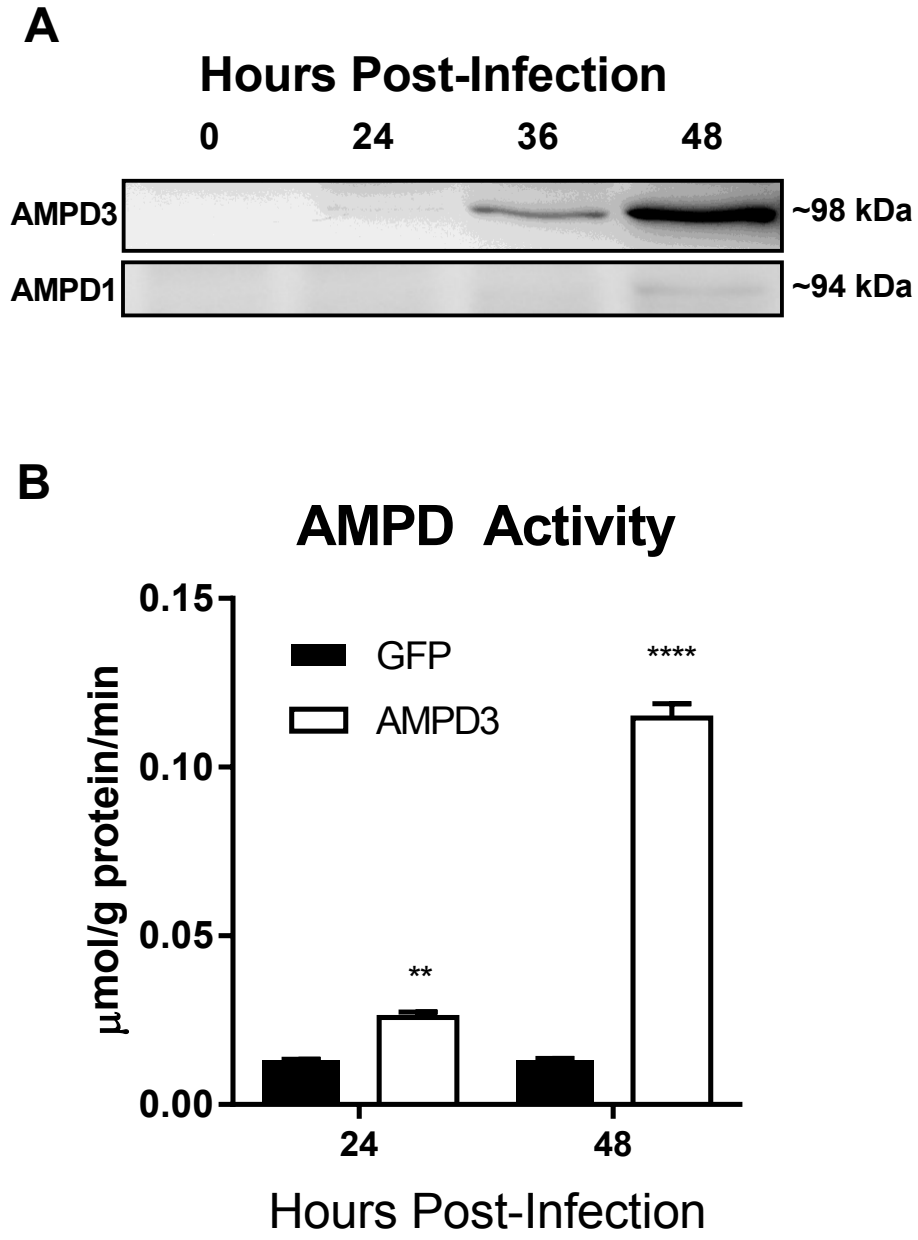

Figure 3.2. AMPD3 overexpression increases total AMPD activity. C2C12 myotubes were infected with GFP or AMPD3 adenovirus. Protein was extracted and AMPD activity was measured at the indicated time points. (A) Representative western blot images for AMPD3 and AMPD1. (B) Total AMPD activity in homogenates. Means ± SEM. n=6 **p<0.01 vs GFP 24 Hour. ****p<0.0001 vs GFP 48 Hour.

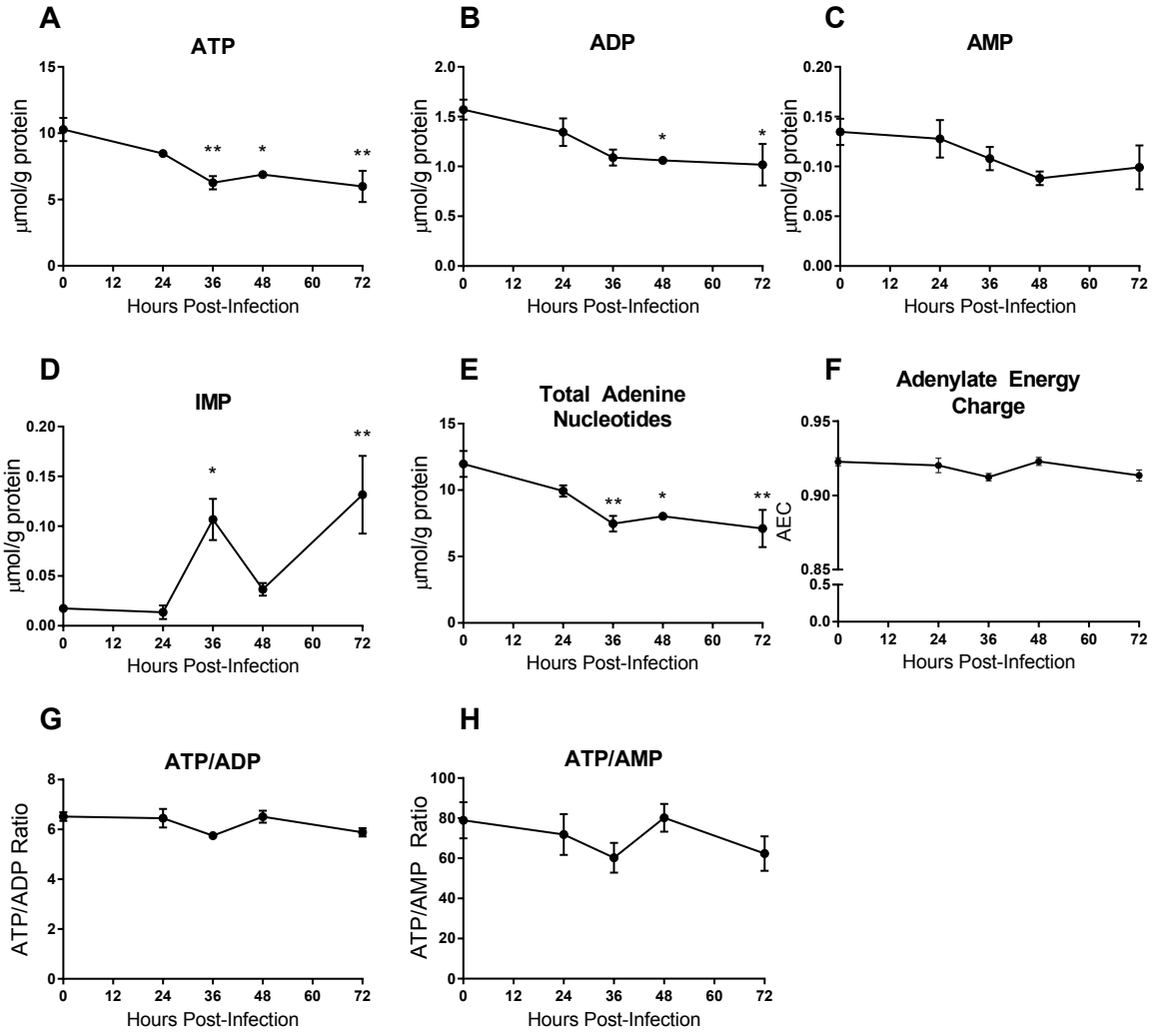

Figure 3.3. AMPD3 degrades the total adenine nucleotide pool while maintaining adenylate energy charge. C2C12 myotube were infected with AMPD3 adenovirus for the indicated times. Nucleotides were extracted on day 7 in perchloric acid and subsequently quantified by UPLC. Measurements of (A) ATP, (B) ADP, (C) AMP, and (D) IMP are expressed as µmol/g of total protein. (E) Total adenine nucleotides (ATP+ADP+AMP), (F) adenylate energy charge was calculated as the mole fraction of ATP plus 0.5 the mole fraction of ADP. (G) ATP/ADP ratio and (H) ATP/AMP ratio. Means ± SEM. n=5 *p<0.05 vs time 0. **p<0.01 vs time 0.

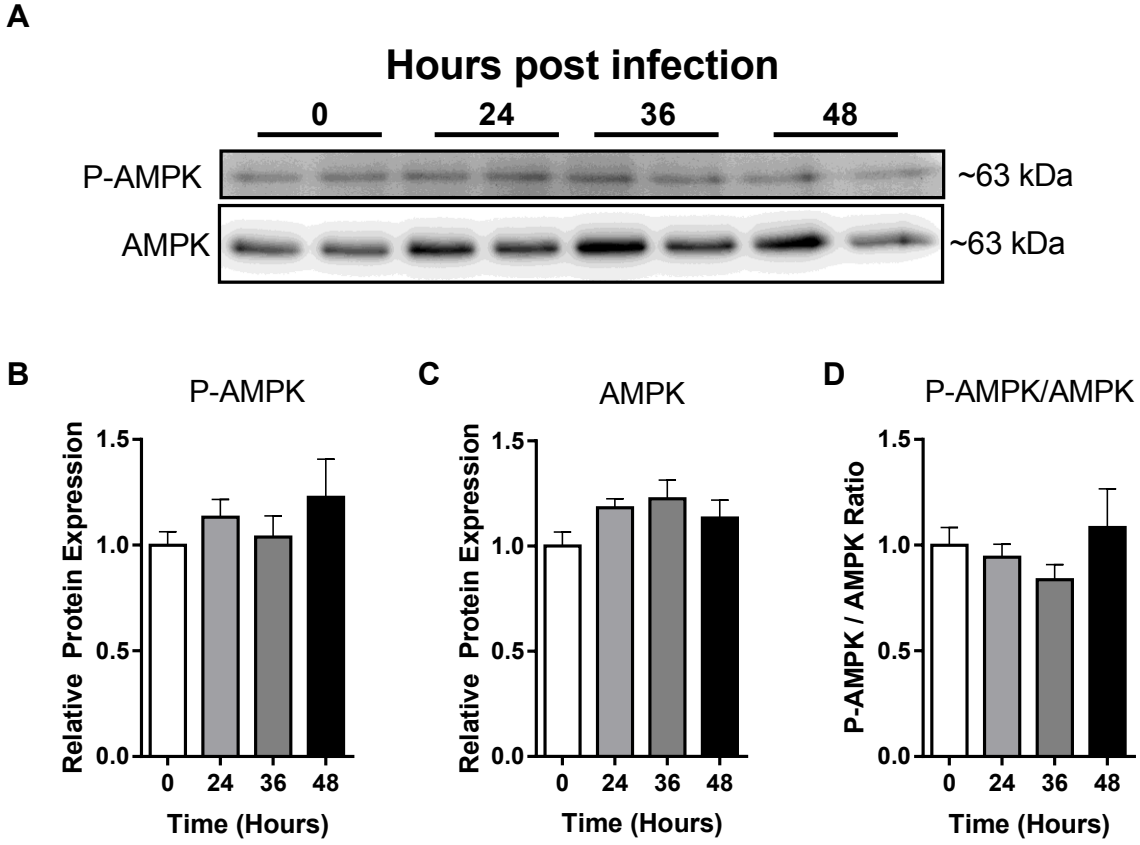

Figure 3.4. Total AMPK and P-AMPK remain constant with AMPD3 overexpression. C2C12 myotube were infected with AMPD3 adenovirus for the indicated times and proteins were extracted on day 7. (A) Western blot images for P-AMPK Thr 172 and AMPKα, samples are paired at time points. Relative protein expression of (B) P-AMPK Thr 172, (C) AMPKα, and (D) the ratio of P-AMPK to AMPK. Means ± SEM. n=5

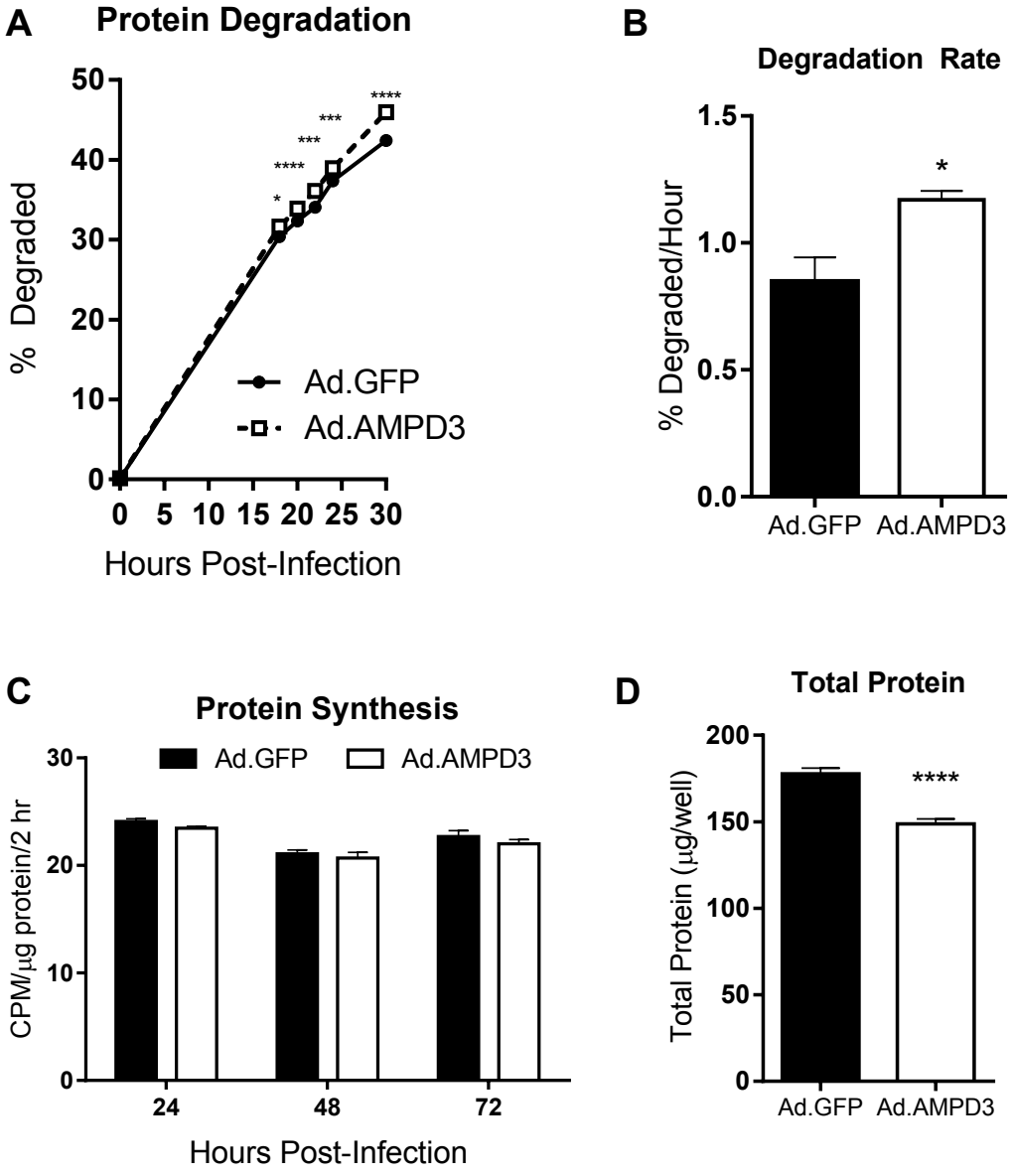

Figure 3.5. AMPD3 overexpression accelerates protein degradation. C2C12 myotubes were infected with GFP or AMPD3 adenovirus for the indicated times. (A) Degradation of long-lived proteins determined by the release of L-[3,5-^{3}H]-tyrosine over time. n=6. (B) Protein degradation rate between 24-30 hours. n=6. (C) Protein synthesis rate determined by the incorporation of L-[3,5-^{3}H]-tyrosine over a two hour pulse. n=4. (D) Total protein per well of a 6-well plate following 72 hours of GFP or AMPD3 overexpression. n=6. Means ± SEM. *p<0.05 vs GFP. ***p<0.001 vs GFP. ****p<0.0001 vs GFP.

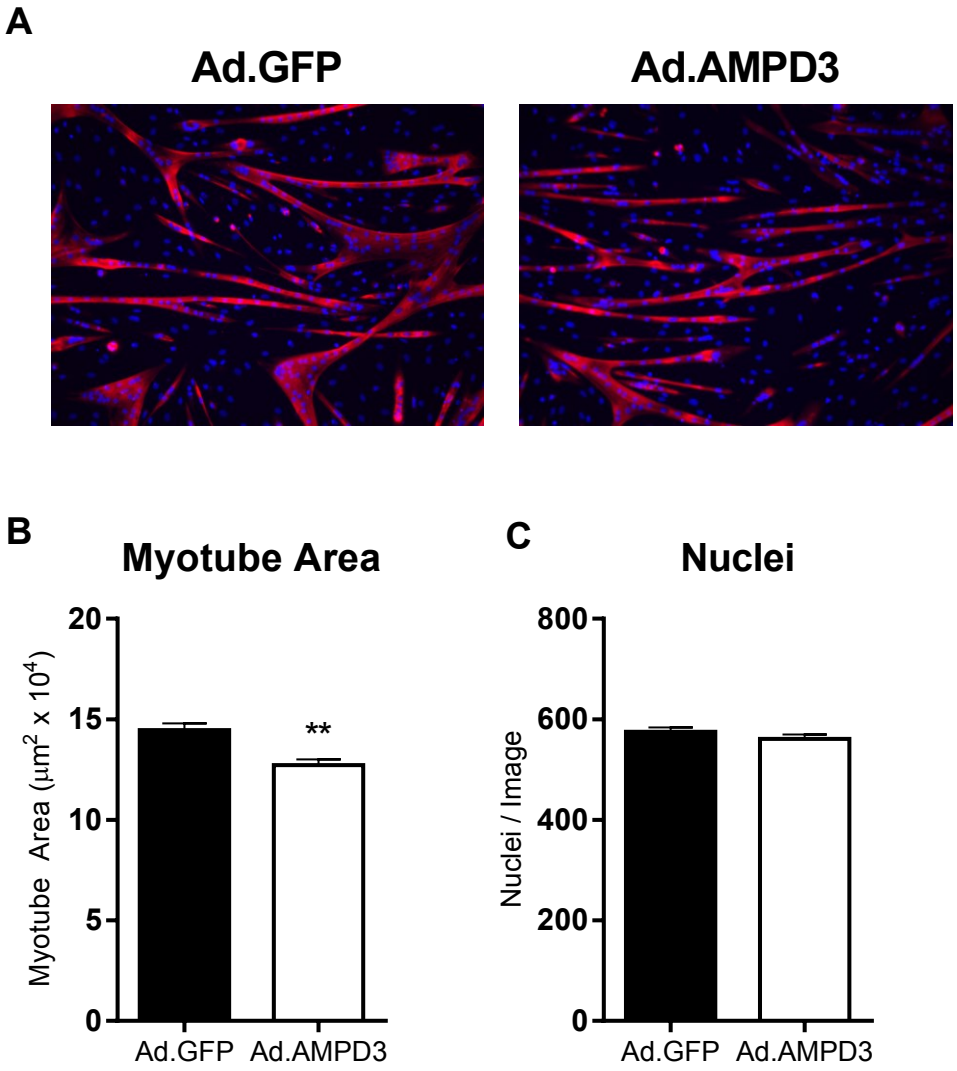

Figure 3.6. Myotubes are smaller with AMPD3 overexpression. C2C12 myotubes were infected with GFP or AMPD3 for 72 hours following which myosin heavy chain was identified by immunofluorescence. Images were captured from 10 evenly dispersed regions of each well of a 6-well plate, and converted to threshold images using ImageJ. The area of positive pixels, representing myosin heavy chain, was measured and averaged for each well. Six wells were imaged in total. (A) Myotube area, (B) number of nuclei per image. (C) Representative images. Means ± SEM n=6 **p<0.01 vs GFP

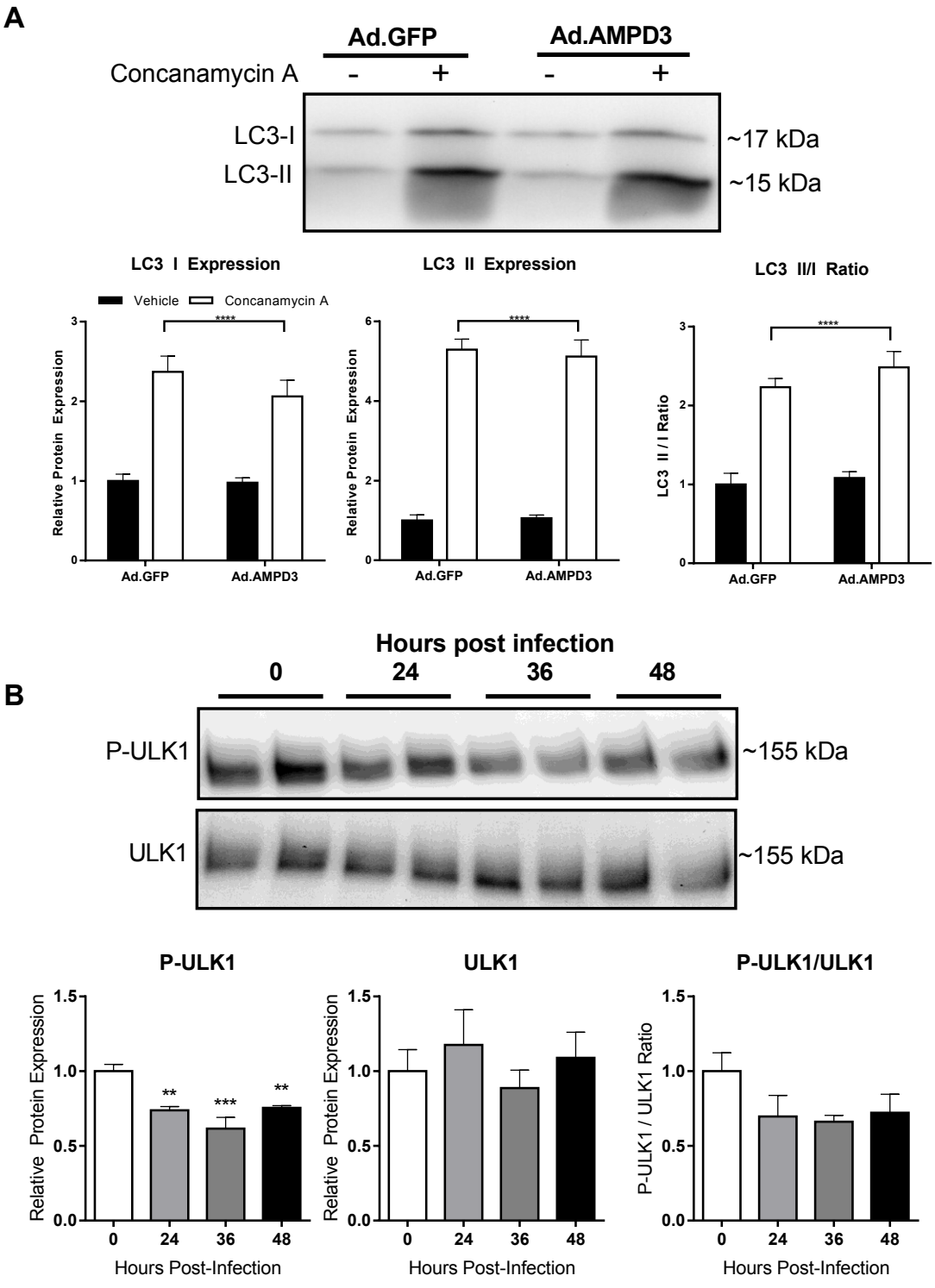

Figure 3.7. AMPD3 does not upregulate Autophagy. (A) C2C12 myotubes were infected with GFP or AMPD3 for 48 hours then treated with concanamycin A or vehicle for 6 hours following which proteins were extracted and LC3 I and LC3 II was identified by western blot. Means ± SEM n=6. ****p<0.0001 vs vehicle. (B) ULK1 and P-ULK1 Ser555 were identified by western blot in GFP or AMPD3 treated myotubes. Means ± SEM n=5. **p<0.01 vs time 0. ***p<0.001 vs time 0.

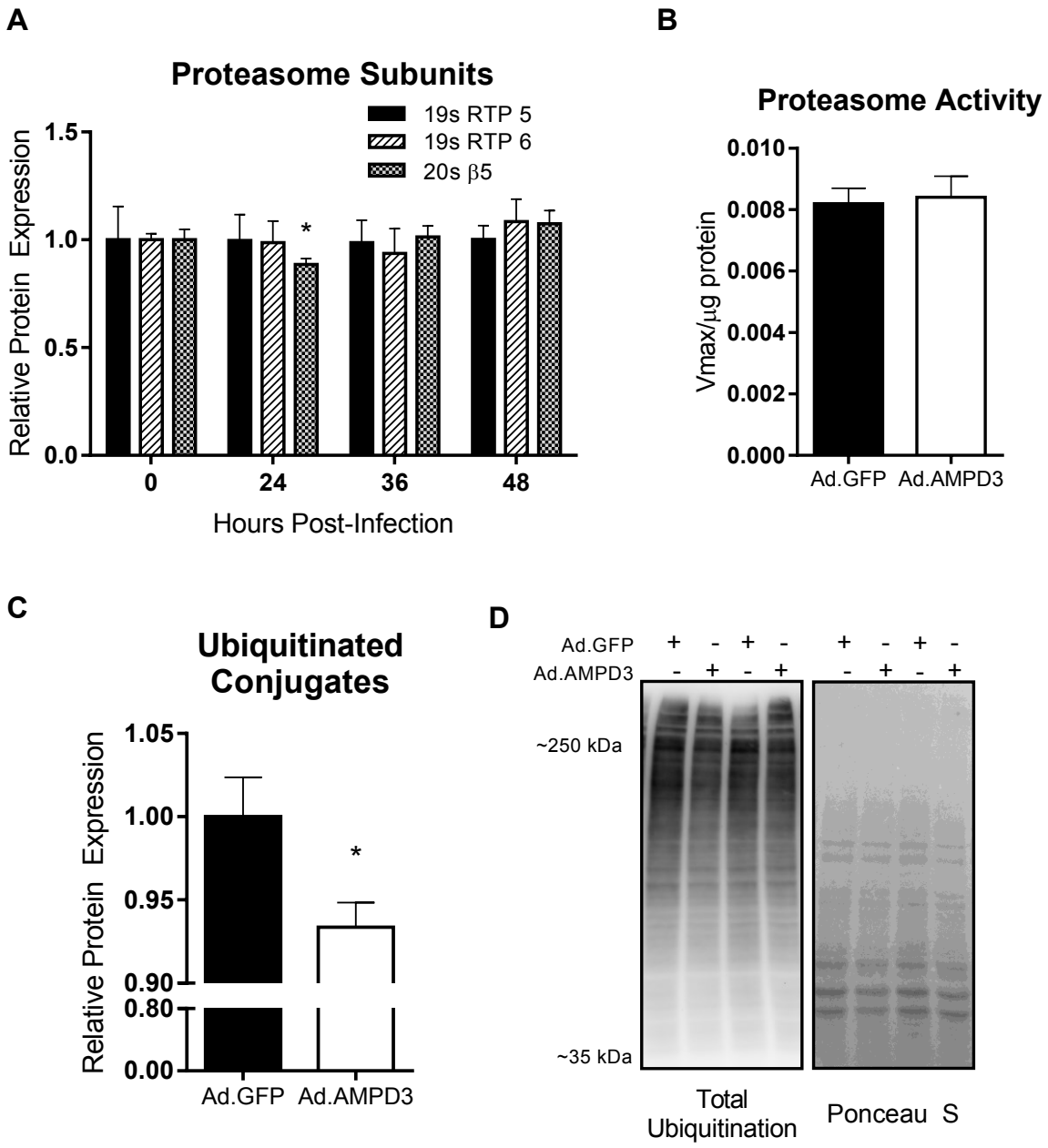

Figure 3.8. Proteasome content is not changed with AMPD3 but total ubiquitination is decreased. (A) C2C12 myotubes were infected with AMPD3 adenovirus for the indicated times following which proteins were extracted on day 7 and proteasome subunits were quantified by western blot. n=5 *p<0.05 vs time 0. (B) Proteasome activity was determined in cytosolic extracts after 48 hours of GFP or AMPD3 infection. n=9 (C) Total mono- and poly-ubiquitin was determine by western blot following 48 hours of GFP or AMPD infection. The intensity of each lane was calculated and averaged. n=5 *p<0.05. (D) Representative western blot image and corresponding Ponceau S staining. Means ± SEM

Chapter Four

Supplemental Data

Methods

Animal Procedures

Adult male CD-1 mice were purchased from Charles River (Raleigh, NC) and housed in Association for Assessment and Accreditation of Laboratory Animal Care approved housing. Mice were approximately 30 grams at the time of muscle collection. They were housed 4 mice per cage, and given free access to food and water and a 12 hr light/dark cycle. All animal procedures were approved by the East Carolina University Animal Care and Use Committee.

Expression or shRNA plasmids were transferred into skeletal muscle by electroporation, as done previously (14). In brief, mice were anesthetized with isoflurane (2-3%) in oxygen and an incision was made in the anterior lower hind limb allowing access to the EDL muscle. Plasmid DNA (0.5 μg/μl knockdown plasmids, 1.0 μg/μl overexpression plasmids) was injected lengthwise into the EDL (10 μl), using a Hamilton microliter syringe. Electrical pulses were applied using BTX ECM 830 electroporator (Holliston, MA) as the muscle was sandwiched between two opposing stainless steel paddles (10 volts, 5x20 ms pulses at 250 ms intervals). Incisions were closed with Vicryl (polyglactin 910) sutures.

Atrophy was induced by sciatic nerve sectioning as done previously at the same time as electroporation (14). An incision was made in the lateral mid-thigh of the hind limb. The sciatic nerve was exposed by blunt dissection and a 2-3 mm section was

removed. Sham operation on the contralateral limb was done to expose the sciatic nerve without sectioning the nerve. The incisions were closed with surgical glue, and buprenex (0.03 mg/kg body weight) was administered sub-cutaneously as a post-operative analgesic.

Muscle Contraction

Mice were anesthetized with isoflurane or ketamine:xylazine (100:10 mg/kg) and euthanized by cervical dislocation. The proximal and distal tendons of EDL muscles were ligated with 2.0 silk sutures and placed in oxygenated (95% O_2, 5% CO_2) Krebs-Henseleit bicarbonate buffer (25 mM $NaHCO_3$, 118 mM NaCl, 4.7 mM KCl, 1.2 mM $MgSO_4 \bullet 7H_2O$, 1.2 mM KH_2PO_4, 1.2 mM $CaCl_2 \bullet 2H_2O$, 5 mM glucose, 0.15 mM sodium pyruvate) at their approximate in vivo resting length. Muscles were maintained in the Krebs-Henseleit buffer at 37°C for approximately 40 minutes prior to contractile measurements. For the anesthesia testing (Figure 4.4), the pre-incubation was approximately five minutes.

Muscles were secured to a dual mode force transducer (Aurora Scientific) and field-stimulated via platinum electrodes (Aurora Scientific). Optimal length was determined using 0.3 ms pulses and the length tension relationship. Following another 5-10 minute rest period, muscles were either subjected to a high intensity (150 Hz pulse frequency, 500 ms train duration, 1 train per second, for 60 seconds) or low intensity (50 Hz pulse frequency, 250 ms train duration, 1 train every 2 seconds, for 600 sec) contraction protocol using 610A DMC v5.4 (Aurora Scientific) or kept at their resting length for approximately 5 additional minutes. Muscles were then rapidly cut from sutures, blotted dry, and snap frozen between liquid nitrogen cooled tongs. Contraction

characteristics were analyzed using 611A DMA software v5.2 (Aurora Scientific). Each contraction was analyzed individually using the high throughput feature. For measurements of half relaxation time, the window for analysis was set to start with the last electrical pulse of each stimulation train and end just prior to the next stimulation. Force-time integral is the area under the force-time curve for each contraction.

Cell Culture

C2C12 myoblasts were grown in Dulbecco's modified Eagle's medium (DMEM) with 10% fetal bovine serum (FBS), penicillin (100 U/mL), and streptomycin (100 µg/mL) until 75-90% confluent. Media was switched to DMEM with 2% horse serum and penicillin/streptomycin to induce differentiation into multinucleated myotubes. Adenovirus was used to overexpress GFP or AMPD3. Custom made adenovirus, serotype 5 (DE1/E3), for the co-expression of AMPD3 and GFP was purchased from Vector Biolabs (Malvern, PA). Adenoviruses infect nearly 100% of myotubes, which was confirmed visually here by GFP fluorescence.

Protein Analysis

Proteins were extracted from cells with RIPA buffer and were then quantified by BCA Assay (Pierce). Equal amounts of protein were separated by SDS-PAGE (8% polyacrylamide depending on target) then transferred to polyvinylidene difluoride (PVDF) membranes. Equal loading and transfer were confirmed by Ponceau S staining. Antibodies were purchased from Cell Signaling (FoxO1 #2880; FoxO3 #2497; P-FoxO1/3 #9464). Secondary antibody conjugated to HRP (Cell Signaling #7074) was used and visualized with Western Chemiluminesence HRP Substrate (EMD Millipore).

Band intensities were captured using a Bio-Rad Chemi Doc XRS imager and analyzed using Image Lab Software (Bio-Rad).

Nucleotide Measurements

Nucleotides were extracted from C2C12 myotubes in ice cold 0.5 N PCA. Cells were lysed by sonication, and protein was pelleted by centrifugation. Protein pellets were re-suspended in 0.2 N NaOH for protein estimation by BCA Assay (Pierce). The supernatants were neutralized by the addition of ice cold 1 N KOH and centrifugation at 4°C. Samples were stored at -80°C until analysis. Adenine nucleotide concentrations (ATP, ADP, AMP) and degradation products (IMP, adenine, and inosine) were determined by ultra-performance liquid chromatography (UPLC) using a Waters Acquity UPLC H-Class system and a Acquity UPLC HSS T3 1.8 µm, 2.1 mm X 150 mm column (Waters) as done previously (15). The adenylate energy charge was calculated as the mole fraction of ATP plus 0.5 the mole fraction of ADP as described by Atkinson (6).

AMP Binding Assay

Six day differentiated C2C12 myotubes were infected with GFP or AMPD3 expressing adenovirus for 48 hours. Media was then switched to low glucose DMEM (1g/L) with 2% horse serum, and 3 µM Nigericin (an ionophore to allow for a fall in intracellular pH) at either pH 6.5 or 7.4 for 30 minutes. A subset of wells received low glucose DMEM, 2% HS, 3 µM Nigericin, and 25 mM 2-deoxyglucose (2DG) at pH 6.5 for 0, 3, 10, or 30 minutes. A final group received low glucose DMEM, 2% HS, 3 µM Nigericin, and 25 mM 2DG at pH 7.4 for 30 minutes. After media treatments nucleotides were extracted in ice cold 0.5 N PCA and UPLC analysis was done as described above.

Tables and Figures

Table 4.1. Nucleotides in resting EDL muscles

	n	ATP*	ADP	AMP**,†	IMP**,††	Adenine	TAN + IMP
Innervated	9	3.80 ± 0.16	0.71 ± 0.04	0.017 ± 0.001	0.033 ± 0.006	0.010 ± 0.001	4.559 ± 0.197
Denervated	10	3.64 ± 0.43	0.93 ± 0.11	0.042 ± 0.011	0.168 ± 0.027	0.017 ± 0.002	4.783 ± 0.562
shAMPD3:Innervated	10	4.01 ± 0.39	0.76 ± 0.05	0.025 ± 0.006	0.036 ± 0.006	0.011 ± 0.001	4.814 ± 0.425
shAMPD3:Denervated	10	2.72 ± 0.32	0.71 ± 0.07	0.093 ± 0.013	0.862 ± 0.013	0.020 ± 0.008	4.377 ± 0.373

Values are expressed as µmol/g. Means ± SEM. TAN=Total Adenine Nucleotides. Main effect of denervation *p<0.05, **p<0.0001, main effect of knockdown †p<0.01, ††p<0.001.

Table 4.2. Nucleotides in high intensity contracted EDL muscles

	Innervated [11]	Denervated [12]	shAMPD3: Innervated [10]	shAMPD3: Denervated [10]
ATP	2.87 ± 0.25	2.43 ± 0.18	2.68 ± 0.20	2.42 ± 0.18
	(-0.93)	(-1.21)	(-1.33)	(-0.30)
ADP	1.02 ± 0.11	0.99 ± 0.07	1.00 ± 0.08	1.04 ± 0.09
	(0.30)	(0.06)	(0.24)	(0.33)
AMP*†	0.035 ± 0.004	0.055 ± 0.005	0.045 ± 0.003	0.069 ± 0.007
	(0.018)	(0.013)	(0.020)	(-0.024)
IMP	0.572 ± 0.108	0.514 ± 0.071	0.579 ± 0.095	0.563 ± 0.088
	(0.539)	(0.346)	(0.543)	(-0.299)
TAN+IMP	4.497 ± 0.442	3.983 ± 0.274	4.302 ± 0.379	4.095 ± 0.322
	(-0.062)	(-0.800)	(-0.512)	(-0.283)

Values are expressed as µmol/g. Means ± SEM. TAN=Total Adenine Nucleotides. Values in ( ) indicate difference from resting levels (Table 1). *$p<0.001$ main effect of denervation, †$p<0.05$ main effect of knockdown. n=[ ]

Table 4.3. Nucleotides in low intensity contracted EDL muscles

	n	ATP**	ADP*	AMP*	IMP	Adenine	TAN + IMP
Innervated	9	2.15 ± 0.20	0.95 ± 0.09	0.062 ± 0.008	0.935 ± 0.115	0.009 ± 0.001	4.091 ± 0.393
Denervated	10	1.55 ± 0.09	0.83 ± 0.06	0.104 ± 0.008	1.091 ± 0.105	0.020 ± 0.006	3.381 ± 0.338
shAMPD3:Innervated	9	2.22 ± 0.25	1.00 ± 0.10	0.083 ± 0.005	0.999 ± 0.160	0.010 ± 0.001	4.297 ± 0.463
shAMPD3:Denervated	9	1.28 ± 0.15	0.66 ± 0.07	0.096 ± 0.012	0.957 ± 0.127	0.020 ± 0.009	2.981 ± 0.315

Values are expressed as µmol/g. Means ± SEM. TAN=Total Adenine Nucleotides. *p<0.01, **p<0.001 main effect of denervation

Table 4.4. Nucleotides in high intensity contracted AMPD3 overexpressing EDL muscles

	n	ATP*	ADP****	AMP****	IMP	Adenine	TAN + IMP
GFP Resting	7	4.72 ± 0.23	0.85 ± 0.04	0.020 ± 0.001	ND	0.017 ± 0.002	5.569 ± 0.271
GFP Contracted	9	3.79 ± 0.22	1.29 ± 0.08	0.050 ± 0.006	0.513 ± 0.076	0.014 ± 0.001	5.822 ± 0.361
AMPD3 Resting	5	4.54 ± 0.08	0.85 ± 0.04	0.021 ± 0.005	ND	0.018 ± 0.002	5.438 ± 0.131
AMPD3 Contracted	11	4.16 ± 0.25	1.35 ± 0.08	0.050 ± 0.004	0.486 ± 0.064	0.017 ± 0.001	6.048 ± 0.380

Values are expressed as µmol/g, ND-Not Detectable. Means ± SEM. TAN=Total Adenine Nucleotides. Main effect of contraction *p<0.05, ****p<0.0001

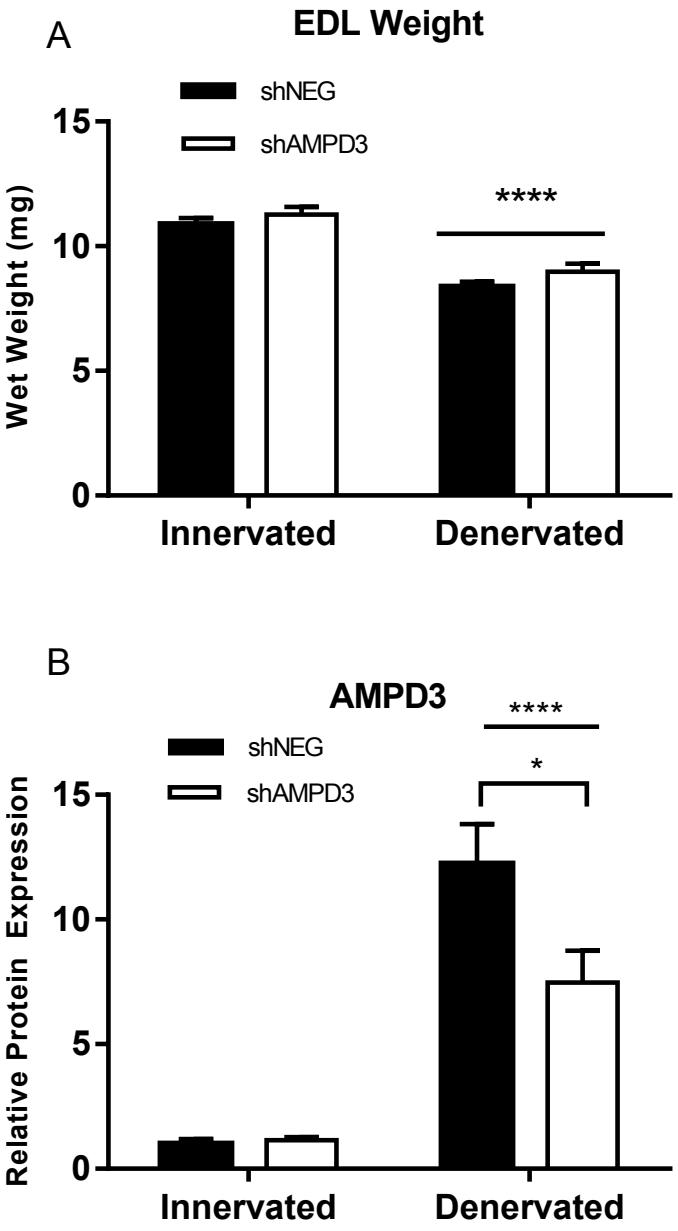

Figure 4.1. Knockdown of AMPD3 reduced AMPD3 protein content. Mouse EDL muscles were electroporated with shAMPD3 or shNEG concurrent with unilateral lower limb denervation. (A) EDL wet weights after 1-week of denervation (B) AMPD3 protein content relative to shNEG:Innervated. n=8 shNEG, 7 shAMPD3. Means ± SEM. *p<0.05 shNEG:Denervated vs. shAMPD3:Denervated, ****p<0.0001 main effect of denervation.

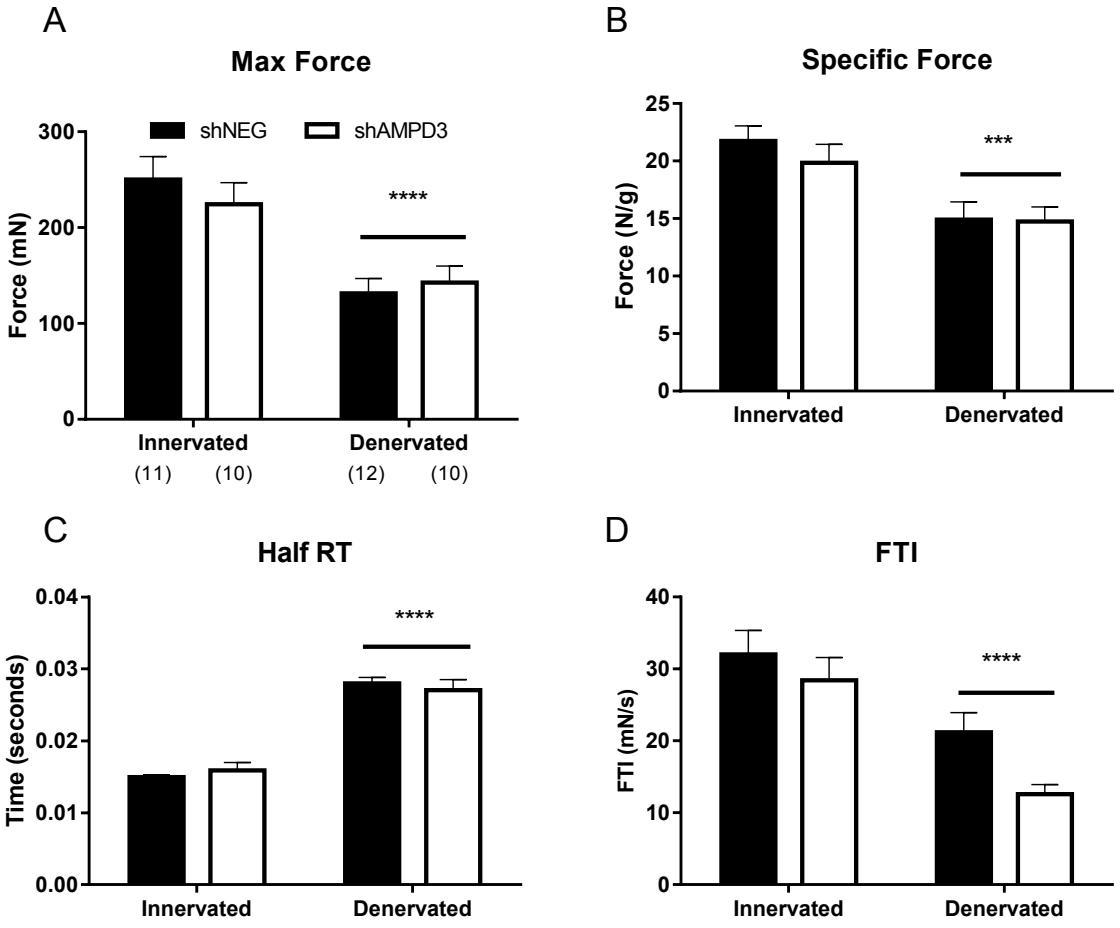

Figure 4.2. Denervation reduces Max Force, Specific Force, FTI, and increase Half RT. Contractile characteristics of the EDL in response to a single 250 Hz 160 ms electrical stimulation. (A) Absolute maximal tetanic force (B) specific tetanic force (C) half relaxation time (D) force-time integral (area under the force-time curve). Means ± SEM, Values in ( ) are n for each group. ****p<0.0001

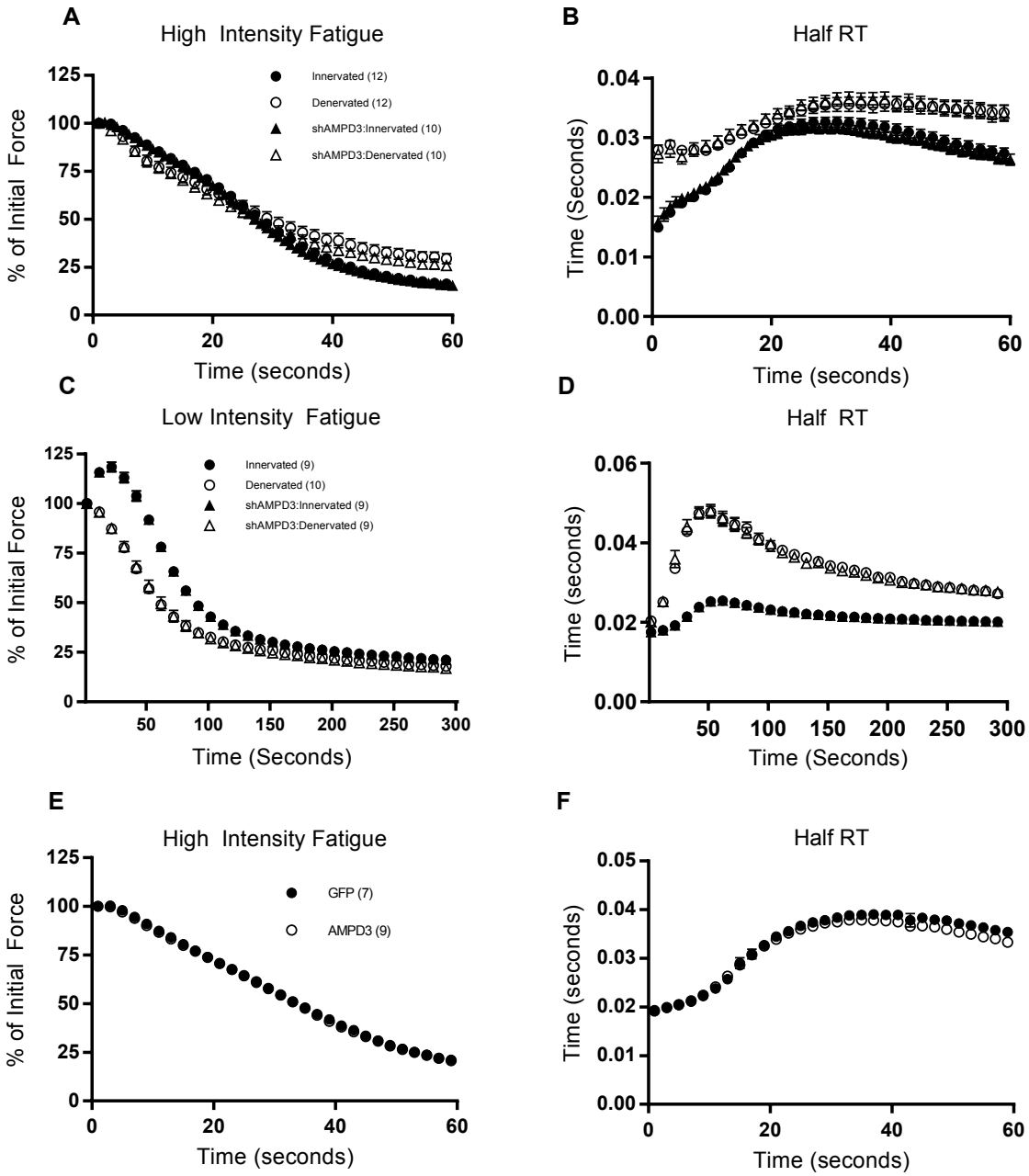

Figure 4.3. Knockdown of AMPD3 does not alter contractile performance of the EDL. Mouse EDL muscle was electrically stimulated with a high intensity fatigue protocol (250 Hz, 160 ms, 1 tetani per second, 60 seconds) or a low intensity fatigue protocol (80 Hz, 300ms, 1 contraction every 2 seconds, 300 seconds). Percent of initial force (A) and half relaxation time (B) during high intensity fatigue protocol. Percent of initial force (C) and half relaxation time (D) during low intensity fatigue protocol. Percent of initial force (E) and half relaxation time (F) in GFP or AMPD3 overexpressing EDL during high intensity fatigue protocol. Every other (A-B, E-F) or 5th contraction (C-D) plotted for clarity. Means ±SEM. n's are indicated in ( ) in figure legends.

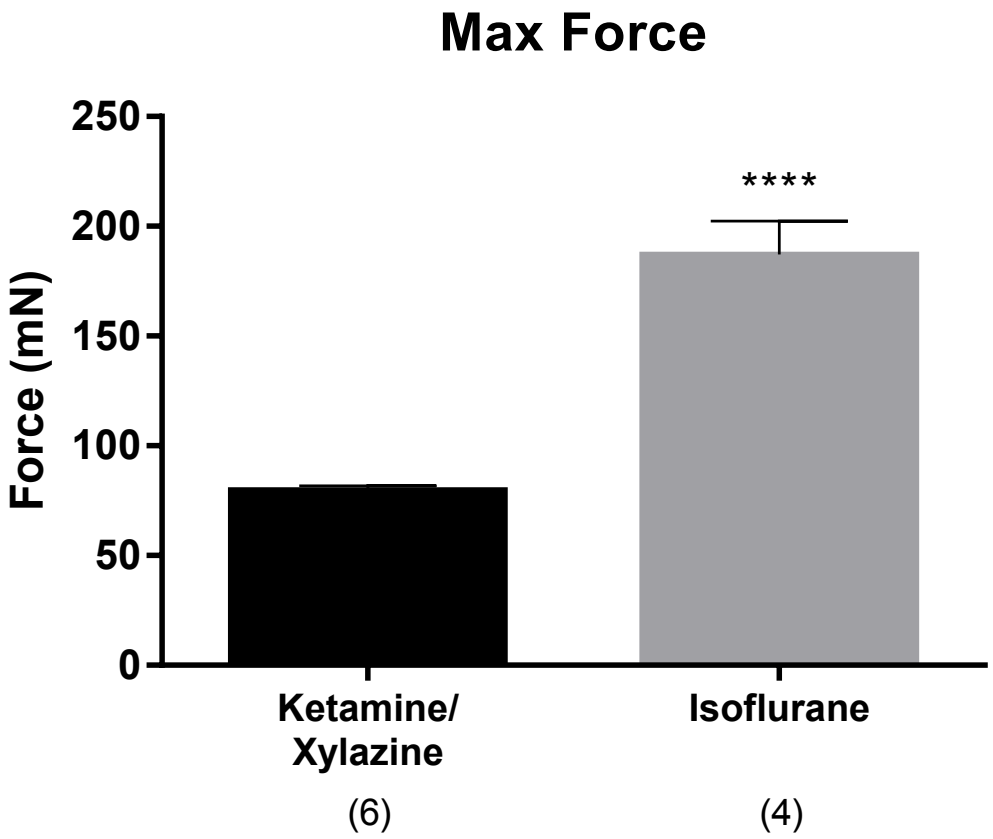

Figure 4.4. Ketamine/Xylazine reduces maximal force output. Mice were anesthetized with an intraperitoneal injection of Ketamine/Xylazine or inhaled isoflurane and euthanized by cervical dislocation. Soleus muscles were removed and stimulated once (300 Hz, 250 ms) while maximal force was recorded. Means ± SEM. n=4-6 per group.

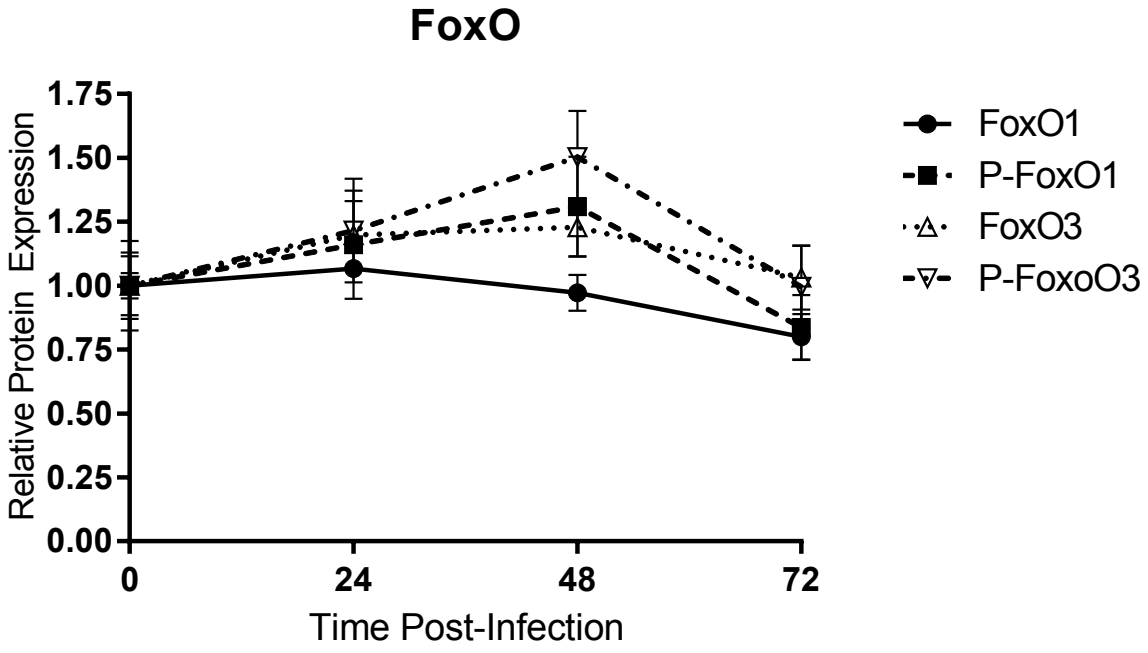

Figure 4.5. FoxO 1 and 3 expression an phosphorylation do not change with AMPD3 overexpression. Western blot analysis of C2C12 myotube homogenates following 0, 24, 48, or 72 hours of AMPD3 overexpression. Means ±SEM n=5 for all groups and time points.

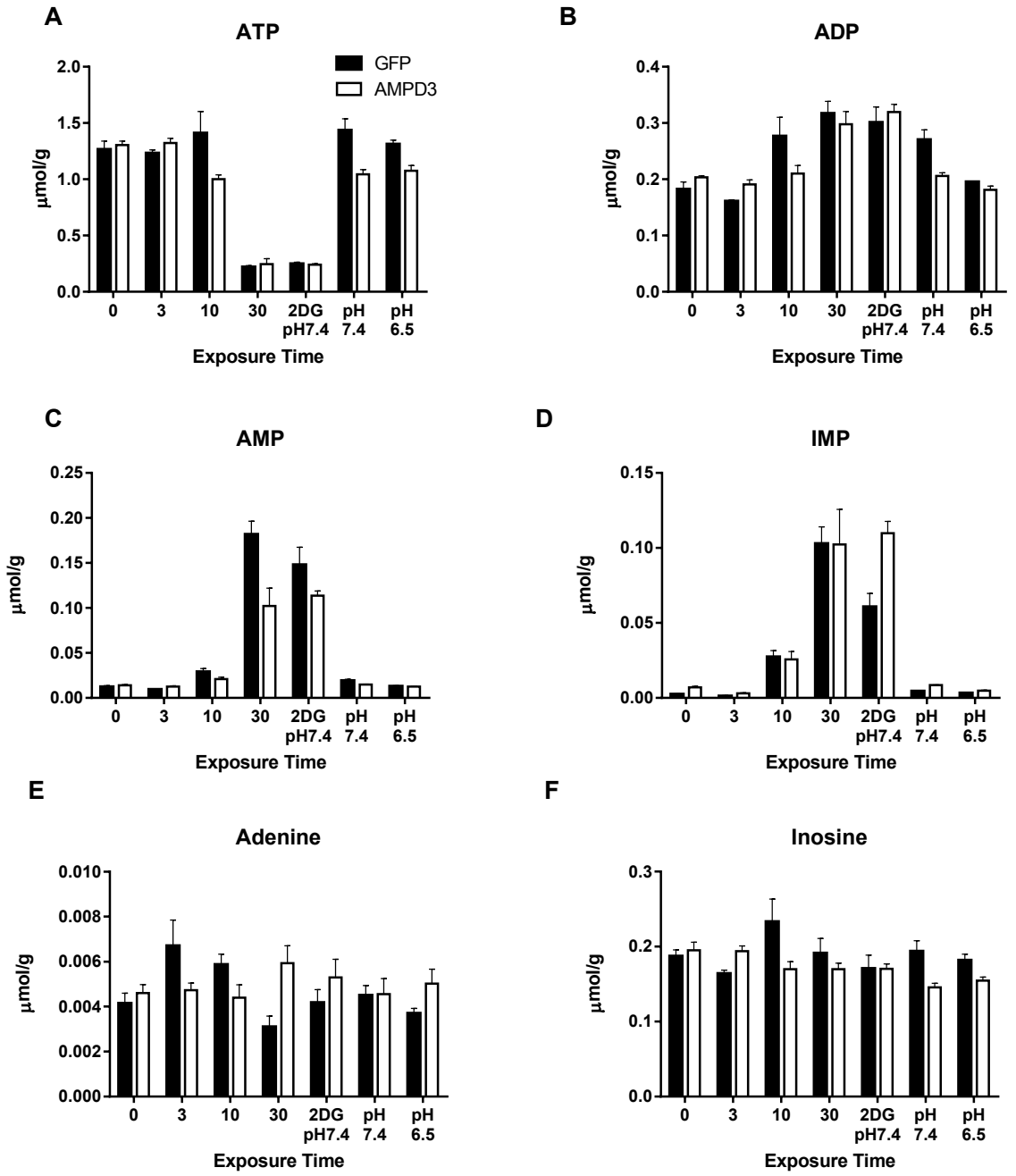

Figure 4.6. In-vivo AMPD activity. C2C12 myotubes were infected with GFP or AMPD3 encoding adenovirus for 48 hours. Media was then switched to low glucose DMEM (1g/L) with 2% horse serum, and 3 µM nigericin at either pH 6.5 (pH 6.5) or 7.4 (pH 7.4) for 30 minutes. A subset of wells received low glucose DMEM, 2% HS, 3 µM nigericin, and 25 mM 2-deoxyglucose (2DG) at pH 6.5 for 0, 3, 10, or 30 minutes (0, 3, 10, 30). A final group received low glucose DMEM, 2% HS, 3 µM Nigericin, and 25 mM 2DG at pH 7.4 for 30 minutes (2DG 7.4). After media treatments nucleotides were extracted in ice cold 0.5 N PCA and analyzed by UPLC. n=4

Chapter Five

Summary and Conclusions

Skeletal muscle atrophy is regulated, at least in part, by a coordinated transcriptional program of atrophy related genes termed atrogenes (81, 130). Since their discovery, research into the regulation, functions, and mechanisms of various individual atrogenes has greatly advanced the understanding of skeletal muscle atrophy. Despite these advances, exercise remains the only effective treatment of atrophy. The discovery of novel regulators of muscle atrophy is a high priority of research within the field. The purpose of the present project was to investigate the potential of AMPD3, one of the most highly upregulated atrogenes (up to 100-fold) (81, 97), to regulate muscle atrophy. Little research on AMPD3 within the context of muscle atrophy has been published.

AMPD has two known functions in skeletal muscle. The first is to provide maintenance of the ΔG_{ATP} during high energy demands (55, 91). The second is to regulate of the size of the total adenine nucleotide pool (20, 132). Interestingly during atrophy there are reductions in both the ΔG_{ATP} (29, 42, 54, 77, 110) and in [ATP] (46, 140), which is the major component of the total adenine nucleotide pool. It is unknown if the upregulation of AMPD3 during atrophy is in response to the reduced ΔG_{ATP}, or if contributes to the atrophic phenotype and reduced [ATP]. In order to better understand the role of AMPD3 in atrophy, two independent studies were designed to answer the following hypotheses; 1) Knockdown of AMPD3 during atrophy will result in impairments of muscle half relaxation time; and 2) Overexpression of AMPD3 will reduced the adenine nucleotide pool and increase protein degradation.

Collectively, this dissertation serves to define the role of AMPD3 upregulation during atrophy. Herein evidence is presented that demonstrates that; i) muscle contractile performance is impaired during atrophy; ii) the upregulation of AMPD3 during atrophy improves muscle half relaxation, iii) increased AMPD3 expression degrades the adenine nucleotide pool; iv) AMPD3 overexpression accelerates overall protein degradation; and v) the ubiquitin proteasome pathway may be activated as a result of AMPD3 overexpression.

Denervation impairs contractile functions

First, muscle contractile performance in isolated soleus and extensor digitorum longus (EDL) muscles of mice were measured after one week of unilateral lower hind limb denervation. Surprisingly, one week of denervation atrophy did not result is a significantly reduced maximal force in soleus muscles (Figure 2.3A) but it did the EDL (Figure 4.2A). A loss of force was anticipated in the denervated muscles similar to the findings of Schulte et al. (139), but other groups have also reported no or little force reduction after only one week of denervation (92, 160). Increased half relaxation time in both the soleus (Figure 2.3C) and EDL (Figure 4.2C) was detected, which is consistent with past findings in denervation (2, 53, 139) as well as other models of atrophy (119, 123). This seems to be due to factors of Ca^{2+} handling unrelated to the energetic state of the cell, as there were no measurable differences in the nucleotides of the resting muscles (Table 2.2). A possible explanation of the increased relaxation time could be partially depolarized mitochondria during atrophy which have been shown to contribute to dysfunctional Ca^{2+} clearance from the sarcoplasm (159). Decreases in parvalbumin

can impair Ca^{2+} clearance but this is an unlikely factor in the soleus muscle since there is little parvalbumin in type I fibers (60).

This study extends the previous findings related to muscle relaxation during atrophy to measure half relaxation time during a 60 second high intensity fatigue protocol. After 5 seconds of intense contractions, half relaxation time is shorter in denervated soleus muscles (Figure 2.4) but not in the EDL (Figure 4.3). This decrease in half relaxation time is transient and by approximately 45 seconds both innervated and denervated muscles have the same half relaxation time. Over this 40 second window, where relaxation is shorter, the muscles are fatiguing which indicates ATP consumption may be outpacing ATP supply, a condition when AMPD activity is very important to maintain muscle performance. The decrease in half relaxation time during the fatigue protocol is likely due to the upregulation of AMPD3 during atrophy, which will be discussed in the next section.

Denervation atrophy results in an increase in the fatigability of the muscle, which agrees with what has been previously reported (53, 92, 131, 160). This was apparent in both high and low intensity fatigue protocols. The increased fatigability of the denervated muscle is likely in response to a reduced mitochondrial content and function, which has been well documented in atrophy (14, 29, 108, 156).

AMPD3 influence on muscle contractile performance

Second, this study shows the role of AMPD3 during atrophy on muscle performance. By electroporating a shRNA plasmid targeted to AMPD3 into muscle the atrophy induced upregulation of AMPD3 was attenuated. This type of study design allowed for the determination of the specific effects of AMPD3 upregulation on muscle

performance. As already mentioned, denervation increases half relaxation time of a single tetanic contraction. Knockdown of AMPD3 combined with denervation has an additive effect to further increase half relaxation time only in the soleus (Figure 2.3C). It appears then that the upregulation of AMPD3 during atrophy attenuates increased muscle relaxation.

During high intensity contractions knockdown of AMPD3 increased relaxation time in both innervated and denervated muscles when compared to the innervated and denervated controls respectively. These differences were not explained by changes in SERCA isoform or content. The most likely explanation for the slowed relaxation of muscles while AMPD3 is knocked down could be reduced SERCA activity due to a reduced ΔG_{ATP}, which would increase the Ca^{2+} transit time and prolong muscle relaxation. SERCA requires a large yield of the ΔG_{ATP} to maintain the ~1:10,000 Ca^{2+} gradient across the endoplasmic reticulum (21, 59). Previous observations put the free energy requirement of the SERCA (ΔG_{SERCA}) around 50 kJ/mol (21, 59, 80), while ΔG_{ATP} in resting muscle typically yields -60-65kJ/mol (21, 56). This small difference in the energy requirements of SERCA and available energy from ATP hydrolysis highlights how important maintenance of the ΔG_{ATP} is to preserve normal function of the muscle. Even with small reductions in the ΔG_{ATP} (<5 kJ/mol), Dawson et al. saw slowed relaxation in frog skeletal muscle (35). Additionally, slowed relaxation has been observed in wild type mice during a high intensity fatigue protocol where the ΔG_{ATP} was -52.8 kJ/mol (56). In the adenylate kinase knockout mouse, relaxation was further impaired during the high intensity contraction protocol, where the calculated ΔG_{ATP} was

-45.6 kJ/mol (56). These previous studies clearly demonstrate the sensitivity of SERCA to ΔG_{ATP} and this study falls in line with those observations.

Taken together, these results indicate that knockdown of AMPD3 in both innervated and denervated muscle slows muscle relaxation during high intensity contractions, likely as a result of a reduced ΔG_{ATP} and reduced SERCA activity. This seems to be somewhat inconsistent with the understanding that AMPD3 is inactivated with a reduced pH (86, 87, 111), such as during contraction. However, there are two possible explanations that could address this inconsistency. First, the affinity of AMPD1 to bind myosin may be greater than affinity of AMPD3 to bind to membranes. This would suggest that any tetramers that contained AMPD1 subunits, would preferentially bind to myosin rather than bind to membranes. The result would be activation of AMPD1 and an increase in activity. The second explanation would be that AMPD3 may act as an AMP sink during high energy demands. In this model, during low pH, AMPD3 would bind to membranes with a subsequent inhibition of its catalytic ability. However, AMP would still to bind to AMPD3 without undergoing catalytic degradation. In this scenario, increased AMP binding would reduce the [AMP] and favor the forward reaction of AK and maintenance of the ΔG_{ATP}. This would be a favorable scenario as this would attenuate the loss of adenine nucleotides during high energy demands. Future studies would need to address the potential of AMPD3 to bind AMP without degrading it.

The lack of any different contractile characteristics in the EDL with AMPD3 knockdown suggests that there is sufficient total AMPD activity from contributions of AMPD1, that the increase in AMPD3 does not supply additional maintenance of the

ΔG_{ATP}. This is supported by previous findings that the EDL has a much higher AMPD1 content and total AMPD activity than the soleus (120).

AMPD3 controls the size of the adenine nucleotide pool.

ATP, ADP, and AMP can all be rapidly interconverted between each other by the transfer, removal, or addition of phosphate groups by ATPases, ATP synthases, adenylate kinase (AK), and creatine kinase. The ratio of free metabolically available ATP/ADP/AMP is maintained roughly around 1,000,000/1,000/1. AMPD reaction is important during high energy demands when the ratio of ATP/ADP/AMP is shifted toward AMP. Removal of AMP helps to shift this ratio back toward ATP. But the removal of AMP over time will decrease the total adenine nucleotide pool. Because of this, AMPD can exercise control over or regulate the total adenine nucleotide pool. Overexpression of AMPD3 in C2C12 myotubes led to a loss of [ATP], [ADP], and total adenine nucleotides (Figure 3.3). Additionally, there was an increase in [IMP] while the adenylate energy charge remained constant. These findings stand in slight contrast to the findings of Plaideau et al., who did not see differences in total adenine nucleotides when AMPD1 or AMPD2 were overexpressed in HEK 293t cells (113). However, this is likely because AMPD3, appears to be the most active of the three isoforms under basal conditions.

All three isoforms have an actomyosin binding domain in the C-terminal while only AMPD1 has an N-terminal sequence that promotes binding to myosin (86). Both AMPD2 and AMPD3 have N-terminal sequences that suppress binding to myosin with AMPD3 exhibiting the stronger suppression (86, 87). AMPD1 will bind to myosin with a resultant increase in activity, during muscle contractions and lower pH (40, 66, 126,

127). Conversely, AMPD3 is more active basally but when pH is reduced, it binds to membranes (111) with a subsequent reduction in activity (87). Little is known about the regulation of AMPD2 and it isn't expressed in skeletal muscle. The increase in AMPD3 during atrophy suggests a shift in the control of AMPD to a more basally active AMPD tetramer and explains the loss of adenine nucleotides seen in this study and likely the loss of [ATP] in other models of atrophy (33, 42, 46, 92, 140).

AMPD3 accelerates protein degradation.

A very exciting finding of this study is that AMPD3 overexpression accelerates protein degradation. When AMPD3 was overexpressed in C2C12 myotubes the degradation of long-lived proteins was accelerated (figure 3.5). The increase in protein degradation rate resulted in, and fully accounted for a loss of total protein. In further support of the increased protein degradation, myotubes atrophied with AMPD3 overexpression. This was demonstrated by smaller myotubes in AMPD3 infected cells (Figure 3.6). There was no change in the protein synthesis rate with AMPD3 overexpression which is in agreement with the net loss of protein.

Protein degradation in dominated by two different pathways, the ubiquitin-proteasome and the autophagy-lysosome. The increase in protein degradation would likely result in an increase of either or both of these protein degradation pathways. However, the increase in total protein degradation was not explained by any change in estimated flux of autophagy or in ULK1 (Figure 3.7). Additionally, the content of the proteasome did not change with AMPD3 overexpression (Figure 3.8). The activity of the chymotrypsin-like site of the proteasome, determined in-vitro with a fixed [ATP] of 0.72 mM, was not different between GFP or AMPD3 groups (Figure 3.8). This measurement

takes place in-vitro with an exogenous supply of ATP which masks intracellular ATP concentration across samples and therefore does not reflect the intracellular ATP conditions Additionally, the Suc-LLVY-AMC peptide does not need to be ubiquitinated in order to enter the proteasome. These are important distinctions to make, since reduced intracellular ATP levels have been shown to activate the proteasome (24, 32, 49, 69, 84) and there is a significant loss of [ATP] in AMPD3 infected cells (Figure 3.3). This mechanism will be discussed in more detail in the next section.

AMPD3 increases protein degradation by activation the 26S proteasome with reduced [ATP]

AMPD3 overexpression resulted in an increase in overall protein degradation but no apparent change in the two major protein degradation pathways, autophagy or proteasome. This was somewhat puzzling as the increase in protein degradation could not be attributed to either of these two pathways. A search of the literature revealed that reduced [ATP] has been shown to activate the 26S proteasome (24, 32, 49, 69, 84). This may explain why the in-vitro proteasome activity assay (Figure 3.8) was unable to detect any differences with AMPD3 overexpression.

The mechanism behind the increased proteasome activity with reduced [ATP] was proposed by Smith et al. (142) who argue that when 4 ATP molecules bind the 19s cap there is suboptimal joining with the 20s core. However, when only 2 ATP molecules bind the 19s cap it allows for a better association with the 20s core to form the 26s proteasome and results in maximal catalytic activity. The likelihood of ATP binding to the 19s cap is dependent on the concentration of ATP within the cell. The reduction in [ATP] with AMPD3 overexpression would be expected to decrease ATP binding to the

19s cap, which results in a greater formation of the 26s proteasome and increased proteasome activity in-vivo.

Furthering the idea that the reduction of [ATP] activates the proteasome is the observation of a reduction in the ubiquitination of protein when AMPD3 is overexpressed. This is in contrast to what happens during atrophy, when total protein ubiquitination increases markedly (6, 31, 32). The activation of the entire set of atrogenes during atrophy (81, 130) directly upregulates the major muscle ubiquitin ligases, Atrogin-1 (135) and MuRF (27). When a single atrogene, AMPD3, is overexpressed, the entire atrogene profile is not expected to be activated, and any increases in Atrogin-1 or MuRF are not anticipated. This is supported by the lack of any increase in content or phosphorylation of the major atrophy related transcription factors (FoxO1 and FoxO3), with AMPD3 treatment (Figure 4.5). If the rate of ubiquitination is unchanged and the activity of the proteasome is increased, it follows that there would be a decrease in the amount of total ubiquitination. This is exactly what was observed in this study (Figure 3.8). These results indicate that AMPD3 overexpression activates the 26S proteasome but does not increase ubiquitination. Future studies will need to address the in-vivo proteasome activity during AMPD3 overexpression to determine if the loss of [ATP] by AMPD3 can activate the proteasome.

Taken together, these studies highlight the known functions of AMPD and their involvement in atrophy. First, AMPD helps to maintain ΔG_{ATP} during high energy demands. During atrophy, the upregulation of AMPD3 helps to maintain or prevent further reductions of the ΔG_{ATP} during intense muscle contraction. This was demonstrated by improved muscle relaxation kinetics when AMPD3 was upregulated

during atrophy and impaired relaxation kinetics when AMPD3 was knockdown during atrophy. The relaxation kinetics of the muscle is indicative of the ΔG_{ATP} because SERCA is dependent on a large ΔG_{ATP}. Secondly, AMPD3 acts as a regulator of the total adenine nucleotide pool. Overexpression of AMPD3 in C2C12 myotubes led to a loss of adenine nucleotides. This seems to be partly due to AMPD3 being more active under basal/resting conditions. Furthermore, the reduction of [ATP] leads to an activation the proteasome and increased protein degradation. These findings are exciting in that they identify AMPD3 as a novel regulator of skeletal muscle performance and protein degradation during atrophy.

As there is currently a lack of practical treatments for skeletal muscle atrophy available, the identification of AMPD3, and perhaps energetics in general, as regulators of atrophy necessitates further investigation into treatments that could inhibit AMPD during atrophy. Clinically, inhibition of AMPD3 during conditions of atrophy may slow the rate of protein degradation and perhaps spare some muscle mass while the underlying cause of the atrophy is treated (i.e. cancer, injury, organ failure, etc.). The inhibition of AMPD3 may lead to slower muscle relaxation in slow type I fibers but not in fast type II fibers. This would likely be of little consequence to the quality of life of an atrophy patient as the need for a rapid succession of contractions is not common. On the other hand, inhibition of AMPD3 may improve maximal tetanic force in type I fibers which may be a large benefit in conditions of atrophy, where maximal force output is being lost. Overall, the benefits of AMPD3 inhibition during atrophy may outweigh the costs, but more research is necessary to fully explore the cost vs benefit balance.

References

1. **Admyre T, Amrot-Fors L, Andersson M, Bauer M, Bjursell M, Drmota T, Hallen S, Hartleib-Geschwindner J, Lindmark B, Liu J, Lofgren L, Rohman M, Selmi N, and Wallenius K**. Inhibition of AMP deaminase activity does not improve glucose control in rodent models of insulin resistance or diabetes. *Chem Biol* 21: 1486-1496, 2014.

2. **Agbulut O, Vignaud A, Hourde C, Mouisel E, Fougerousse F, Butler-Browne GS, and Ferry A**. Slow myosin heavy chain expression in the absence of muscle activity. *Am J Physiol Cell Physiol* 296: C205-214, 2009.

3. **Allen MD, Kimpinski K, Doherty TJ, and Rice CL**. Decreased muscle endurance associated with diabetic neuropathy may be attributed partially to neuromuscular transmission failure. *J Appl Physiol (1985)* 118: 1014-1022, 2015.

4. **Anker SD, Ponikowski P, Varney S, Chua TP, Clark AL, Webb-Peploe KM, Harrington D, Kox WJ, Poole-Wilson PA, and Coats AJ**. Wasting as independent risk factor for mortality in chronic heart failure. *Lancet* 349: 1050-1053, 1997.

5. **Ashley Z, Salmons S, Boncompagni S, Protasi F, Russold M, Lanmuller H, Mayr W, Sutherland H, and Jarvis JC**. Effects of chronic electrical stimulation on long-term denervated muscles of the rabbit hind limb. *J Muscle Res Cell Motil* 28: 203-217, 2007.

6. **Atkinson DE**. The energy charge of the adenylate pool as a regulatory parameter. Interaction with feedback modifiers. *Biochemistry* 7: 4030-4034, 1968.

7. **Begum SJ, Reddy MM, Ramakrishna O, Indira K, and Swami KS**. Skeletal muscle protein metabolism under denervation atrophy in dog, Canis domesticus. *Indian J Physiol Pharmacol* 30: 341-346, 1986.

8. **Berg HE, Larsson L, and Tesch PA**. Lower limb skeletal muscle function after 6 wk of bed rest. *J Appl Physiol (1985)* 82: 182-188, 1997.

9. **Bernard S, LeBlanc P, Whittom F, Carrier G, Jobin J, Belleau R, and Maltais F**. Peripheral muscle weakness in patients with chronic obstructive pulmonary disease. *Am J Respir Crit Care Med* 158: 629-634, 1998.

10. **Blazkiewicz M, Sundar L, Healy A, Ramachandran A, Chockalingam N, and Naemi R**. Assessment of lower leg muscle force distribution during isometric ankle dorsi and plantar flexion in patients with diabetes: a preliminary study. *J Diabetes Complications* 29: 282-287, 2015.

11. **Bodine SC, Latres E, Baumhueter S, Lai VK, Nunez L, Clarke BA, Poueymirou WT, Panaro FJ, Na E, Dharmarajan K, Pan ZQ, Valenzuela DM,**

DeChiara TM, Stitt TN, Yancopoulos GD, and Glass DJ. Identification of ubiquitin ligases required for skeletal muscle atrophy. *Science* 294: 1704-1708, 2001.

12. **Bollinger LM, Powell JJ, Houmard JA, Witczak CA, and Brault JJ**. Skeletal muscle myotubes in severe obesity exhibit altered ubiquitin-proteasome and autophagic/lysosomal proteolytic flux. *Obesity (Silver Spring)* 23: 1185-1193, 2015.

13. **Bollinger LM, Witczak CA, Houmard JA, and Brault JJ**. SMAD3 augments FoxO3-induced MuRF-1 promoter activity in a DNA-binding-dependent manner. *Am J Physiol Cell Physiol* 307: C278-287, 2014.

14. **Brault JJ, Jespersen JG, and Goldberg AL**. Peroxisome proliferator-activated receptor gamma coactivator 1alpha or 1beta overexpression inhibits muscle protein degradation, induction of ubiquitin ligases, and disuse atrophy. *J Biol Chem* 285: 19460-19471, 2010.

15. **Brault JJ, Pizzimenti NM, Dentel JN, and Wiseman RW**. Selective inhibition of ATPase activity during contraction alters the activation of p38 MAP kinase isoforms in skeletal muscle. *J Cell Biochem* 114: 1445-1455, 2013.

16. **Brault JJ, and Terjung RL**. Purine salvage to adenine nucleotides in different skeletal muscle fiber types. *J Appl Physiol* 91: 231-238, 2001.

17. **Brocca L, Cannavino J, Coletto L, Biolo G, Sandri M, Bottinelli R, and Pellegrino MA**. The time course of the adaptations of human muscle proteome to bed rest and the underlying mechanisms. *J Physiol* 590: 5211-5230, 2012.

18. **Cannavino J, Brocca L, Sandri M, Grassi B, Bottinelli R, and Pellegrino MA**. The role of alterations in mitochondrial dynamics and PGC-1alpha over-expression in fast muscle atrophy following hindlimb unloading. *J Physiol* 593: 1981-1995, 2015.

19. **Chapman AG, and Atkinson DE**. Stabilization of adenylate energy charge by the adenylate deaminase reaction. *J Biol Chem* 248: 8309-8312, 1973.

20. **Chapman AG, Miller AL, and Atkinson DE**. Role of the adenylate deaminase reaction in regulation of adenine nucleotide metabolism in Ehrlich ascites tumor cells. *Cancer Res* 36: 1144-1150, 1976.

21. **Chen W, Steenbergen C, Levy LA, Vance J, London RE, and Murphy E**. Measurement of free Ca2+ in sarcoplasmic reticulum in perfused rabbit heart loaded with 1,2-bis(2-amino-5,6-difluorophenoxy)ethane-N,N,N',N'-tetraacetic acid by 19F NMR. *J Biol Chem* 271: 7398-7403, 1996.

22. **Cheng J, Morisaki H, Toyama K, Ikawa M, Okabe M, and Morisaki T**. AMPD3-deficient mice exhibit increased erythrocyte ATP levels but anemia not improved due to PK deficiency. *Genes Cells* 17: 913-922, 2012.

23. **Chetty CS, Naidu RC, Rajendra W, Indira K, and Swami KS**. AMP-deaminase activity in denervation atrophy of the amphibian skeletal muscle. *Arch Int Physiol Biochim* 89: 51-55, 1981.

24. **Chu-Ping M, Vu JH, Proske RJ, Slaughter CA, and DeMartino GN**. Identification, purification, and characterization of a high molecular weight, ATP-dependent activator (PA700) of the 20 S proteasome. *J Biol Chem* 269: 3539-3547, 1994.

25. **Ciciliot S, Rossi AC, Dyar KA, Blaauw B, and Schiaffino S**. Muscle type and fiber type specificity in muscle wasting. *Int J Biochem Cell Biol* 45: 2191-2199, 2013.

26. **Clark BC, and Manini TM**. Functional consequences of sarcopenia and dynapenia in the elderly. *Curr Opin Clin Nutr Metab Care* 13: 271-276, 2010.

27. **Cohen S, Brault JJ, Gygi SP, Glass DJ, Valenzuela DM, Gartner C, Latres E, and Goldberg AL**. During muscle atrophy, thick, but not thin, filament components are degraded by MuRF1-dependent ubiquitylation. *J Cell Biol* 185: 1083-1095, 2009.

28. **Cohen S, Zhai B, Gygi SP, and Goldberg AL**. Ubiquitylation by Trim32 causes coupled loss of desmin, Z-bands, and thin filaments in muscle atrophy. *J Cell Biol* 198: 575-589, 2012.

29. **Constantinou C, Fontes de Oliveira CC, Mintzopoulos D, Busquets S, He J, Kesarwani M, Mindrinos M, Rahme LG, Argiles JM, and Tzika AA**. Nuclear magnetic resonance in conjunction with functional genomics suggests mitochondrial dysfunction in a murine model of cancer cachexia. *Int J Mol Med* 27: 15-24, 2011.

30. **Cooke R, and Pate E**. The effects of ADP and phosphate on the contraction of muscle fibers. *Biophys J* 48: 789-798, 1985.

31. **Cortopassi F, Celli B, Divo M, and Pinto-Plata V**. Longitudinal changes in hand grip strength, hyperinflation and 6-minute walk distance in COPD patients and a control group. *Chest* 2015.

32. **Dahlmann B, Kuehn L, and Reinauer H**. Studies on the activation by ATP of the 26 S proteasome complex from rat skeletal muscle. *Biochem J* 309 (Pt 1): 195-202, 1995.

33. **Daneryd P, Karlberg I, Schersten T, and Soussi B**. Cytochrome c oxidase and purine nucleotides in skeletal muscle in tumour-bearing exercising rats. *Eur J Cancer* 28A: 773-777, 1992.

34. **Davies JM, Poole RJ, and Sanders D**. The computed free energy change of hydrolysis of inorganic pyrophosphate and ATP: apparent significance. for inorganic-pyrophosphate-driven reactions of intermediary metabolism. *Biochimica et Biophysica Acta (BBA) - Bioenergetics* 1141: 29-36, 1993.

35. **Dawson MJ, Gadian DG, and Wilkie DR**. Mechanical relaxation rate and metabolism studied in fatiguing muscle by phosphorus nuclear magnetic resonance. *J Physiol* 299: 465-484, 1980.

36. **de Boer MD, Selby A, Atherton P, Smith K, Seynnes OR, Maganaris CN, Maffulli N, Movin T, Narici MV, and Rennie MJ**. The temporal responses of protein synthesis, gene expression and cell signalling in human quadriceps muscle and patellar tendon to disuse. *J Physiol* 585: 241-251, 2007.

37. **Debold EP, Dave H, and Fitts RH**. Fiber type and temperature dependence of inorganic phosphate: implications for fatigue. *Am J Physiol Cell Physiol* 287: C673-681, 2004.

38. **Desplanches D, Mayet MH, Sempore B, and Flandrois R**. Structural and functional responses to prolonged hindlimb suspension in rat muscle. *J Appl Physiol* 63: 558-563, 1987.

39. **DiMauro S, Miranda AF, Hays AP, Franck WA, Hoffman GS, Schoenfeldt RS, and Singh N**. Myoadenylate deaminase deficiency--muscle biopsy and muscle culture in a patient with gout. *J Neurol Sci* 47: 191-202, 1980.

40. **Dudley GA, and Terjung RL**. Influence of acidosis on AMP deaminase activity in contracting fast-twitch muscle. *Am J Physiol* 248: C43-50, 1985.

41. **Dudley GA, Tullson PC, and Terjung RL**. Influence of mitochondrial content on the sensitivity of respiratory control. *J Biol Chem* 262: 9109-9114, 1987.

42. **Fewell JG, and Moerland TS**. Responses of mouse fast and slow skeletal muscle to streptozotocin diabetes: myosin isoenzymes and phosphorous metabolites. *Mol Cell Biochem* 148: 147-154, 1995.

43. **Fischer H, Esbjornsson M, Sabina RL, Stromberg A, Peyrard-Janvid M, and Norman B**. AMP deaminase deficiency is associated with lower sprint cycling performance in healthy subjects. *J Appl Physiol* 103: 315-322. Epub 2007 Apr 2026., 2007.

44. **Fishbein WN, Armbrustmacher VW, and Griffin JL**. Myoadenylate deaminase deficiency: a new disease of muscle. *Science* 200: 545-548, 1978.

45. **Fishbein WN, Sabina RL, Ogasawara N, and Holmes EW**. Immunologic evidence for three isoforms of AMP deaminase (AMPD) in mature skeletal muscle. *Biochimica et Biophysica Acta (BBA) - Protein Structure and Molecular Enzymology* 1163: 97-104, 1993.

46. **Fontes-Oliveira CC, Busquets S, Toledo M, Penna F, Aylwin MP, Sirisi S, Silva AP, Orpi M, Garcia A, Sette A, Genovese MI, Olivan M, Lopez-Soriano FJ, and Argiles JM**. Mitochondrial and sarcoplasmic reticulum abnormalities in cancer cachexia: Altered energetic efficiency? *Biochim Biophys Acta* 2012.

47. **Fortuin FD, Morisaki T, and Holmes EW**. Subunit composition of AMPD varies in response to changes in AMPD1 and AMPD3 gene expression in skeletal muscle. *Proc Assoc Am Physicians* 108: 329-333., 1996.

48. **Geiger PC, Cody MJ, Macken RL, Bayrd ME, and Sieck GC**. Effect of unilateral denervation on maximum specific force in rat diaphragm muscle fibers. *J Appl Physiol (1985)* 90: 1196-1204, 2001.

49. **Geng Q, Romero J, Saini V, Baker TA, Picken MM, Gamelli RL, and Majetschak M**. A subset of 26S proteasomes is activated at critically low ATP concentrations and contributes to myocardial injury during cold ischemia. *Biochem Biophys Res Commun* 390: 1136-1141, 2009.

50. **Gineviciene V, Jakaitiene A, Pranculis A, Milasius K, Tubelis L, and Utkus A**. AMPD1 rs17602729 is associated with physical performance of sprint and power in elite Lithuanian athletes. *BMC Genet* 15: 58, 2014.

51. **Glass D, and Roubenoff R**. Recent advances in the biology and therapy of muscle wasting. *Ann N Y Acad Sci* 1211: 25-36, 2010.

52. **Glitsch HG, and Tappe A**. Change of Na+ pump current reversal potential in sheep cardiac Purkinje cells with varying free energy of ATP hydrolysis. *J Physiol* 484 (Pt 3): 605-616, 1995.

53. **Gundersen K**. Early effects of denervation on isometric and isotonic contractile properties of rat skeletal muscles. *Acta Physiol Scand* 124: 549-555, 1985.

54. **Hamaguchi M**. The study of energy metabolism in denervated skeletal muscle with 31P-NMR. *Comp Biochem Physiol A Comp Physiol* 97: 433-437, 1990.

55. **Hancock CR, Brault JJ, and Terjung RL**. Protecting the cellular energy state during contractions: role of AMP deaminase. *J Physiol Pharmacol* 57 Suppl 10: 17-29, 2006.

56. **Hancock CR, Janssen E, and Terjung RL**. Skeletal muscle contractile performance and ADP accumulation in adenylate kinase-deficient mice. *Am J Physiol Cell Physiol* 288: C1287-1297, 2005.

57. **Hanisch F, Joshi P, and Zierz S**. AMP deaminase deficiency in skeletal muscle is unlikely to be of clinical relevance. *J Neurol* 255: 318-322, 2008.

58. **Hanson S, McCartan K, Sabina RL, Holmes EW, and Ullman B**. Adenylate deaminase deficiency in a mutant murine T cell lymphoma cell line. *J Biol Chem* 265: 11474-11481, 1990.

59. **Hasselbach W, and Oetliker H**. Energetics and electrogenicity of the sarcoplasmic reticulum calcium pump. *Annu Rev Physiol* 45: 325-339, 1983.

60. **Heizmann CW, Berchtold MW, and Rowlerson AM**. Correlation of parvalbumin concentration with relaxation speed in mammalian muscles. *Proc Natl Acad Sci U S A* 79: 7243-7247, 1982.

61. **Hellsten Y, Richter EA, Kiens B, and Bangsbo J**. AMP deamination and purine exchange in human skeletal muscle during and after intense exercise. *Journal of Physiology-London* 520: 909-920, 1999.

62. **Hibberd MG, Dantzig JA, Trentham DR, and Goldman YE**. Phosphate release and force generation in skeletal muscle fibers. *Science* 228: 1317-1319, 1985.

63. **Hickson RC**. Skeletal muscle cytochrome c and myoglobin, endurance, and frequency of training. *Journal of Applied Physiology* 51: 746-749, 1981.

64. **Hickson RC, Czerwinski SM, Falduto MT, and Young AP**. Glucocorticoid antagonism by exercise and androgenic-anabolic steroids. *Med Sci Sports Exerc* 22: 331-340, 1990.

65. **Hilliard-Robertson PC, Schneider SM, Bishop SL, and Guilliams ME**. Strength gains following different combined concentric and eccentric exercise regimens. *Aviation Space and Environmental Medicine* 74: 342-347, 2003.

66. **Hisatome I, Morisaki T, Kamma H, Sugama T, Morisaki H, Ohtahara A, and Holmes EW**. Control of AMP deaminase 1 binding to myosin heavy chain. *Am J Physiol* 275: C870-881, 1998.

67. **Holloszy JO**. Biochemical adaptations in muscle. Effects of exercise on mitochondrial oxygen uptake and respiratory enzyme activity in skeletal muscle. *J Biol Chem* 242: 2278-2282, 1967.

68. **Holloszy JO, and Coyle EF**. Adaptations of skeletal muscle to endurance exercise and their metabolic consequences. *J Appl Physiol* 56: 831-838, 1984.

69. **Huang H, Zhang X, Li S, Liu N, Lian W, McDowell E, Zhou P, Zhao C, Guo H, Zhang C, Yang C, Wen G, Dong X, Lu L, Ma N, Dong W, Dou QP, Wang X, and Liu J**. Physiological levels of ATP negatively regulate proteasome function. *Cell Res* 20: 1372-1385, 2010.

70. **Huey KA, and Bodine SC**. Changes in myosin mRNA and protein expression in denervated rat soleus and tibialis anterior. *Eur J Biochem* 256: 45-50, 1998.

71. **Hvid LG, Suetta C, Aagaard P, Kjaer M, Frandsen U, and Ortenblad N**. Four days of muscle disuse impairs single fiber contractile function in young and old healthy men. *Exp Gerontol* 48: 154-161, 2013.

72. **Jagoe RT, Lecker SH, Gomes M, and Goldberg AL**. Patterns of gene expression in atrophying skeletal muscles: response to food deprivation. *FASEB J* 16: 1697-1712, 2002.

73. **Janssen I, Heymsfield SB, and Ross R**. Low relative skeletal muscle mass (sarcopenia) in older persons is associated with functional impairment and physical disability. *J Am Geriatr Soc* 50: 889-896, 2002.

74. **Janssen I, Shepard DS, Katzmarzyk PT, and Roubenoff R**. The healthcare costs of sarcopenia in the United States. *J Am Geriatr Soc* 52: 80-85, 2004.

75. **Jubrias SA, Odderson IR, Esselman PC, and Conley KE**. Decline in isokinetic force with age: muscle cross-sectional area and specific force. *Pflugers Arch* 434: 246-253, 1997.

76. **Kalliainen LK, Jejurikar SS, Liang LW, Urbanchek MG, and Kuzon WM, Jr.** A specific force deficit exists in skeletal muscle after partial denervation. *Muscle Nerve* 25: 31-38, 2002.

77. **Kauffman FC, and Albuquerque EX**. Effect of ischemia and denervation on metabolism of fast and slow mammalian skeletal muscle. *Exp Neurol* 28: 46-63, 1970.

78. **Kisselev AF, and Goldberg AL**. Monitoring activity and inhibition of 26S proteasomes with fluorogenic peptide substrates. *Methods Enzymol* 398: 364-378, 2005.

79. **Klionsky DJ, Abdalla FC, Abeliovich H, Abraham RT, Acevedo-Arozena A, Adeli K, Agholme L, Agnello M, Agostinis P, Aguirre-Ghiso JA, Ahn HJ, Ait-Mohamed O, Ait-Si-Ali S, Akematsu T, Akira S, Al-Younes HM, Al-Zeer MA, Albert ML, Albin RL, Alegre-Abarrategui J, Aleo MF, Alirezaei M, Almasan A, Almonte-Becerril M, Amano A, Amaravadi R, Amarnath S, Amer AO, Andrieu-Abadie N, Anantharam V, Ann DK, Anoopkumar-Dukie S, Aoki H, Apostolova N, Arancia G, Aris JP, Asanuma K, Asare NY, Ashida H, Askanas V, Askew DS, Auberger P, Baba M, Backues SK, Baehrecke EH, Bahr BA, Bai XY, Bailly Y, Baiocchi R, Baldini G, Balduini W, Ballabio A, Bamber BA, Bampton ET, Banhegyi G, Bartholomew CR, Bassham DC, Bast RC, Jr., Batoko H, Bay BH, Beau I, Bechet DM, Begley TJ, Behl C, Behrends C, Bekri S, Bellaire B, Bendall LJ, Benetti L, Berliocchi L, Bernardi H, Bernassola F, Besteiro S, Bhatia-Kissova I, Bi X, Biard-Piechaczyk M, Blum JS, Boise LH, Bonaldo P, Boone DL, Bornhauser BC, Bortoluci KR, Bossis I, Bost F, Bourquin JP, Boya P, Boyer-Guittaut M, Bozhkov PV, Brady NR, Brancolini C, Brech A, Brenman JE, Brennand A, Bresnick EH, Brest P, Bridges D, Bristol ML, Brookes PS, Brown EJ, Brumell JH, Brunetti-Pierri N, Brunk UT, Bulman DE, Bultman SJ, Bultynck G, Burbulla LF, Bursch W, Butchar JP, Buzgariu W, Bydlowski SP, Cadwell K, Cahova M, Cai D, Cai J, Cai Q, Calabretta B, Calvo-Garrido J, Camougrand N, Campanella M, Campos-Salinas J, Candi E, Cao L, Caplan AB, Carding SR, Cardoso SM, Carew JS, Carlin CR, Carmignac V, Carneiro LA, Carra S, Caruso RA, Casari G, Casas C, Castino R, Cebollero E, Cecconi F, Celli J, Chaachouay H, Chae HJ, Chai CY, Chan DC, Chan EY, Chang RC, Che CM, Chen CC, Chen GC, Chen GQ, Chen M, Chen Q, Chen SS, Chen W, Chen X, Chen YG, Chen Y, Chen YJ, Chen Z, Cheng A, Cheng CH, Cheng Y, Cheong H, Cheong JH, Cherry S, Chess-Williams R, Cheung ZH, Chevet E,**

Chiang HL, Chiarelli R, Chiba T, Chin LS, Chiou SH, Chisari FV, Cho CH, Cho DH, Choi AM, Choi D, Choi KS, Choi ME, Chouaib S, Choubey D, Choubey V, Chu CT, Chuang TH, Chueh SH, Chun T, Chwae YJ, Chye ML, Ciarcia R, Ciriolo MR, Clague MJ, Clark RS, Clarke PG, Clarke R, Codogno P, Coller HA, Colombo MI, Comincini S, Condello M, Condorelli F, Cookson MR, Coombs GH, Coppens I, Corbalan R, Cossart P, Costelli P, Costes S, Coto-Montes A, Couve E, Coxon FP, Cregg JM, Crespo JL, Cronje MJ, Cuervo AM, Cullen JJ, Czaja MJ, D'Amelio M, Darfeuille-Michaud A, Davids LM, Davies FE, De Felici M, de Groot JF, de Haan CA, De Martino L, De Milito A, De Tata V, Debnath J, Degterev A, Dehay B, Delbridge LM, Demarchi F, Deng YZ, Dengjel J, Dent P, Denton D, Deretic V, Desai SD, Devenish RJ, Di Gioacchino M, Di Paolo G, Di Pietro C, Diaz-Araya G, Diaz-Laviada I, Diaz-Meco MT, Diaz-Nido J, Dikic I, Dinesh-Kumar SP, Ding WX, Distelhorst CW, Diwan A, Djavaheri-Mergny M, Dokudovskaya S, Dong Z, Dorsey FC, Dosenko V, Dowling JJ, Doxsey S, Dreux M, Drew ME, Duan Q, Duchosal MA, Duff K, Dugail I, Durbeej M, Duszenko M, Edelstein CL, Edinger AL, Egea G, Eichinger L, Eissa NT, Ekmekcioglu S, El-Deiry WS, Elazar Z, Elgendy M, Ellerby LM, Eng KE, Engelbrecht AM, Engelender S, Erenpreisa J, Escalante R, Esclatine A, Eskelinen EL, Espert L, Espina V, Fan H, Fan J, Fan QW, Fan Z, Fang S, Fang Y, Fanto M, Fanzani A, Farkas T, Farre JC, Faure M, Fechheimer M, Feng CG, Feng J, Feng Q, Feng Y, Fesus L, Feuer R, Figueiredo-Pereira ME, Fimia GM, Fingar DC, Finkbeiner S, Finkel T, Finley KD, Fiorito F, Fisher EA, Fisher PB, Flajolet M, Florez-McClure ML, Florio S, Fon EA, Fornai F, Fortunato F, Fotedar R, Fowler DH, Fox HS, Franco R, Frankel LB, Fransen M, Fuentes JM, Fueyo J, Fujii J, Fujisaki K, Fujita E, Fukuda M, Furukawa RH, Gaestel M, Gailly P, Gajewska M, Galliot B, Galy V, Ganesh S, Ganetzky B, Ganley IG, Gao FB, Gao GF, Gao J, Garcia L, Garcia-Manero G, Garcia-Marcos M, Garmyn M, Gartel AL, Gatti E, Gautel M, Gawriluk TR, Gegg ME, Geng J, Germain M, Gestwicki JE, Gewirtz DA, Ghavami S, Ghosh P, Giammarioli AM, Giatromanolaki AN, Gibson SB, Gilkerson RW, Ginger ML, Ginsberg HN, Golab J, Goligorsky MS, Golstein P, Gomez-Manzano C, Goncu E, Gongora C, Gonzalez CD, Gonzalez R, Gonzalez-Estevez C, Gonzalez-Polo RA, Gonzalez-Rey E, Gorbunov NV, Gorski S, Goruppi S, Gottlieb RA, Gozuacik D, Granato GE, Grant GD, Green KN, Gregorc A, Gros F, Grose C, Grunt TW, Gual P, Guan JL, Guan KL, Guichard SM, Gukovskaya AS, Gukovsky I, Gunst J, Gustafsson AB, Halayko AJ, Hale AN, Halonen SK, Hamasaki M, Han F, Han T, Hancock MK, Hansen M, Harada H, Harada M, Hardt SE, Harper JW, Harris AL, Harris J, Harris SD, Hashimoto M, Haspel JA, Hayashi S, Hazelhurst LA, He C, He YW, Hebert MJ, Heidenreich KA, Helfrich MH, Helgason GV, Henske EP, Herman B, Herman PK, Hetz C, Hilfiker S, Hill JA, Hocking LJ, Hofman P, Hofmann TG, Hohfeld J, Holyoake TL, Hong MH, Hood DA, Hotamisligil GS, Houwerzijl EJ, Hoyer-Hansen M, Hu B, Hu CA, Hu HM, Hua Y, Huang C, Huang J, Huang S, Huang WP, Huber TB, Huh WK, Hung TH, Hupp TR, Hur GM, Hurley JB, Hussain SN, Hussey PJ, Hwang JJ, Hwang S, Ichihara A, Ilkhanizadeh S, Inoki K, Into T, Iovane V, Iovanna JL, Ip NY, Isaka Y, Ishida H, Isidoro C, Isobe K, Iwasaki A, Izquierdo M, Izumi Y, Jaakkola PM, Jaattela M, Jackson GR, Jackson WT, Janji B, Jendrach M, Jeon JH, Jeung EB, Jiang H, Jiang JX, Jiang M, Jiang Q, Jiang X, Jimenez A, Jin M, Jin S, Joe CO, Johansen T, Johnson DE, Johnson GV, Jones NL, Joseph B,

Joseph SK, Joubert AM, Juhasz G, Juillerat-Jeanneret L, Jung CH, Jung YK, Kaarniranta K, Kaasik A, Kabuta T, Kadowaki M, Kagedal K, Kamada Y, Kaminskyy VO, Kampinga HH, Kanamori H, Kang C, Kang KB, Kang KI, Kang R, Kang YA, Kanki T, Kanneganti TD, Kanno H, Kanthasamy AG, Kanthasamy A, Karantza V, Kaushal GP, Kaushik S, Kawazoe Y, Ke PY, Kehrl JH, Kelekar A, Kerkhoff C, Kessel DH, Khalil H, Kiel JA, Kiger AA, Kihara A, Kim DR, Kim DH, Kim EK, Kim HR, Kim JS, Kim JH, Kim JC, Kim JK, Kim PK, Kim SW, Kim YS, Kim Y, Kimchi A, Kimmelman AC, King JS, Kinsella TJ, Kirkin V, Kirshenbaum LA, Kitamoto K, Kitazato K, Klein L, Klimecki WT, Klucken J, Knecht E, Ko BC, Koch JC, Koga H, Koh JY, Koh YH, Koike M, Komatsu M, Kominami E, Kong HJ, Kong WJ, Korolchuk VI, Kotake Y, Koukourakis MI, Kouri Flores JB, Kovacs AL, Kraft C, Krainc D, Kramer H, Kretz-Remy C, Krichevsky AM, Kroemer G, Kruger R, Krut O, Ktistakis NT, Kuan CY, Kucharczyk R, Kumar A, Kumar R, Kumar S, Kundu M, Kung HJ, Kurz T, Kwon HJ, La Spada AR, Lafont F, Lamark T, Landry J, Lane JD, Lapaquette P, Laporte JF, Laszlo L, Lavandero S, Lavoie JN, Layfield R, Lazo PA, Le W, Le Cam L, Ledbetter DJ, Lee AJ, Lee BW, Lee GM, Lee J, Lee JH, Lee M, Lee MS, Lee SH, Leeuwenburgh C, Legembre P, Legouis R, Lehmann M, Lei HY, Lei QY, Leib DA, Leiro J, Lemasters JJ, Lemoine A, Lesniak MS, Lev D, Levenson VV, Levine B, Levy E, Li F, Li JL, Li L, Li S, Li W, Li XJ, Li YB, Li YP, Liang C, Liang Q, Liao YF, Liberski PP, Lieberman A, Lim HJ, Lim KL, Lim K, Lin CF, Lin FC, Lin J, Lin JD, Lin K, Lin WW, Lin WC, Lin YL, Linden R, Lingor P, Lippincott-Schwartz J, Lisanti MP, Liton PB, Liu B, Liu CF, Liu K, Liu L, Liu QA, Liu W, Liu YC, Liu Y, Lockshin RA, Lok CN, Lonial S, Loos B, Lopez-Berestein G, Lopez-Otin C, Lossi L, Lotze MT, Low P, Lu B, Lu Z, Luciano F, Lukacs NW, Lund AH, Lynch-Day MA, Ma Y, Macian F, MacKeigan JP, Macleod KF, Madeo F, Maiuri L, Maiuri MC, Malagoli D, Malicdan MC, Malorni W, Man N, Mandelkow EM, Manon S, Manov I, Mao K, Mao X, Mao Z, Marambaud P, Marazziti D, Marcel YL, Marchbank K, Marchetti P, Marciniak SJ, Marcondes M, Mardi M, Marfe G, Marino G, Markaki M, Marten MR, Martin SJ, Martinand-Mari C, Martinet W, Martinez-Vicente M, Masini M, Matarrese P, Matsuo S, Matteoni R, Mayer A, Mazure NM, McConkey DJ, McConnell MJ, McDermott C, McDonald C, McInerney GM, McKenna SL, McLaughlin B, McLean PJ, McMaster CR, McQuibban GA, Meijer AJ, Meisler MH, Melendez A, Melia TJ, Melino G, Mena MA, Menendez JA, Menna-Barreto RF, Menon MB, Menzies FM, Mercer CA, Merighi A, Merry DE, Meschini S, Meyer CG, Meyer TF, Miao CY, Miao JY, Michels PA, Michiels C, Mijaljica D, Milojkovic A, Minucci S, Miracco C, Miranti CK, Mitroulis I, Miyazawa K, Mizushima N, Mograbi B, Mohseni S, Molero X, Mollereau B, Mollinedo F, Momoi T, Monastyrska I, Monick MM, Monteiro MJ, Moore MN, Mora R, Moreau K, Moreira PI, Moriyasu Y, Moscat J, Mostowy S, Mottram JC, Motyl T, Moussa CE, Muller S, Munger K, Munz C, Murphy LO, Murphy ME, Musaro A, Mysorekar I, Nagata E, Nagata K, Nahimana A, Nair U, Nakagawa T, Nakahira K, Nakano H, Nakatogawa H, Nanjundan M, Naqvi NI, Narendra DP, Narita M, Navarro M, Nawrocki ST, Nazarko TY, Nemchenko A, Netea MG, Neufeld TP, Ney PA, Nezis IP, Nguyen HP, Nie D, Nishino I, Nislow C, Nixon RA, Noda T, Noegel AA, Nogalska A, Noguchi S, Notterpek L, Novak I, Nozaki T, Nukina N, Nurnberger T, Nyfeler B, Obara K, Oberley TD, Oddo S, Ogawa M, Ohashi T, Okamoto K, Oleinick NL, Oliver FJ,

Olsen LJ, Olsson S, Opota O, Osborne TF, Ostrander GK, Otsu K, Ou JH, Ouimet M, Overholtzer M, Ozpolat B, Paganetti P, Pagnini U, Pallet N, Palmer GE, Palumbo C, Pan T, Panaretakis T, Pandey UB, Papackova Z, Papassideri I, Paris I, Park J, Park OK, Parys JB, Parzych KR, Patschan S, Patterson C, Pattingre S, Pawelek JM, Peng J, Perlmutter DH, Perrotta I, Perry G, Pervaiz S, Peter M, Peters GJ, Petersen M, Petrovski G, Phang JM, Piacentini M, Pierre P, Pierrefite-Carle V, Pierron G, Pinkas-Kramarski R, Piras A, Piri N, Platanias LC, Poggeler S, Poirot M, Poletti A, Pous C, Pozuelo-Rubio M, Praetorius-Ibba M, Prasad A, Prescott M, Priault M, Produit-Zengaffinen N, Progulske-Fox A, Proikas-Cezanne T, Przedborski S, Przyklenk K, Puertollano R, Puyal J, Qian SB, Qin L, Qin ZH, Quaggin SE, Raben N, Rabinowich H, Rabkin SW, Rahman I, Rami A, Ramm G, Randall G, Randow F, Rao VA, Rathmell JC, Ravikumar B, Ray SK, Reed BH, Reed JC, Reggiori F, Regnier-Vigouroux A, Reichert AS, Reiners JJ, Jr., Reiter RJ, Ren J, Revuelta JL, Rhodes CJ, Ritis K, Rizzo E, Robbins J, Roberge M, Roca H, Roccheri MC, Rocchi S, Rodemann HP, Rodriguez de Cordoba S, Rohrer B, Roninson IB, Rosen K, Rost-Roszkowska MM, Rouis M, Rouschop KM, Rovetta F, Rubin BP, Rubinsztein DC, Ruckdeschel K, Rucker EB, 3rd, Rudich A, Rudolf E, Ruiz-Opazo N, Russo R, Rusten TE, Ryan KM, Ryter SW, Sabatini DM, Sadoshima J, Saha T, Saitoh T, Sakagami H, Sakai Y, Salekdeh GH, Salomoni P, Salvaterra PM, Salvesen G, Salvioli R, Sanchez AM, Sanchez-Alcazar JA, Sanchez-Prieto R, Sandri M, Sankar U, Sansanwal P, Santambrogio L, Saran S, Sarkar S, Sarwal M, Sasakawa C, Sasnauskiene A, Sass M, Sato K, Sato M, Schapira AH, Scharl M, Schatzl HM, Scheper W, Schiaffino S, Schneider C, Schneider ME, Schneider-Stock R, Schoenlein PV, Schorderet DF, Schuller C, Schwartz GK, Scorrano L, Sealy L, Seglen PO, Segura-Aguilar J, Seiliez I, Seleverstov O, Sell C, Seo JB, Separovic D, Setaluri V, Setoguchi T, Settembre C, Shacka JJ, Shanmugam M, Shapiro IM, Shaulian E, Shaw RJ, Shelhamer JH, Shen HM, Shen WC, Sheng ZH, Shi Y, Shibuya K, Shidoji Y, Shieh JJ, Shih CM, Shimada Y, Shimizu S, Shintani T, Shirihai OS, Shore GC, Sibirny AA, Sidhu SB, Sikorska B, Silva-Zacarin EC, Simmons A, Simon AK, Simon HU, Simone C, Simonsen A, Sinclair DA, Singh R, Sinha D, Sinicrope FA, Sirko A, Siu PM, Sivridis E, Skop V, Skulachev VP, Slack RS, Smaili SS, Smith DR, Soengas MS, Soldati T, Song X, Sood AK, Soong TW, Sotgia F, Spector SA, Spies CD, Springer W, Srinivasula SM, Stefanis L, Steffan JS, Stendel R, Stenmark H, Stephanou A, Stern ST, Sternberg C, Stork B, Stralfors P, Subauste CS, Sui X, Sulzer D, Sun J, Sun SY, Sun ZJ, Sung JJ, Suzuki K, Suzuki T, Swanson MS, Swanton C, Sweeney ST, Sy LK, Szabadkai G, Tabas I, Taegtmeyer H, Tafani M, Takacs-Vellai K, Takano Y, Takegawa K, Takemura G, Takeshita F, Talbot NJ, Tan KS, Tanaka K, Tang D, Tanida I, Tannous BA, Tavernarakis N, Taylor GS, Taylor GA, Taylor JP, Terada LS, Terman A, Tettamanti G, Thevissen K, Thompson CB, Thorburn A, Thumm M, Tian F, Tian Y, Tocchini-Valentini G, Tolkovsky AM, Tomino Y, Tonges L, Tooze SA, Tournier C, Tower J, Towns R, Trajkovic V, Travassos LH, Tsai TF, Tschan MP, Tsubata T, Tsung A, Turk B, Turner LS, Tyagi SC, Uchiyama Y, Ueno T, Umekawa M, Umemiya-Shirafuji R, Unni VK, Vaccaro MI, Valente EM, Van den Berghe G, van der Klei IJ, van Doorn W, van Dyk LF, van Egmond M, van Grunsven LA, Vandenabeele P, Vandenberghe WP, Vanhorebeek I, Vaquero EC, Velasco G,

Vellai T, Vicencio JM, Vierstra RD, Vila M, Vindis C, Viola G, Viscomi MT, Voitsekhovskaja OV, von Haefen C, Votruba M, Wada K, Wade-Martins R, Walker CL, Walsh CM, Walter J, Wan XB, Wang A, Wang C, Wang D, Wang F, Wang G, Wang H, Wang HG, Wang HD, Wang J, Wang K, Wang M, Wang RC, Wang X, Wang YJ, Wang Y, Wang Z, Wang ZC, Wansink DG, Ward DM, Watada H, Waters SL, Webster P, Wei L, Weihl CC, Weiss WA, Welford SM, Wen LP, Whitehouse CA, Whitton JL, Whitworth AJ, Wileman T, Wiley JW, Wilkinson S, Willbold D, Williams RL, Williamson PR, Wouters BG, Wu C, Wu DC, Wu WK, Wyttenbach A, Xavier RJ, Xi Z, Xia P, Xiao G, Xie Z, Xu DZ, Xu J, Xu L, Xu X, Yamamoto A, Yamashina S, Yamashita M, Yan X, Yanagida M, Yang DS, Yang E, Yang JM, Yang SY, Yang W, Yang WY, Yang Z, Yao MC, Yao TP, Yeganeh B, Yen WL, Yin JJ, Yin XM, Yoo OJ, Yoon G, Yoon SY, Yorimitsu T, Yoshikawa Y, Yoshimori T, Yoshimoto K, You HJ, Youle RJ, Younes A, Yu L, Yu SW, Yu WH, Yuan ZM, Yue Z, Yun CH, Yuzaki M, Zabirnyk O, Silva-Zacarin E, Zacks D, Zacksenhaus E, Zaffaroni N, Zakeri Z, Zeh HJ, 3rd, Zeitlin SO, Zhang H, Zhang HL, Zhang J, Zhang JP, Zhang L, Zhang MY, Zhang XD, Zhao M, Zhao YF, Zhao Y, Zhao ZJ, Zheng X, Zhivotovsky B, Zhong Q, Zhou CZ, Zhu C, Zhu WG, Zhu XF, Zhu X, Zhu Y, Zoladek T, Zong WX, Zorzano A, Zschocke J, and Zuckerbraun B. Guidelines for the use and interpretation of assays for monitoring autophagy. *Autophagy* 8: 445-544, 2012.

80. **Kodama T**. Thermodynamic analysis of muscle ATPase mechanisms. *Physiol Rev* 65: 467-551, 1985.

81. **Lecker SH, Jagoe RT, Gilbert A, Gomes M, Baracos V, Bailey J, Price SR, Mitch WE, and Goldberg AL**. Multiple types of skeletal muscle atrophy involve a common program of changes in gene expression. *FASEB J* 18: 39-51, 2004.

82. **Levine B, and Klionsky DJ**. Development by self-digestion: molecular mechanisms and biological functions of autophagy. *Dev Cell* 6: 463-477, 2004.

83. **Levine S, Nguyen T, Taylor N, Friscia ME, Budak MT, Rothenberg P, Zhu J, Sachdeva R, Sonnad S, Kaiser LR, Rubinstein NA, Powers SK, and Shrager JB**. Rapid disuse atrophy of diaphragm fibers in mechanically ventilated humans. *N Engl J Med* 358: 1327-1335, 2008.

84. **Liu CW, Li X, Thompson D, Wooding K, Chang TL, Tang Z, Yu H, Thomas PJ, and DeMartino GN**. ATP binding and ATP hydrolysis play distinct roles in the function of 26S proteasome. *Mol Cell* 24: 39-50, 2006.

85. **Macpherson PC, Wang X, and Goldman D**. Myogenin regulates denervation-dependent muscle atrophy in mouse soleus muscle. *J Cell Biochem* 112: 2149-2159, 2011.

86. **Mahnke-Zizelman DK, and Sabina RL**. Localization of N-terminal sequences in human AMP deaminase isoforms that influence contractile protein binding. *Biochem Biophys Res Commun* 285: 489-495, 2001.

87. **Mahnke-Zizelman DK, and Sabina RL**. N-terminal sequence and distal histidine residues are responsible for pH-regulated cytoplasmic membrane binding of human AMP deaminase isoform E. *J Biol Chem* 277: 42654-42662, 2002.

88. **Mahnke DK, and Sabina RL**. Calcium activates erythrocyte AMP deaminase [isoform E (AMPD3)] through a protein-protein interaction between calmodulin and the N-terminal domain of the AMPD3 polypeptide. *Biochemistry* 44: 5551-5559, 2005.

89. **Majetschak M**. Regulation of the proteasome by ATP: implications for ischemic myocardial injury and donor heart preservation. *Am J Physiol Heart Circ Physiol* 305: H267-278, 2013.

90. **Mammucari C, Milan G, Romanello V, Masiero E, Rudolf R, Del Piccolo P, Burden SJ, Di Lisi R, Sandri C, Zhao J, Goldberg AL, Schiaffino S, and Sandri M**. FoxO3 controls autophagy in skeletal muscle in vivo. *Cell Metab* 6: 458-471, 2007.

91. **Manfredi JP, and Holmes EW**. Control of the purine nucleotide cycle in extracts of rat skeletal muscle: effects of energy state and concentrations of cycle intermediates. *Arch Biochem Biophys* 233: 515-529, 1984.

92. **Matar W, Lunde JA, Jasmin BJ, and Renaud JM**. Denervation enhances the physiological effects of the K(ATP) channel during fatigue in EDL and soleus muscle. *Am J Physiol Regul Integr Comp Physiol* 281: R56-65, 2001.

93. **Medina R, Wing SS, and Goldberg AL**. Increase in levels of polyubiquitin and proteasome mRNA in skeletal muscle during starvation and denervation atrophy. *Biochem J* 307 (Pt 3): 631-637, 1995.

94. **Metter EJ, Talbot LA, Schrager M, and Conwit R**. Skeletal muscle strength as a predictor of all-cause mortality in healthy men. *J Gerontol A Biol Sci Med Sci* 57: B359-365, 2002.

95. **Meyer RA, Dudley GA, and Terjung RL**. Ammonia and IMP in different skeletal muscle fibers after exercise in rats. *J Appl Physiol Respir Environ Exerc Physiol* 49: 1037-1041, 1980.

96. **Meyer RA, and Terjung RL**. AMP deamination and IMP reamination in working skeletal muscle. *American Journal of Physiology - Cell Physiology* 239: C32-C38, 1980.

97. **Milan G, Romanello V, Pescatore F, Armani A, Paik JH, Frasson L, Seydel A, Zhao J, Abraham R, Goldberg AL, Blaauw B, DePinho RA, and Sandri M**. Regulation of autophagy and the ubiquitin-proteasome system by the FoxO transcriptional network during muscle atrophy. *Nat Commun* 6: 6670, 2015.

98. **Min K, Smuder AJ, Kwon OS, Kavazis AN, Szeto HH, and Powers SK**. Mitochondrial-targeted antioxidants protect skeletal muscle against immobilization-induced muscle atrophy. *J Appl Physiol* 111: 1459-1466, 2011.

99. **Morisaki T, Gross M, Morisaki H, Pongratz D, Zollner N, and Holmes EW**. Molecular basis of AMP deaminase deficiency in skeletal muscle. *Proc Natl Acad Sci U S A* 89: 6457-6461, 1992.

100. **Morisaki T, Sabina RL, and Holmes EW**. Adenylate deaminase. A multigene family in humans and rats. *J Biol Chem* 265: 11482-11486, 1990.

101. **Morley JE, Thomas DR, and Wilson MM**. Cachexia: pathophysiology and clinical relevance. *Am J Clin Nutr* 83: 735-743, 2006.

102. **Murphy KT, Chee A, Trieu J, Naim T, and Lynch GS**. Importance of functional and metabolic impairments in the characterization of the C-26 murine model of cancer cachexia. *Dis Model Mech* 5: 533-545, 2012.

103. **Nevitt MC, Cummings SR, Kidd S, and Black D**. Risk factors for recurrent nonsyncopal falls. A prospective study. *JAMA* 261: 2663-2668, 1989.

104. **Norman B, Glenmark B, and Jansson E**. Muscle AMP deaminase deficiency in 2% of a healthy population. *Muscle Nerve* 18: 239-241, 1995.

105. **Nosek TM, Fender KY, and Godt RE**. It is diprotonated inorganic phosphate that depresses force in skinned skeletal muscle fibers. *Science* 236: 191-193, 1987.

106. **O'Leary MF, Vainshtein A, Carter HN, Zhang Y, and Hood DA**. Denervation-induced mitochondrial dysfunction and autophagy in skeletal muscle of apoptosis-deficient animals. *Am J Physiol Cell Physiol* 303: C447-454, 2012.

107. **Oka C, Cha CY, and Noma A**. Characterization of the cardiac Na+/K+ pump by development of a comprehensive and mechanistic model. *J Theor Biol* 265: 68-77, 2010.

108. **Pellegrino C, and Franzini C**. An Electron Microscope Study of Denervation Atrophy in Red and Which Skeletal Muscle Fibers. *J Cell Biol* 17: 327-349, 1963.

109. **Perez M, Martin MA, Canete S, Rubio JC, Fernandez-Moreira D, San Juan AF, Gomez-Gallego F, Santiago C, Arenas J, and Lucia A**. Does the C34T mutation in AMPD1 alter exercise capacity in the elderly? *Int J Sports Med* 27: 429-435, 2006.

110. **Pichard C, Vaughan C, Struk R, Armstrong RL, and Jeejeebhoy KN**. Effect of dietary manipulations (fasting, hypocaloric feeding, and subsequent refeeding) on rat muscle energetics as assessed by nuclear magnetic resonance spectroscopy. *J Clin Invest* 82: 895-901, 1988.

111. **Pipoly GM, Nathans GR, Chang D, and Deuel TF**. Regulation of the interaction of purified human erythrocyte AMP deaminase and the human erythrocyte membrane. *J Clin Invest* 63: 1066-1076, 1979.

112. **Plaideau C, Lai YC, Kviklyte S, Zanou N, Lofgren L, Andersen H, Vertommen D, Gailly P, Hue L, Bohlooly YM, Hallen S, and Rider MH**. Effects of pharmacological AMP deaminase inhibition and Ampd1 deletion on nucleotide levels and AMPK activation in contracting skeletal muscle. *Chem Biol* 21: 1497-1510, 2014.

113. **Plaideau C, Liu J, Hartleib-Geschwindner J, Bastin-Coyette L, Bontemps F, Oscarsson J, Hue L, and Rider MH**. Overexpression of AMP-metabolizing enzymes controls adenine nucleotide levels and AMPK activation in HEK293T cells. *The FASEB Journal* 26: 2685-2694, 2012.

114. **Potma EJ, van Graas IA, and Stienen GJ**. Influence of inorganic phosphate and pH on ATP utilization in fast and slow skeletal muscle fibers. *Biophys J* 69: 2580-2589, 1995.

115. **Quy PN, Kuma A, Pierre P, and Mizushima N**. Proteasome-dependent activation of mammalian target of rapamycin complex 1 (mTORC1) is essential for autophagy suppression and muscle remodeling following denervation. *J Biol Chem* 288: 1125-1134, 2013.

116. **Raffaello A, Laveder P, Romualdi C, Bean C, Toniolo L, Germinario E, Megighian A, Danieli-Betto D, Reggiani C, and Lanfranchi G**. Denervation in murine fast-twitch muscle: short-term physiological changes and temporal expression profiling. *Physiol Genomics* 25: 60-74, 2006.

117. **Raffaello A, Milan G, Masiero E, Carnio S, Lee D, Lanfranchi G, Goldberg AL, and Sandri M**. JunB transcription factor maintains skeletal muscle mass and promotes hypertrophy. *J Cell Biol* 191: 101-113, 2010.

118. **Rantanen T, Harris T, Leveille SG, Visser M, Foley D, Masaki K, and Guralnik JM**. Muscle strength and body mass index as long-term predictors of mortality in initially healthy men. *J Gerontol A Biol Sci Med Sci* 55: M168-173, 2000.

119. **Rassier DE, Tubman LA, and MacIntosh BR**. Inhibition of Ca2+ release in rat atrophied gastrocnemius muscle. *Exp Physiol* 82: 665-676, 1997.

120. **Ren JM, and Holloszy JO**. Adaptation of rat skeletal muscle to creatine depletion: AMP deaminase and AMP deamination. *J Appl Physiol (1985)* 73: 2713-2716, 1992.

121. **Rennie MJ, Selby A, Atherton P, Smith K, Kumar V, Glover EL, and Philips SM**. Facts, noise and wishful thinking: muscle protein turnover in aging and human disuse atrophy. *Scand J Med Sci Sports* 20: 5-9, 2010.

122. **Rico-Sanz J, Rankinen T, Joanisse DR, Leon AS, Skinner JS, Wilmore JH, Rao DC, and Bouchard C**. Associations between cardiorespiratory responses to exercise and the C34T AMPD1 gene polymorphism in the HERITAGE Family Study. *Physiol Genomics* 14: 161-166, 2003.

123. **Roberts BM, Frye GS, Ahn B, Ferreira LF, and Judge AR**. Cancer cachexia decreases specific force and accelerates fatigue in limb muscle. *Biochem Biophys Res Commun* 435: 488-492, 2013.

124. **Rock KL, Gramm C, Rothstein L, Clark K, Stein R, Dick L, Hwang D, and Goldberg AL**. Inhibitors of the proteasome block the degradation of most cell proteins and the generation of peptides presented on MHC class I molecules. *Cell* 78: 761-771, 1994.

125. **Romanello V, Guadagnin E, Gomes L, Roder I, Sandri C, Petersen Y, Milan G, Masiero E, Del Piccolo P, Foretz M, Scorrano L, Rudolf R, and Sandri M**. Mitochondrial fission and remodelling contributes to muscle atrophy. *Embo J* 29: 1774-1785, 2010.

126. **Rundell KW, Tullson PC, and Terjung RL**. Altered kinetics of AMP deaminase by myosin binding. *Am J Physiol* 263: C294-299, 1992.

127. **Rundell KW, Tullson PC, and Terjung RL**. AMP deaminase binding in contracting rat skeletal muscle. *Am J Physiol* 263: C287-293, 1992.

128. **Rush JW, Tullson PC, and Terjung RL**. Molecular and kinetic alterations of muscle AMP deaminase during chronic creatine depletion. *Am J Physiol* 274: C465-471, 1998.

129. **Russell RC, Tian Y, Yuan H, Park HW, Chang YY, Kim J, Kim H, Neufeld TP, Dillin A, and Guan KL**. ULK1 induces autophagy by phosphorylating Beclin-1 and activating VPS34 lipid kinase. *Nat Cell Biol* 15: 741-750, 2013.

130. **Sacheck JM, Hyatt JP, Raffaello A, Jagoe RT, Roy RR, Edgerton VR, Lecker SH, and Goldberg AL**. Rapid disuse and denervation atrophy involve transcriptional changes similar to those of muscle wasting during systemic diseases. *FASEB J* 21: 140-155, 2007.

131. **Saeman MR, DeSpain K, Liu MM, Carlson BA, Song J, Baer LA, Wade CE, and Wolf SE**. Effects of exercise on soleus in severe burn and muscle disuse atrophy. *J Surg Res* 2015.

132. **Sahlin K, and Broberg S**. Adenine nucleotide depletion in human muscle during exercise: causality and significance of AMP deamination. *Int J Sports Med* 11 Suppl 2: S62-67, 1990.

133. **Sanchez AM, Candau RB, Csibi A, Pagano AF, Raibon A, and Bernardi H**. The role of AMP-activated protein kinase in the coordination of skeletal muscle turnover and energy homeostasis. *Am J Physiol Cell Physiol* 303: C475-485, 2012.

134. **Sandri M, Lin JD, Handschin C, Yang WL, Arany ZP, Lecker SH, Goldberg AL, and Spiegelman BM**. PGC-1 alpha a protects skeletal muscle from atrophy by

suppressing Fox03 action and atrophy-specific gene transcription. *Proc Natl Acad Sci U S A* 103: 16260-16265, 2006.

135. **Sandri M, Sandri C, Gilbert A, Skurk C, Calabria E, Picard A, Walsh K, Schiaffino S, Lecker SH, and Goldberg AL**. Foxo transcription factors induce the atrophy-related ubiquitin ligase atrogin-1 and cause skeletal muscle atrophy. *Cell* 117: 399-412, 2004.

136. **Sato K, Katayama K, Hotta N, Ishida K, and Akima H**. Aerobic exercise capacity and muscle volume after lower limb suspension with exercise countermeasure. *Aviat Space Environ Med* 81: 1085-1091, 2010.

137. **Sayer AA, Syddall HE, Martin HJ, Dennison EM, Roberts HC, and Cooper C**. Is grip strength associated with health-related quality of life? Findings from the Hertfordshire Cohort Study. *Age Ageing* 35: 409-415, 2006.

138. **Schiaffino S, Dyar KA, Ciciliot S, Blaauw B, and Sandri M**. Mechanisms regulating skeletal muscle growth and atrophy. *FEBS J* 280: 4294-4314, 2013.

139. **Schulte L, Peters D, Taylor J, Navarro J, and Kandarian S**. Sarcoplasmic reticulum Ca2+ pump expression in denervated skeletal muscle. *Am J Physiol* 267: C617-622, 1994.

140. **Shah PK, Ye F, Liu M, Jayaraman A, Baligand C, Walter G, and Vandenborne K**. In vivo (31)P NMR spectroscopy assessment of skeletal muscle bioenergetics after spinal cord contusion in rats. *Eur J Appl Physiol* 114: 847-858, 2014.

141. **Sims B, Mahnke-Zizelman DK, Profit AA, Prestwich GD, Sabina RL, and Theibert AB**. Regulation of AMP deaminase by phosphoinositides. *J Biol Chem* 274: 25701-25707, 1999.

142. **Smith DM, Fraga H, Reis C, Kafri G, and Goldberg AL**. ATP binds to proteasomal ATPases in pairs with distinct functional effects, implying an ordered reaction cycle. *Cell* 144: 526-538, 2011.

143. **Szabo A, Wuytack F, and Zador E**. The effect of passive movement on denervated soleus highlights a differential nerve control on SERCA and MyHC isoforms. *J Histochem Cytochem* 56: 1013-1022, 2008.

144. **Szulc P, Munoz F, Marchand F, Chapurlat R, and Delmas PD**. Rapid loss of appendicular skeletal muscle mass is associated with higher all-cause mortality in older men: the prospective MINOS study. *Am J Clin Nutr* 91: 1227-1236, 2010.

145. **Tanida I, Ueno T, and Kominami E**. LC3 conjugation system in mammalian autophagy. *Int J Biochem Cell Biol* 36: 2503-2518, 2004.

146. **Thom JM, Thompson MW, Ruell PA, Bryant GJ, Fonda JS, Harmer AR, Janse de Jonge XA, and Hunter SK**. Effect of 10-day cast immobilization on

sarcoplasmic reticulum calcium regulation in humans. *Acta Physiol Scand* 172: 141-147, 2001.

147. **Tovmasian EK, Hairapetian RL, Bykova EV, Severin SE, Jr., and Haroutunian AV**. Phosphorylation of the skeletal muscle AMP-deaminase by protein kinase C. *FEBS Lett* 259: 321-323, 1990.

148. **Trappe TA, Burd NA, Louis ES, Lee GA, and Trappe SW**. Influence of concurrent exercise or nutrition countermeasures on thigh and calf muscle size and function during 60 days of bed rest in women. *Acta Physiol (Oxf)* 191: 147-159, 2007.

149. **Trombetti A, Reid KF, Hars M, Herrmann FR, Pasha E, Phillips EM, and Fielding RA**. Age-associated declines in muscle mass, strength, power, and physical performance: impact on fear of falling and quality of life. *Osteoporos Int* 2015.

150. **Tullson PC, Arabadjis PG, Rundell KW, and Terjung RL**. IMP reamination to AMP in rat skeletal muscle fiber types. *American Journal of Physiology-Cell Physiology* 270: C1067-C1074, 1996.

151. **Tullson PC, Rush JW, Wieringa B, and Terjung RL**. Alterations in AMP deaminase activity and kinetics in skeletal muscle of creatine kinase-deficient mice. *Am J Physiol* 274: C1411-1416, 1998.

152. **Tullson PC, and Terjung RL**. Adenine nucleotide degradation in striated muscle. *Int J Sports Med* 11 Suppl 2: S47-55, 1990.

153. **Udaka J, Terui T, Ohtsuki I, Marumo K, Ishiwata S, Kurihara S, and Fukuda N**. Depressed contractile performance and reduced fatigue resistance in single skinned fibers of soleus muscle after long-term disuse in rats. *J Appl Physiol (1985)* 111: 1080-1087, 2011.

154. **Umeki D, Ohnuki Y, Mototani Y, Shiozawa K, Suita K, Fujita T, Nakamura Y, Saeki Y, and Okumura S**. Protective Effects of Clenbuterol against Dexamethasone-Induced Masseter Muscle Atrophy and Myosin Heavy Chain Transition. *PLoS One* 10: e0128263, 2015.

155. **Wackerhage H, Hoffmann U, Essfeld D, Leyk D, Mueller K, and Zange J**. Recovery of free ADP, Pi, and free energy of ATP hydrolysis in human skeletal muscle. *J Appl Physiol (1985)* 85: 2140-2145, 1998.

156. **Wagatsuma A, Kotake N, Kawachi T, Shiozuka M, Yamada S, and Matsuda R**. Mitochondrial adaptations in skeletal muscle to hindlimb unloading. *Mol Cell Biochem* 350: 1-11, 2011.

157. **Weber MA, Krakowski-Roosen H, Schroder L, Kinscherf R, Krix M, Kopp-Schneider A, Essig M, Bachert P, Kauczor HU, and Hildebrandt W**. Morphology, metabolism, microcirculation, and strength of skeletal muscles in cancer-related cachexia. *Acta Oncol* 48: 116-124, 2009.

158. **Webster DM, and Bressler BH**. Changes in isometric contractile properties of extensor digitorum longus and soleus muscles of C57BL/6J mice following denervation. *Can J Physiol Pharmacol* 63: 681-686, 1985.

159. **Weiss N, Andrianjafiniony T, Dupre-Aucouturier S, Pouvreau S, Desplanches D, and Jacquemond V**. Altered myoplasmic Ca(2+) handling in rat fast-twitch skeletal muscle fibres during disuse atrophy. *Pflugers Arch* 459: 631-644, 2010.

160. **Wicks KL, and Hood DA**. Mitochondrial adaptations in denervated muscle: relationship to muscle performance. *Am J Physiol* 260: C841-850, 1991.

161. **Wing SS, and Goldberg AL**. Glucocorticoids activate the ATP-ubiquitin-dependent proteolytic system in skeletal muscle during fasting. *Am J Physiol* 264: E668-676, 1993.

162. **Yoshida D, Suzuki T, Shimada H, Park H, Makizako H, Doi T, Anan Y, Tsutsumimoto K, Uemura K, Ito T, and Lee S**. Using two different algorithms to determine the prevalence of sarcopenia. *Geriatr Gerontol Int* 14 Suppl 1: 46-51, 2014.

163. **Zhao J, Brault JJ, Schild A, Cao P, Sandri M, Schiaffino S, Lecker SH, and Goldberg AL**. FoxO3 coordinately activates protein degradation by the autophagic/lysosomal and proteasomal pathways in atrophying muscle cells. *Cell Metab* 6: 472-483, 2007.

Apendix A: Institutional Animal Care and Use Committee Approval

East Carolina University

Animal Care and Use Commitee
212 Ed Warren Life Sciences Building
East Carolina University
Greenville, NC 27834

252-744-2436 office
252-744-2355 fax

September 25, 2013

Jeffrey Brault, Ph.D.
Department of Kinesiology
Ward Sports Medicine
East Carolina University

Dear Dr. Brault:

Your Animal Use Protocol entitled, "Impaired Cellular Energetics and Atrophy of Skeletal Muscle" (AUP #P063a) was reviewed by this institution's Animal Care and Use Committee on 9/25/13. The following action was taken by the Committee:

"Approved as submitted"

Please contact Dale Aycock at 744-2997 prior to hazard use

A copy is enclosed for your laboratory files. Please be reminded that all animal procedures must be conducted as described in the approved Animal Use Protocol. Modifications of these procedures cannot be performed without prior approval of the ACUC. The Animal Welfare Act and Public Health Service Guidelines require the ACUC to suspend activities not in accordance with approved procedures and report such activities to the responsible University Official (Vice Chancellor for Health Sciences or Vice Chancellor for Academic Affairs) and appropriate federal Agencies.

Sincerely yours,

Susan McRae, Ph.D.
Chair, Animal Care and Use Committee

SM/jd

Enclosure

East Carolina University

Animal Care and Use Commitee
212 Ed Warren Life Sciences Building
East Carolina University
Greenville, NC 27834

252-744-2436 office
252-744-2355 fax

July 21, 2014

Jeffrey Brault, Ph.D.
Department of Kinesiology
Brody 6N-98
ECU Brody School of Medicine

Dear Dr. Brault:

The Amendment to your Animal Use Protocol entitled, "Impaired Cellular Energetics and Atrophy of Skeletal Muscle", (AUP #P063a) was reviewed by this institution's Animal Care and Use Committee on 7/21/14. The following action was taken by the Committee:

"Approved as amended"

****Please contact Dale Aycock prior to any hazard use**

A copy of the Amendment is enclosed for your laboratory files. Please be reminded that all animal procedures must be conducted as described in the approved Animal Use Protocol. Modifications of these procedures cannot be performed without prior approval of the ACUC. The Animal Welfare Act and Public Health Service Guidelines require the ACUC to suspend activities not in accordance with approved procedures and report such activities to the responsible University Official (Vice Chancellor for Health Sciences or Vice Chancellor for Academic Affairs) and appropriate federal Agencies. **Please ensure that all personnel associated with this protocol have access to this approved copy of the AUP/Amendment and are familiar with its contents.**

Sincerely yours,

Susan McRae, Ph.D.
Chair, Animal Care and Use Committee

SM/jd

enclosure